Sensitive detection of foodborne *E. coli* O157:H7 by dendrimer-aptamer modified microchannels - with RCA signal intensifications

Yuqian Jiang

Thesis submitted in partial fulfillment of the requirements for the

Doctorate in Philosophy Degree in Chemical Engineering

Department of Chemical and Biological Engineering

Faculty of Engineering

University of Ottawa

Abstract

Foodborne pathogenic bacterial infection is one of the main causes for food poisoning cases. Therefore there is an urgent need for rapid, sensitive and cost-effective detection methods in order to avoid or to respond to outbreaks of such diseases in a timely manner. To this end, a dendrimer-aptamer modified microfluidic detection system with rolling circle amplification (RCA) is developed to detect *E. coli* O157:H7. In the proposed detection system, poly(amidoamine (PAMAM) dendrimers are immobilized onto inner surfaces of polydimethyl siloxane (PDMS) microchannels to avoid non-specific binding and to provide more binding sites to subsequently conjugate capturing aptamers as recognition elements. Surface modifications by the PAMAM dendrimers and the aptamers are characterized. To further enhance detection sensitivity, RCA is employed to intensify fluorescence signals for detection. To better understand the RCA process and optimize its reaction conditions, the RCA reaction processes are followed over time using atomic force microscopy and agarose gel electrophoresis. Subsequently, the optimized RCA reaction conditions are used in a dendrimer-aptamer microfluidic whole-cell detection system for *E. coli* O157:H7 detection with signal RCA (sRCA) signal intensifications. To further improve the detection sensitivity, a new set of RCA sequences for capturing target bacterial cells (*i.e.* cRCA) are designed to produce tandem repeat aptamer units (*i.e.* cRCA-aptamers) for more efficient target captures. In situ cRCA synthesis on microchannel inner surface is characterized and optimized for its application in capturing *E. coli* O157:H7 cells. The cRCA approach shows better capturing ability and further increased the fluorescence

detection signals. Our results suggest that the proposed platform is a promising method for sensitive and rapid detection of pathogenic bacterial cells.

Résumé

La majorité des cas d'intoxication alimentaire sont causés par des bactéries pathogènes. Donc, il y a un besoin urgent pour des méthodes de détection rapides, sensibles et rentables pour éviter ou répondre aux flambées de ces maladies en temps opportun. Pour cet objective, un système de détection microfluidique modifié par des dendrimère-aptamères avec une amplification en cercle tournant (ACT) est développé pour détecter *E. coli* O157:H7. Dans le système de détection proposé, les dendrimères PAMAM sont immobilisés sur les surfaces internes des microcanaux PDMS pour éviter la liaison non spécifique et pour fournir plus de sites de liaison qui ensuite conjugue les aptamères de capture comme éléments de reconnaissance. Les modifications de surface par les dendrimères PAMAM et les aptamères sont caractérisées. Pour améliorer encore la sensibilité de détection, ACT est utilisé pour intensifier les signaux de la détection de fluorescence. Pour mieux comprendre le ACT procédé et optimiser ses conditions de réaction, les procédés de réaction ACT sont suivis au fil du temps en utilisant la microscopie à force atomique et l'électrophorèse sur gel d'agarose. Ensuite, les conditions de réaction ACT optimisées sont utilisées dans un système de détection dendrimère-aptamère microfluidique de cellule entière pour la détection de *E. coli* O157: H7 avec des intensités de signal RCA (S-ACT). Pour améliorer encore la sensibilité de détection, un nouvel ensemble de séquences ACT pour capturer des cellules bactériennes cibles (p. ex. C-ACT) est dessiné pour produire des unités aptamères répétées en tandem (p. ex. poly-aptamères) pour des captures cibles plus efficaces. La synthèse de C-ACT in situ sur une surface interne de microcanaux est caractérisée et optimisée pour son application à la capture de cellules *E. coli* O157:H7. L'approche C-ACT montre une meilleure capacité de

capture et augmente encore les signaux de détection de fluorescence. Nos résultats indiquent que la plate-forme proposée est une méthode prometteuse pour la détection sensible et rapide des cellules bactériennes pathogènes.

Statement of contributions of collaborators

I hereby declare that I am the sole author of this thesis.

I designed the methodologies of the project and performed all the experiments and data analysis. The scientific guidance and editorial comments for the written work were provided by my supervisors Dr. Cao and Dr. Zou.

Dr. Zou helped to improve the AFM characterizations and relevant data analysis.

Other sources of assistance in academic discussion and comments will be listed as co-authors in relevant journal papers.

Acknowledgments

I would like to express my sincere appreciation to my supervisors Dr. Xudong Cao and Dr. Shan Zou for offering valuable opportunities for joining their groups in University of Ottawa and National Research Council Canada, respectively. I also appreciate their patient guidance, continued encouragement and understanding, as well as financial support during my PhD study. Both of my supervisors are mentors and friends for me not only in labs but also in life. Many thanks to them for supporting and encouraging me whenever I encountered difficulties and challenges.

I would like to acknowledge and appreciate University of Ottawa for waiving my tuitions, and China Scholarship Council for covering my living expenses.

I also would like to take the opportunity to thank professors and faculty members in our department for providing academic services, technical supports, accesses and trainings to lab equipment. Many thanks to Francine Pétrin, Sylvie Saindon, Frantz Célestin, Louis Tremblay, and Franco Ziroldo. I would like to extend my gratitude to colleagues in National Research Council for their kind supports and helps.

I would like to extend my thanks to my colleagues and friends in the department. I thank Yubo Qin and Xingkai Hao for their friendship, instruction and suggestions to my research work. I thank Zhiliang Yang for sharing his knowledge and biological techniques. I also feel lucky and grateful to have other colleagues and friends during my PhD study and they are Jian Tang, Taisa Stumpf, Zheng Dai, Zizhen Li, Shuying Li and Xiangchao Meng.

I would like to acknowledge Canadian Food Inspection Agency (CFIA) for providing bacterial samples. I also would like to acknowledge the work of undergraduate students Abenaya Murali, Ying Lin and Xun Xun Shi for their participations to this project.

Last but not least, sincere thanks to my parents who helped taking care of my little son so that I could work on my studies. I also thank my husband and my son for their love and accompanies.

Table of contents

List of figures

List of tables

Nomenclature, abbreviations and symbols

Nomenclature

AuNP	gold nanoparticle
CdSe	cadmium selenide
-COOH	carboxyl group
Fe_3O_4	iron(II,III) oxide
GO	graphene oxide
H_2O_2	hydrogen peroxide
$MgCl_2$	magnesium chloride
$-NH_2$	amino group
$NiCl_2$	nickel chloride
ZnS	zinc sulfide

Abbreviations

AFM	atomic force microscopy
AGE	agarose gel electrophoresis
APTMS	(3-aminopropyl)-trimethoxysilane
ATP	adenosine triphosphate
CFU	colony forming unit
cRCA	rolling circle amplification for capturing bacteria
Cy3	cyanine 3
DNA	deoxyribonucleic acid

dNTP	deoxynucleotide
dsDNA	double stranded deoxynucleotide
DTT	dithiothreitol
EB	ethidium bromide
E. coli	*Escherichia coli*
EDC	1-(3-dimethylaminopropyl)-3-ethylcarbodiimide
EDTA	ethylenediaminetetraacetic acid
ELISA	enzyme-linked immunosorbent assay
FITC	fluorescein isothiocyanate
F probe	fluorescence probe
GC	gas chromatography
G4	generation 4
G7	generation 7
HACCP	hazard analysis and critical control points
HRP	horseradish peroxidase
LAMP	loop mediated isothermal amplification
LC	liquid chromatography
LCR	ligase chain reaction
LOC	lab-on-a-chip
LOD	limit of detection
MMD	miniaturized microfluidic device
mPCR	multiplex polymerase chain reaction

MS	mass spectrometry
NHS	N-hydroxysuccinimide
NP	nanoparticle
PAMAM	poly(amidoamine)
PBS	phosphate-buffered saline
PC	polycarbonates
PCR	polymerase chain reaction
PDMS	polydimethyl siloxane
PET	polyethylene terephthalate
PMMA	polymethyl methacrylate
PS	polystyrene
QD	quantum dot
RCA	rolling circle amplification
RCAP	rolling circle amplification product
RNA	ribonucleic acid
SDA	strand displacement amplification
SiNP	silica nanoparticle
SELEX	systematic evolution by exponential enrichment
SPCE	screen-printed carbon electrode
SPR	surface plasmon resonance
sRCA	rolling circle amplification for signal intensification
ssDNA	single stranded deoxyribonucleic acid

TBE	tris/boric acid/EDTA
UV	ultra violet
µTAS	micro total analysis system

Symbols

a.u.	arbitrary unit
bp	base pair
°C	degree Celsius
h	hour
kbp	kilo base pair
min	minute
nt	nucleotide

Chapter 1 Introduction

Chapter 1

Introduction

1.1 General introduction

Rapid detection of foodborne pathogens and real time monitoring on food quality are of great importance to food industry. With a growing need for fresh food products from customers, fast transportation of food products is desired. Conventional methods usually take several days to obtain results of pathogen detection, which delayed the food products getting into circulation. Rapid detection of foodborne pathogenic bacteria is of great importance to the food industry and public health [1-3]. *E. coli* O157:H7 is one of the key pathogenic bacteria that is associated with foodborne illnesses, and its infective dose is estimated to be as low as 10 cells [4-6]. The typical symptom of *E. coli* O157:H7 infection is hemorrhagic colitis or bloody diarrhea [7, 8]. The food poisoning cases caused by *E. coli* O157:H7 are not as many as those caused by *Salmonella* or *Campylobacter* spp., however, they lead to more diseases and even deaths [9]. Therefore, sensitive detection of this highly threatening pathogen is a pressing issue. Currently, the most commonly used detection methods for *E. coli* O157:H7 include plate culture, enzyme-linked immunosorbent assay (ELISA) and polymerase chain reaction (PCR). Plate culture is the conventional method to detect pathogens, which takes several days to get results and involves laborious procedures [10, 11]. In comparison, ELISA and PCR are sensitive and can give fast result turn-around. However, sample pre-treatment steps such as cell enrichment and DNA extraction are often

required, significantly increasing the overall detection time [12, 13]. More sensitive and rapid detection methods have been continuously expected. Since the late 1980s, lab-on-a-chip (LOC) technique or micro total analysis system (μTAS) that offers portability, high sensitivity, low cost and reduced reagent consumption has attracted growing research interests [13-17]. The reduced size also improves the analytical performance of microfluidic devices. The potential to integrate with automated analytical modules and develop on-site detection devices further increases their research popularity. Although these newly developed detection methods have promoted more efficient and sensitive approaches for identification and to monitor pathogenic bacteria, there are still growing needs and desires for simple and sensitive detection methods.

The principle of detection in biosensors is to transduce recognition reactions (specific interaction between target and recognition element, such as antigen and antibody, or target protein and its aptamer) into readable signals; therefore strategies to improve detection sensitivities are based on enhancing recognitions between targets and sensing elements, as well as intensifying transduced detection signals. To meet this goal, recognition elements and detection signal intensifications are imperative for sensitive detections. Nucleic acid aptamers have been studied in many applications in foodborne pathogen detections due to their advantages, including ease of synthesis and modification, good reproducibility, and high sensitivity [18-23]. Aptamers are *in vitro* selected single-stranded DNA/RNA oligonucleotides that can recognize and bind to specific targets through folding into defined tertiary structures [24-26]. The selection procedure is called systematic evolution by exponential enrichment (SELEX) from DNA/RNA libraries of random sequences [25, 27].

Compared with antibodies, aptamers possess some distinct advantages including small sizes (1-2 nm), stable structures to undergo repeated denaturation and renaturation, broad detection targets and high specificities [16, 28-30]. Once selected, they can be synthesized commercially with high purity and reproducibility. Besides, it is versatile and convenient for aptamers to be chemically modified and labeled, making them easier to be functionalized with nanoparticles, microbeads or conjugated with surfaces. As a result, aptamers have been used in microfluidic devices as a substitute for antibody [31]. In addition, aptamers can be linked with a primer DNA to initiate signal amplifications, especially nucleic acid based amplifications, such as rolling circle amplification (RCA).

1.2 Thesis objectives

The overall objective of this study was to develop a simple and sensitive microfluidic device to detect foodborne pathogenic bacteria. To achieve this, there are 3 sub-objectives: (1) To modify *E. coli* O157:H7 aptamers on a previously developed dendrimer coated PDMS microchannel. As a recognition element, the immobilized aptamers are tested to specifically recognize and capture the target *E. coli* O157:H7 cells; (2) To develop a RCA signal intensification system for transducing the recognition interaction into readable signals. In addition, RCA was employed upon this dendrimer-aptamer detection system to improve the signal intensity and detection capability. By visualizing RCA products using fluorescence probes, detection signals were collected and analyzed; (3) To further improve the detection sensitivity of the established detection system. Poly-aptamers produced by cRCA reaction were employed to replace the initial monolayer aptamers modified on the dendrimer PDMS microchannel. These cRCA-aptamers containing tandem repeated

aptamers were supposed to work like long capturing arms aiming to target *E. coli* O157:H7 cells, which were combined with the initial signal intensification RCA (sRCA) to form a dual-RCA detection system for *E. coli* O157:H7 cells.

1.3 Thesis structure and scientific contributions

This thesis consists of 6 chapters: Chapter 2 is modified based on a publish review article; Chapters 3, 4 and 5 are independent original research papers, either published or submitted to peer reviewed scientific journals. Chapters 2-5 are presented using journal paper formats and are modified accordingly to achieve format consistence in this thesis. Chapter 1 is general background introduction and Chapter 6 is general discussion, conclusions, and recommendations.

The details of the thesis organization are described as followed.

Chapter 1: Introduction

A background on the field of foodborne pathogen detection and an overview on the projects in this thesis are presented. The objectives, research novelty and strategies are also outlined.

Chapter 2: Literature review

Contributions:

Published paper

Yuqian Jiang, Shan Zou, Xudong Cao*, Rapid and ultra-sensitive detection of foodborne pathogens by using miniaturized microfluidic devices: a review, Analytical Methods 8 (2016) 6668-6681. (IF 2016 = 1.9)

Chapter 3: A simple dendrimer-aptamer based microfluidic platform for *E. coli* O157:H7 detection and signal intensification by rolling circle amplification

Contributions:

Published paper

Yuqian Jiang, Shan Zou, Xudong Cao*, A simple dendrimer-aptamer based microfluidic platform for *E. coli* O157: H7 detection and signal intensification by rolling circle amplification, Sensors and Actuators B: Chemical 251 (2017) 976-984. (IF 2016 = 5.4)

Submitted manuscript

Xingkai Hao, Po Ying Yeh, Yubo Qin, **Yuqian Jiang**, Zhenyu Qiu, Xudong Cao*, Aptamer surface functionalization of microfluidic devices via dendrimers as multi-handled templates and its application in sensitive detections of foodborne pathogenic bacteria, submitted.

Poster competition

Yuqian Jiang, Xingkai Hao, Zheng Dai, Xudong Cao*, Effective detection of foodborne pathogen using PAMAM dendrimer and aptamer coated microfluidic channel. Faculty's

7th Edition of the Engineering and Computer Science Poster Competition, 2nd prize was awarded.

Chapter 4: A study on rolling circle amplification and its signal enhancement in a dendrimer-PDMS microfluidic detection system

Contributions:

Submitted manuscript

Yuqian Jiang, Zhenyu Qiu, Tao Le, Shan Zou, Xudong Cao*, A study on rolling circle amplification and its signal enhancing application in a dendrimer-PDMS microfluidic system, submitted.

Conference presentation

Yuqian Jiang, Shan Zou, Xudong Cao*, A study on rolling circle amplification and its signal enhancing application in a dendrimer-PDMS microfluidic system. 67th Canadian Chemical Engineering Conference, Oct. 22-25, Edmonton.

Chapter 5: Developing a dual-RCA aptamer-based microfluidic platform for sensitive whole-cell detection of *E. coli* O157:H7

Contributions:

Submitted manuscript

Yuqian Jiang, Shan Zou, Xudong Cao*. Developing a dual-RCA aptamer-based microfluidic platform for sensitive whole-cell detection of *E. coli* O157:H7. In preparation of submission.

Chapter 6: Discussion and conclusion

An overall summary and conclusions are included. Recommendations for further work based on the presented work in this thesis are discussed.

1.4 References

1. Scallan, E., et al., *Foodborne Illness Acquired in the United States—Major Pathogens.* Emerging Infectious Diseases, 2011. **17**(1): p. 7-15.
2. Tauxe, R.V., *Emerging foodborne pathogens.* International Journal of Food Microbiology, 2002. **78**(1): p. 31-41.
3. Painter, J.A., et al., *Attribution of foodborne illnesses, hospitalizations, and deaths to food commodities by using outbreak data, United States, 1998–2008.* Emerging Infectious Diseases, 2013. **19**(3): p. 407.
4. Jalalpour, S., *Food borne diseases bacteria; frequency antibiotic resistance bacteria in Iranian foods.* African Journal of Microbiol Research, 2012. **6**(4): p. 719-723.
5. Sharma, H. and R. Mutharasan, *Review of biosensors for foodborne pathogens and toxins.* Sensors and Actuators B: Chemical, 2013. **183**: p. 535-549.
6. Radke, S.M. and E.C. Alocilja, *A high density microelectrode array biosensor for detection of E. coli O157: H7.* Biosensors and Bioelectronics, 2005. **20**(8): p. 1662-1667.
7. Griffin, P.M. and R.V. Tauxe, *The epidemiology of infections caused by Escherichia coli O157: H7, other enterohemorrhagic E. coli, and the associated hemolytic uremic syndrome.* Epidemiologic Reviews, 1991. **13**(1): p. 60-98.
8. Carter, A.O., et al., *A severe outbreak of Escherichia coli O157: H7–associated hemorrhagic colitis in a nursing home.* New England Journal of Medicine, 1987. **317**(24): p. 1496-1500.

9. Lim, J.Y., J.W. Yoon, and C.J. Hovde, *A brief overview of Escherichia coli O157: H7 and its plasmid O157.* Journal of Microbiology and Biotechnology, 2010. **20**(1): p. 5.
10. Gracias, K.S. and J.L. McKillip, *A review of conventional detection and enumeration methods for pathogenic bacteria in food.* Canadian Journal of Microbiology, 2004. **50**(11): p. 883-890.
11. de Boer, E. and R.R. Beumer, *Methodology for detection and typing of foodborne microorganisms.* International Journal of Food Microbiology, 1999. **50**(1): p. 119-130.
12. Lazcka, O., F.J. Del Campo, and F.X. Munoz, *Pathogen detection: a perspective of traditional methods and biosensors.* Biosensors and Bioelectronics, 2007. **22**(7): p. 1205-1217.
13. Jiang, Y., S. Zou, and X. Cao, *Rapid and ultra-sensitive detection of foodborne pathogens by miniaturized microfluidic devices: a review.* Analytical Methods, 2016. **8**(37): p. 6668-6681.
14. Chin, C.D., V. Linder, and S.K. Sia, *Lab-on-a-chip devices for global health: Past studies and future opportunities.* Lab on a Chip, 2007. **7**(1): p. 41-57.
15. Yoon, J.Y. and B. Kim, *Lab-on-a-chip pathogen sensors for food safety.* Sensors, 2012. **12**(8): p. 10713-10741.
16. Mairhofer, J., K. Roppert, and P. Ertl, *Microfluidic systems for pathogen sensing: a review.* Sensors, 2009. **9**(6): p. 4804-4823.
17. Foudeh, A.M., et al., *Microfluidic designs and techniques using lab-on-a-chip devices for pathogen detection for point-of-care diagnostics.* Lab on a Chip, 2012. **12**(18): p. 3249-3266.
18. Lee, H.J., et al., *A sensitive method to detect Escherichia coli based on immunomagnetic separation and real-time PCR amplification of aptamers.* Biosensors and Bioelectronics, 2009. **24**(12): p. 3550-3555.
19. Queirós, R.B., et al., *A label-free DNA aptamer-based impedance biosensor for the detection of E. coli outer membrane proteins.* Sensors and Actuators B: Chemical, 2013. **181**: p. 766-772.
20. Wu, W., et al., *A sensitive lateral flow biosensor for Escherichia coli O157: H7 detection based on aptamer mediated strand displacement amplification.* Analytica Chimica Acta, 2015. **861**: p. 62-68.
21. Ma, X., et al., *An aptamer-based electrochemical biosensor for the detection of Salmonella.* Journal of Microbiological Methods, 2014. **98**: p. 94-98.

22. Fang, Z., et al., *Lateral flow biosensor for DNA extraction-free detection of salmonella based on aptamer mediated strand displacement amplification.* Biosensors and Bioelectronics, 2014. **56**: p. 192-197.
23. Yuan, J., et al., *A visual detection method for Salmonella typhimurium based on aptamer recognition and nanogold labeling.* Food Control, 2014. **37**: p. 188-192.
24. Zhou, W., et al., *Aptamer-based biosensors for biomedical diagnostics.* Analyst, 2014. **139**(11): p. 2627-2640.
25. Nutiu, R. and Y. Li, *Structure-switching signaling aptamers.* Journal of the American Chemical Society, 2003. **125**(16): p. 4771-4778.
26. Cho, E.J., J.W. Lee, and A.D. Ellington, *Applications of aptamers as sensors.* Annual Review of Analytical Chemistry, 2009. **2**: p. 241-264.
27. Schachermeyer, S., J. Ashby, and W. Zhong, *Aptamer-Protein Binding Detected by Asymmetric Flow Field Flow Fractionation.* Journal of Chromatography A, 2013. **1295**: p.107-113.
28. Torres-Chavolla, E. and E.C. Alocilja, *Aptasensors for detection of microbial and viral pathogens.* Biosensors and Bioelectronics, 2009. **24**(11): p. 3175-3182.
29. Binning, J.M., D.W. Leung, and G.K. Amarasinghe, *Aptamers in virology: recent advances and challenges.* Frontiers in Microbiology, 2012. **3**: p. 29.
30. Georgianna, W.E. and D.D. Young, *Development and utilization of non-coding RNA–small molecule interactions.* Organic & Biomolecular Chemistry, 2011. **9**(23): p. 7969-7978.
31. Toh, S.Y., et al., *Aptamers as a replacement for antibodies in enzyme-linked immunosorbent assay.* Biosensors and Bioelectronics, 2015. **64**: p. 392-403.

Chapter 2 Literature review

Chapter 2

Literature review

Rapid and ultra-sensitive detection of foodborne pathogens by miniaturized microfluidic devices

Yuqian Jiang, Shan Zou, Xudong Cao

The following chapter mainly consists of the paper entitled *Rapid and ultra-sensitive detection of foodborne pathogens by using miniaturized microfluidic devices: a review*, published in Analytical Methods. Authors of this review article include Yuqian Jiang, Shan Zou and Xudong Cao. Formatting and minor modification (such as figure number and labels) were made on the published version and a new section (2.5) on fabrication and modification of minimized microfluidic PDMS devices was added to provide information on materials and techniques commonly used in the detection systems which are also closely relevant to my work in this thesis.

A literature review on rapid and sensitive detection methods based on miniaturized microfluidic devices to detect foodborne pathogenic bacteria were presented in this chapter. Detection principles, features of detection methods, and techniques or strategies for facilitating ultra-sensitive detection were discussed. In addition, emphasis was put on

microfluidic detection conducted on the miniaturized devices with excellent detection performance reported in the most recent years.

Abstract

Identification and quantification of foodborne pathogens is becoming increasingly important to public health and food safety since pathogenic bacteria cause a large amount of foodborne illnesses and even deaths. Conventional methods for foodborne pathogen detection are time-consuming and laborious due to the requirement of a series of processes including cell enrichment, isolation and biochemical identification. Therefore the demand for rapid, sensitive, inexpensive and convenient approaches to detect foodborne pathogenic bacteria has emerged in recent years. Among those new approaches, microfluidic chip-based detection has generated growing interests because of their miniaturized size, improved sensitivity and reduced detection time. In addition, the application of nanomaterials and magnetic microbeads has further facilitated target recognition and signal transduction processes in microfluidic pathogen detections. The lab-on-a-chip technique has developed into an alternative to conventional methods to detect foodborne pathogens owing to its potential to offer desired sensitivity and to respond in a short test time. Most recently, smartphones and 3-D printing technologies are attracting growing attentions for enhanced detection performance. This paper reviews the most recent development and trend of miniaturized microfluidic devices based on different recognition principles and signal amplification methods to detect foodborne pathogens. In particular, emphasis will be put on those that offer both rapid detection result turn-around and ultra-low detection limit of 10^2 - 10^3 cells/mL or even single-cell detection.

Keywords: Food safety; Bacteria detection; Microfluidic devices; Signal amplification; Biosensor; Lab on a chip; Single-cell detection.

2.1 Introduction

Food safety is one of the major concerns to public health. It is estimated that there are nearly 76 million cases of foodborne illness in the US annually, resulting in more than 300,000 hospitalizations and 5,000 deaths every year [1-3]. Food safety greatly depends on rapid and sensitive detection of harmful agents, such as pathogens, viruses and toxins, which could be brought into the food chain at any point during procedures such as food production, transportation, processing, storage, retailing, and handling [4, 5]. To monitor food safety and regulate food hygiene, Hazard Analysis and Critical Control Points (HACCP) programs have been implemented to critically control potential contamination points during food processing. This has significantly improved our food safety [6, 7]. However, there are still millions of people around the world facing illnesses caused by food [8]. While food poisoning and foodborne illness can be caused by harmful chemicals, heavy metals, parasites, fungi, viruses and bacteria. In the US, the bacteria related food poisoning cases are mostly caused by *Salmonella*, Norovirus (Norwalk Virus), *Campylobacter*, *E. coli*, *Listeria*, *Clostridium perfringens* [9]. Unfortunately, conventional methods for foodborne pathogen detection - generally involving multiple laborious steps - take up to several days to get results, demonstrating an unmet need for rapid and sensitive detection of foodborne pathogens [6, 10-12].

To solve this problem, several alternative detection methods have been developed. For instance, liquid or gas chromatography (LC or GC) in combination with mass spectrometry (MS) have been used to detect *E. coli* O157:H7 and *Salmonella typhimurium* by ways of analyzing their metabolites [13]. The main problem of this approach is the requirement of

sophisticated instruments and highly trained personnel, making it inappropriate or even impossible to be applied as a routine method for pathogen detection and monitoring. Immunoassays such as enzyme-linked immunosorbent assay (ELISA), and nucleic acid technologies such as polymerase chain reaction (PCR) have also been used in an attempt to rapidly detect foodborne pathogens with high sensitivities [14-16]. Table 2-1 summarizes assays commonly used to detect foodborne pathogens, their limits of detection (LODs), and overall detection time when pre-enrichment samples are considered. It should be mentioned that while molecular detections are highly specific and sensitive, they still require pre-enrichment steps that account for most of the overall detection time (see pre-enrichment time vs. detection time shown in Table 2-1). As indicated in Table 2-1, microchip-based biosensors offer better sensitivity and shorter response time in detection, although the need for prior cultural enrichment is still debatable.

Table 2-1 Detection of pathogenic bacteria in water or food matrix by different methods

Method	Pathogen	Sample type	Limit of detection (LOD)	Pre-enrichment time	Detection time	Ref.
Plate culture	*E. coli* O157: H7	Apple cider	10^5 CFU/mL	48 - 72 h	--	[17]
PCR	E. coli O157	Water	1 CFU/mL	16 - 20 h	~ 3 h	[18]
PCR-ELISA	*E. coli*	Milk	10^2 CFU/mL	16 h	~ 4 h	[19]
ELISA	*E. coli* O157	Cultures from food	~ 10^3 CFU/mL	24 h	~ 4 h	[20]
ELISA	*Shigella dysenteriae*	Buffer and chicken carcass wash	~ 10^4 CFU/mL	48 h	~ 4 h	[21]
PCR-ELISA	*Salmonella* spp.	Milk and meat sample	10^3 CFU/mL	18 h	~ 5 h	[22]
Immune-based microchip	*E. coli*	Milk	50 CFU/mL	16 h	~ 3 h	[23]
Fiber optic biosensor	*Listeria*, *E. coli* O157:H7, *Salmonella*	Ready-to-eat meat samples	~ 10^3 CFU/mL Each	24 h	~ 2 h	[24]
Aptamer based biosensor	*E. coli* O157:H7	Bacteria in PBS buffer	10 CFU/mL	16 h	~ 1.5 h	[25]

While these new techniques offer significant improvements for detecting foodborne pathogens, they also leave much more to be desired. Restrictive regulations have been implemented as some diseases caused by foodborne pathogens or their toxins happen at

very low doses. For example, in Canada, the acceptable limit of *Listeria monocytogenes* in ready-to-eat food is 100 CFU/g (colony forming unit), while it is zero-tolerance for infants or people with special medical conditions [26]. Another example is that the infective dose of *E. coli* O157:H7 is estimated to be as low as 10 cells [27, 28]. Therefore, it is critically important to be able to detect foodborne pathogenic bacteria at low concentrations to safeguard food safety and ensure timely response to outbreaks.

Miniaturized microfluidic devices (MMDs) - also known as lab-on-a-chip (LOC) or micro total analysis system (μTAS) - emerged in the 1990s [29]. It has been demonstrated that the microfluidic technology can integrate multiple operations and parallel identifications on a single miniaturized device with high throughput analysis [30]. In the past decades, growing research efforts have been focused on the detection of foodborne pathogens using microfluidic approaches [8, 29, 31-33]. In this paper, we will review detection principles and characteristics of MMDs in terms of their recognition and signal amplification mechanisms. It includes most recent studies and new trends in MMD designs with outstanding performance at ultra-low detection limits and short detection time. In addition, challenges and potential opportunities for developments of these microfluidic devices for the detection of foodborne pathogens will also be discussed.

2.2 Working principles of microfluidic detection

Microfluidic sensing systems can be divided into different categories according to their working mechanisms, recognition process, and signal transduction. The general recognition process takes place after samples are introduced into the detection system and

this can be summarized into two steps: 1) target bacteria contained in samples are identified by the recognition elements via bio-specific interactions; and 2) the bio-specific interactions subsequently induce changes via biochemical reactions that can be transmitted into readable signals [34]. Figure 2-1 is a brief illustration of the detection of foodborne pathogens by bio-sensing devices. As the food matrix is very complex, depending on the characteristics of food samples, several sample preparation steps are needed to treat the food samples before the bio-recognition process. In target identification, common interactions between targets and recognition elements include antibody/antigen, enzyme/substrate, DNA or RNA/their complementary sequences, and aptamers or bacteriophages/whole bacterial cells [8, 32, 35]. Readable electrochemical or optical signals can be transduced from bio-specific interactions by signal modules or external instruments.

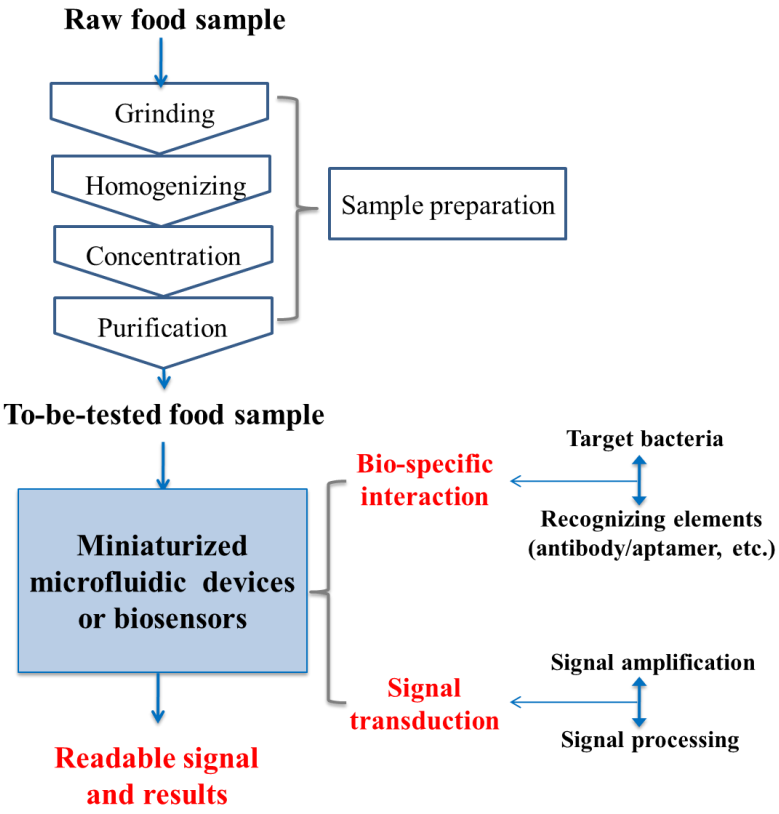

Figure 2-1 Flowchart of general food sample preparation and main steps involved to detect foodborne pathogens by bio-sensing systems.

2.3 Recognition and identification

2.3.1 Antibody based detection

Among all recognition principles, specific interactions between antibodies and antigens are the most widely used recognition mechanism [34, 36, 37]. Antibody/antigen based immunoassay can achieve rapid detection of foodborne pathogens because of direct recognitions between antibodies and whole cells, avoiding target lysis steps to extract DNA or RNA products [38]. In general, the LOD of antibody-based MMDs is reported to be

~100 CFU/mL (or higher) [39]. While antibodies can be readily obtained nowadays, the batch-to-batch variability, the possibility of cross-reactions when targets are closely related, and the inability to distinguish viable from nonviable bacteria are some of the main drawbacks associated with using antibodies/antigen interactions as the recognition mechanisim [40]. Using antibody based lateral flow immunoassay, Cho et al. recently described detection of *E. coli* O157:H7 with a LOD of 10^2 CFU/mL, which was completed within 15 min [41]. Most microfluidic device based assays for foodborne pathogen detection employing antibody-antigen recognition mechanism have reported LODs ranging from 10^0 to 10^3 CFU/mL [42-50].

2.3.2 Nucleic acid based detection

Nucleic acids (DNA or RNA molecules) have been used as specific and sensitive recognition elements to identify foodborne pathogens via specific sequence base-pairing interactions. Typically, complementary nucleic acid probes modified with fluorescent dyes are used to generate readable signals [40]. While this type of identification is of great specificity and accuracy, the requirement for cell lysis and enrichment of DNA fragments makes the whole detection process time consuming. Recently, a special type of nucleic acid molecules called aptamers, which are single-stranded DNA or RNA oligonucleotides that form their own complex or structures, have emerged and attracted growing attention [51, 52]. Compared with nucleic acid base-pairing hybridization, the most outstanding advantage of aptamers is that they can recognize specific surface proteins on bacteria as whole cells without cell lysis and DNA extraction [53]. Aptamers are selected through a cyclic process named systematic evolution by exponential enrichment (SELEX) from

DNA/RNA libraries of random sequences. They have been produced with binding specificity to many different targets [54, 55]. They can recognize specific targets through folding into defined tertiary structures with high affinity [56, 57]. Once selected, they can be synthesized with high purity and reproducibility. Nucleic acids have stable structures to undergo repeated denaturation and renaturation cycles. When applied in MMDs, nucleic acid aptamers are versatile and can be chemically immobilized onto nanoparticles, microbeads or substrates [58]. To date, nucleic acid based microfluidic detection systems have been reported to achieve LOD ranging from 2 CFU/mL to 10^2 CFU/mL [59-64].

2.3.3 Bacteriophage based detection

As an alternative recognition element, bacteriophages have also attracted much research attention for foodborne pathogen detection [65-70]. Bacteriophages are viruses that can bind to and infect host bacteria by injecting their DNA into the host bacteria followed by their efficient replication. The use of bacteriophages has two advantages: 1) high specificity to target bacteria: the specific phages can be selected from phage libraries and used to recognize particular bacteria via certain proteins, lipids and sugars of bacterial cells [71]; and 2) infection of only live bacterial cells: bacteriophages are able to discriminate viable from nonviable bacterial cells and only infect live cells. As viruses, bacteriophages are inexpensive with long shelf life [67, 72]. Furthermore, genetic modifications of phages can be carried out to allow incorporation of reporter genes, which can be expressed to produce detectable signals to characterize the existence of the target bacterial cells [71]. Bacteriophages have been used to detect foodborne pathogens such as *Staphylococcus*

aureus and *E. coli* O157:H7, and the LODs are reported to be 10^1 - 10^4 CFU/mL [66, 73-75].

As each different detection mechanism is more suitable for specific sample conditions (*i.e.* whole cells vs. cell lysis) and detection requirements (*i.e.* live cell vs. dead cell detection), all three detection mechanisms have applicability for use in microfluidic devices.

2.4 Signal transduction and amplification

The common goal of signal transduction is to convert specific biochemical reactions into readable signals to qualify or quantify the target bacteria. Those signals are usually electric, thermometric, piezoelectric, magnetic, micromechanical, photonic, or optical, and can be transduced by techniques such as surface plasmon resonance (SPR), surface acoustic wave, fluorescence/phosphorescence spectrometry and bio-/chem-iluminescence [76]. The transduced signals are then detected by spectrophotometers or fluorescence microscopes, which are often connected to computers to further process the signals when necessary [39, 77]. In order to achieve ultra-high detection sensitivity, additional signal amplifications are often required. Currently three methods are commonly employed in MMDs to amplify detection signals. These are nucleic acid amplification, nano-scale particles, and magnetic microbeads.

2.4.1 Nucleic acid amplification

As mentioned above, nucleic acids are being used as a type of recognition elements to identify target bacteria. Moreover, they can be replicated by nucleic acid polymerases

based on designed templates, which can be applied to enhance detection signals. This signal enhancing mechanism has been used in many applications, such as polymerase chain reaction (PCR), ligase chain reaction (LCR), strand displacement amplification (SDA), rolling circle amplification (RCA), and loop mediated isothermal amplification (LAMP) [32]. For example, PCR is widely used to amplify target nucleic acids with very high sensitivity, but it always requires incubation, cell lysis and multiple purification steps to obtain target DNA or RNA; in addition, thermal cyclers are required to achieve exponential amplification of target DNA [78-80]. Recently, isothermal amplification methods, such as RCA and LAMP, have attracted growing attention due to their high efficiencies and isothermal temperature requirements [81, 82]. As shown in Figure 2-2A, RCA products are long single stranded DNAs or RNAs containing repeated sequences that are propagated based on a circular template. Once the RCA products are generated, they can be readily visualized by complementary probes modified with fluorophores that will give off fluorescent signals for detection. It is evident that the detection method shown in Figure 2-2B (rolling circle amplification) binds significantly more fluorescent probes than a method without rolling circle amplification, as shown in Figure 2-2C. Nucleic acid-based amplification approaches are often combined with both aptamer and antibody recognition steps. For instance, Fischer *et al.* described a method in which amplifiable DNA sequences (including primer) were incorporated into an aptamer to obtain bio-readout ability [83]. An aptamer was used to recognize the target while the primer was used for the RCA reaction, respectively. Nucleic acid-based signal amplification approaches can also be incorporated into antibody based detection system [84-86]. In a study by Schweitzer *et al*., an antibody was conjugated with a 5’ thiol oligonucleotide that contained a primer for RCA, and the

RCA products were detected by hybridization with fluorescently labeled oligonucleotides. By using this immuno-RCA system, the immunoassay sensitivity was enhanced by more than two orders of magnitude when compared with conventional immunoassays [85].

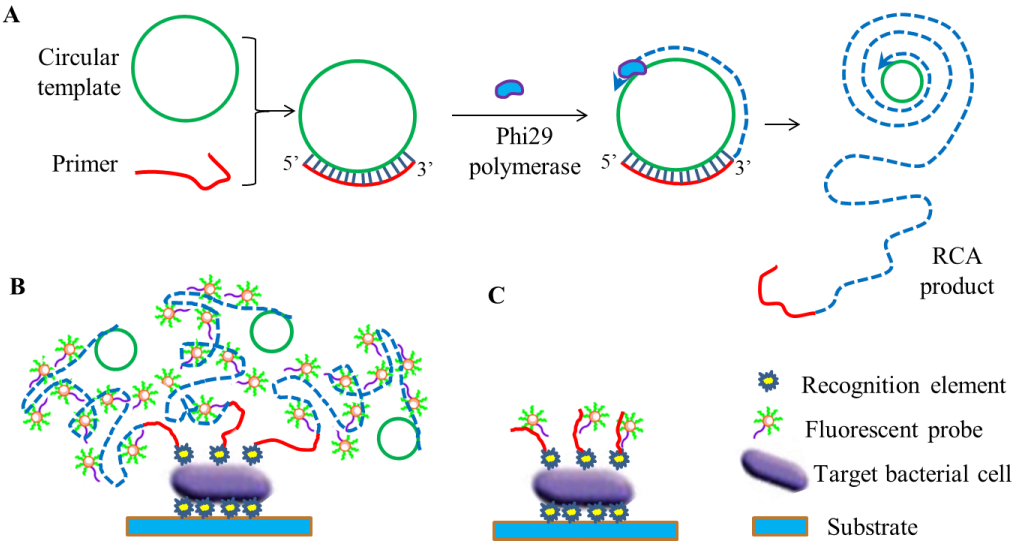

Figure 2-2 Signal amplification of RCA in detection system: A. working principle of RCA; B. detection by fluorescent probes with RCA amplifications - with signal enhancement; and C. detection by fluorescent probes without RCA amplifications - no signal enhancement

Similarly, LAMP has also been widely used in microfluidic devices for signal amplification. In comparison with RCA, LAMP amplifies DNA sequences utilizing several specific primers [87, 88]. For example, Sayad *et al.* developed a lab-on-a-disc microfluidic device to detect *Salmonella* using LAMP amplification [89]. This portable device successfully integrated sample preparation and detection on a microfluidic disc and achieved a detection limit of 5 pg/µl DNA from *Salmonella*. Notably, the whole procedure was completely

automated, and the detection was completed within 70 min. Using a lab-on-a-chip system, Sun *et al*. reported detection of *Salmonella* at a LOD of 10^3 cells/ml when the signal was amplified using LAMP [90]. Interestingly, LAMP was also used to detect *Listeria monocytogenes* on food contact surfaces with an impressive reported lower LOD of 1 CFU/100 cm^2 [91]. Besides RCA and LAMP, other isothermal DNA amplification techniques have also been used in microfluidic systems to assist bacterial cell detection or DNA detection [87].

2.4.2 Nanoparticles

Developments in optoelectronics and electromechanical technology have facilitated bio-recognition and signal transduction at the nanometer scale [34]. By virtue of their unique physical, optical and electrical properties, nanomaterials are increasingly utilized to significantly improve detection sensitivities [31, 92, 93]. For example, nanoparticles (NPs) possess better fluorescence properties than traditional organic fluorophores, facilitating signal transduction and intensifying signals in MMDs [31]. It has been reported that a variety of NPs, such as gold and silver NPs, quantum dots (QDs), and magnetic NPs have been used in bacterial detection to enhance both detection signals and detection sensitivities [8, 94-99]. For instance, semiconductor QDs (CdSe core with ZnS shell) were used in a fluorometric assay in combination with antibodies to capture *E. coli* O157:H7 cells. This biosensor exhibited two orders of magnitude in sensitivity (LOD is 2.3 CFU/mL) compared to that using a traditional organic dye [100]. In addition, Rotem *et al*. reported a method to detect bacteria using a QD modified bacteriophage. The researchers showed a LOD of 10 cells/mL, which had a signal intensity of about 100-fold above the background signal [101].

Additionally, nanomaterials can be used to simplify detection procedures. Zuo *et al*. conducted an excellent piece of work by incorporating graphene oxide (GO) and aptamer into a microfluidic system [102]. As shown in Figure 2-3, the inner surface of the microfluidic channels was functionalized with GO and fluorophore modified aptamers. In the absence of targets, the fluorescence was quenched as the aptamers were physically adsorbed on the surface of the GO. However when the target pathogens were present, aptamers were released from the GO surface and specifically bound to the the target pathogens. The binding event resulted in re-appearance of fluorescence, indicating the existence of target pathogens (Figure 2-3B). By virtue of switching the fluorescent properties of the surface on and off, the use of GO enabled a simple one-step detection of multiple pathogens. This device was reported to have a LOD of 11 CFU/mL using *Lactobacillus acidophilus* as a model bacterium [102]. It is also worth noting that the detection only took about 10 min to complete.

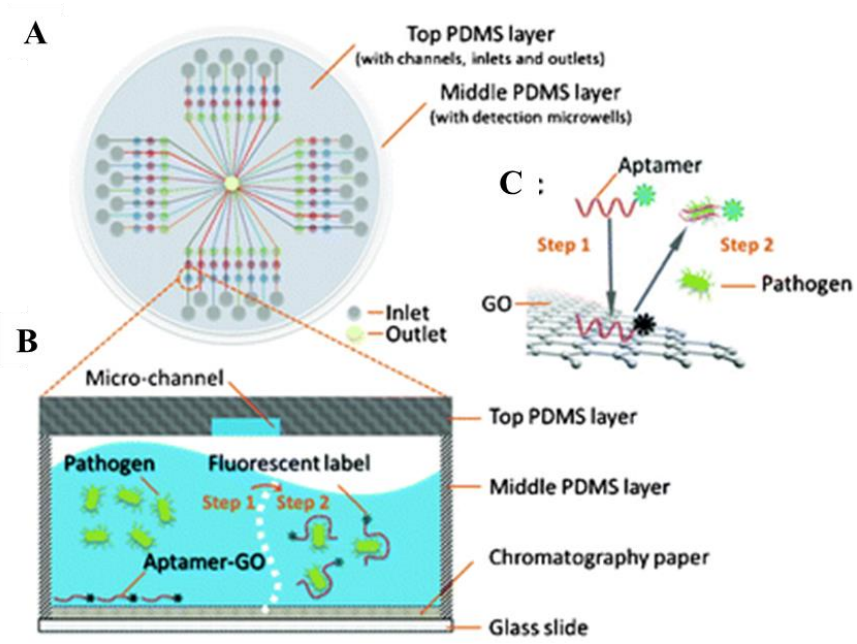

Figure 2-3 Schematic illustration of PDMS/paper hybrid microfluidic biosensor functionalized by aptamer and GO for detection of multiple pathogens: A. overall view of PDMS microfluidic device design; B. modification of microchannel and target pathogen capture by aptamer-GO; C. illustration of fluorescence signal "on" and "off" states: fluorescence on the aptamer is quenched by GO (off) and the fluorescence is restored after target pathogen binds to aptamer and liberates aptamer from the GO surface (on). Figures were adapted from Ref. [102] with permission from The Royal Society of Chemistry.

Nanomaterials have facilitated the development of biosensors and significantly improved the development of miniaturized microfluidic detection. Indeed, various functions of NPs in microfluidic detection have been exploited in recent years. Generally, modified NPs help to recognize, capture and concentrate bacterial cells in samples [103-105]. While the application of nanomaterials in MMDs is still in its infancy, it certainly has a promising outlook in the detection of foodborne pathogens.

2.4.3 Magnetic microbeads

Magnetic microbeads, similar to nanoparticles, have large surface-to-volume ratios; in addition, their magnetic properties can be utilized to simplify detection procedures and to enhance detection signals. The surface of magnetic microbeads can be functionalized with recognition elements while the magnetic property allows the microbeads to be conveniently manipulated by externally applied magnetic fields. Therefore, magnetic microbeads have been used in various steps in lab-on-a-chip detections, including fluid mixing, analyte labelling and capturing, and immuno-magnetic separation [106-108]. For example, Qiu *et al.* used microbeads (1 - 5 μm in diameter) modified with antibodies to capture and separate target bacteria from background particles using an externally applied magnetic field without any centrifugation or filtration, as shown in Figure 2-4A [109]. This process also enriched target cells in suspension, therefore enabling detection of low target concentration in samples. In another study by Ozalp and colleagues, a quartz crystal microbalance sensor was developed to detect *Salmonella* cells in food samples, which was assisted by magnetic bead separation [110]. As shown in Figure 2-4B, the magnetic beads were functionalized with an aptamer specific to *Salmonella*. This enabled *Salmonella* cell capture on the aptamer-functionalized magnetic bead surfaces, achieving rapid enrichment of target *Salmonella* cells in less than 10 min and ultimate detection of *Salmonella* cells at a LOD of 100 CFU/mL in milk samples. Similar approaches have been used to modify microbeads with appropriate antibodies for foodborne pathogen detection with high specificities and sensitivities [111, 112]. It is interesting to note that while most of the studies employed magnetic microbeads modified with antibodies or aptamers for foodborne pathogen capture

and subsequent separation, smaller sized particles, such as sub-micron-sized particles and nano-sized particles have also been reported in the literature [113]. For example, in a recent study, Zhu *et al.* used a Fe_3O_4/Vancomycin/PEG magnetic nanocarrier with diameters 100 - 200 nm to efficiently enrich *Listeria monocytogenes* samples, and used an electrochemiluminescence based DNA sensor to detect the bacterial cells at a LOD as low as 10 CFU/mL [114].

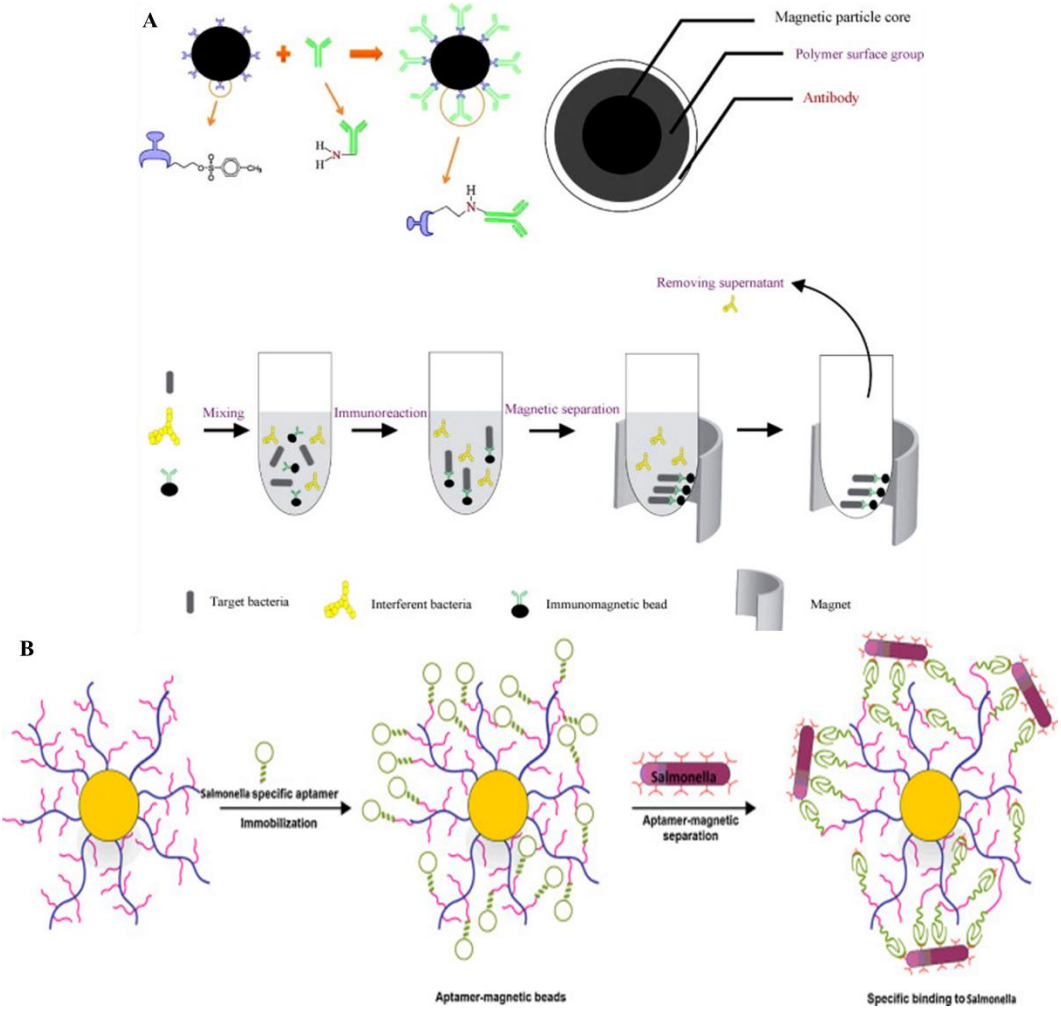

Figure 2-4 Schematic illustration of magnetic separation and concentration of samples. A. Immunomagnetic separation and concentration of target bacteria using magnetic

microbeads modified with antibodies. Reprinted from Ref. [109], Copyright (2009), with permission from Elsevier; B. An aptamer-based detection for *Salmonalla* using magnetic microbeads to concentrate samples. Reprinted from Ref. [110], Copyright (2014), with permission from Elsevier.

2.5 Fabrication and modification of PDMS devices

2.5.1 Polymeric materials

In comparison with glass and silicon, polymeric substrates have been favored to fabricate microfluidic devices due to the advantages of low cost, high chemical resistance and excellent optical properties [115]. The most commonly used polymeric materials in device fabrication include polymethyl methacrylate (PMMA), polydimethyl siloxane (PDMS), Polycarbonates (PC), polystyrene (PS), and polyethylene terephthalate (PET) [116]. PDMS is one of the most commonly developed polymers for microfluidic device fabrication with merits of ease to use, low cost, flexibility, optical transparency, low toxicity and chemically stable properties. PDMS is capable to fabricate structures at microscale (sub-0.1-μm) levels with very low shrinkage rates, making it a good stamp resin for soft lithography [117]. PDMS microfluidic channels have been extensively employed in various microfluidic devices. Applications of PDMS fabricated microfluidic devices include biochemical assays [118-121], detection of pathogens [122-124], cell culture and enrichment [125-127], cell analysis and sorting [128-132], fluid flow control [133, 134], microfluidic mixing [135, 136], etc.

2.5.2 Photolithography and soft lithography

Soft lithography is a technique to construct structures using elastomeric stamps, molds and conformable photomasks on micro- or even nano- scale. This technique has been extensively used in fields of biomedical diagnosis, analysis and detection [137, 138]. PDMS devices are commonly fabricated by soft lithography [139, 140]. A master (or mold), usually made of silicon wafer with desired channel structures, is generally produced by photolithography techniques (Figure 2-5A). Briefly, negative photoresist such as SU-8 is spin-coated on a substrate silicon wafer (step i in Figure 2-5A). A photomask with designed structures is layered on the negative photoresist and exposed to UV light (step ii in Figure 2-5A) to form a protruding part which will be the major straight and plain channel structure by etching and striping (step iii in Figure 2-5A). Subsequently, the developed master is used to mold PDMS for fabricating a microfluidic device. This process can be briefly summarized as 3 steps shown in Figure 2-5B. Step (i): deposit the mixture of PDMS monomer (base) and cross-linker agent (curing agent) onto the master; step (ii): cure the PDMS mold by heating and release the hardened PDMS from the master; and step (iii): cut the PDMS stamp and create access ports before bonding to a glass slide by O_2 plasma treatment.

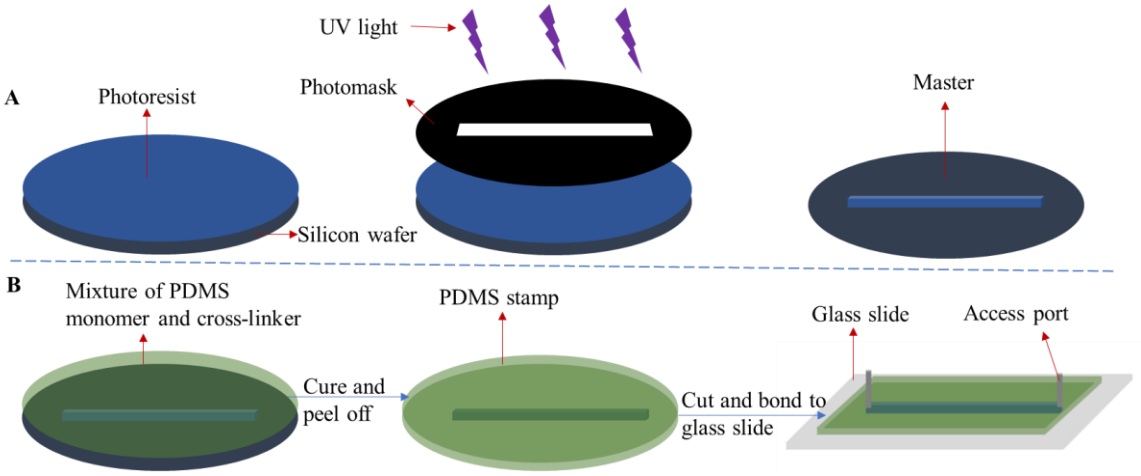

Figure 2-5 Schemes for soft lithography. A. master fabrication process; B. PDMS microfluidic device assembling.

2.5.3 PAMAM dendrimer

Dendrimers are highly branched polymers of ideally symmetric skeletal structure and a unique molar mass [141]. Synthesis of dendrimers started in the 1970s and has become a major research focus since the late 1980s [141, 142]. Dendrimers possess many unique properties such as ease of dissolution, low viscosity and non-crystallization [143]. The poly(amidoamine) (PAMAM) dendrimer family has been studied extensively, which is well synthesized, characterized and commercialized [144, 145]. The molecular structure of PAMAM dendrimers is shown in Figure 2-6. Divergent methods have been used to synthesize PAMAM dendrimer, where branch cell multiplicity initiates from a central core and forms concentric shells (generations) [141]. As the core-shell architecture grows (generation number increases), PAMAM dendrimers become globular in shape and the surface groups exponentially increase [145]. From generation 1 to 7, the surface functional

groups increase from 4 to 512 (Figure 2-6). Those surface functional groups can be modified to link with a variety of molecules via chemical linkage, hydrogen bond, or hydrophobic interaction [146, 147] for different applications, such as sensing [148-150], drug delivery [151, 152] and gene transportation [153, 154]. Specifically, as a type of polymeric nanoparticles, PAMAM dendrimers have been applied to reduce non-specific binding and enhance detection sensitivity in detection systems for proteins, nucleic acids, pathogens and other chemicals [155, 156]. In a study by Chang and colleagues, PAMAM dendrimer (G4, 64 surface functional groups) and SYTOX Green dye were employed to construct a sensing film for detection of *Pseudomonas aeruginosa* [157]. As a result, PAMAM dendrimer enhanced the fluorescence intensity of the sensing system by 350%. In another work reported by Ji *et al*., PAMAM dendrimer films (G4) were used for cell capture and collection in an optical sensor, where the dendrimer worked as an adhesive element to capture bacteria (this was semi-selective sensor, not specific to one type of bacteria) [158]. The sensitivity of the sensor was dramatically increased in flowing water and achieved a LOD of 10^4 cells/ml.

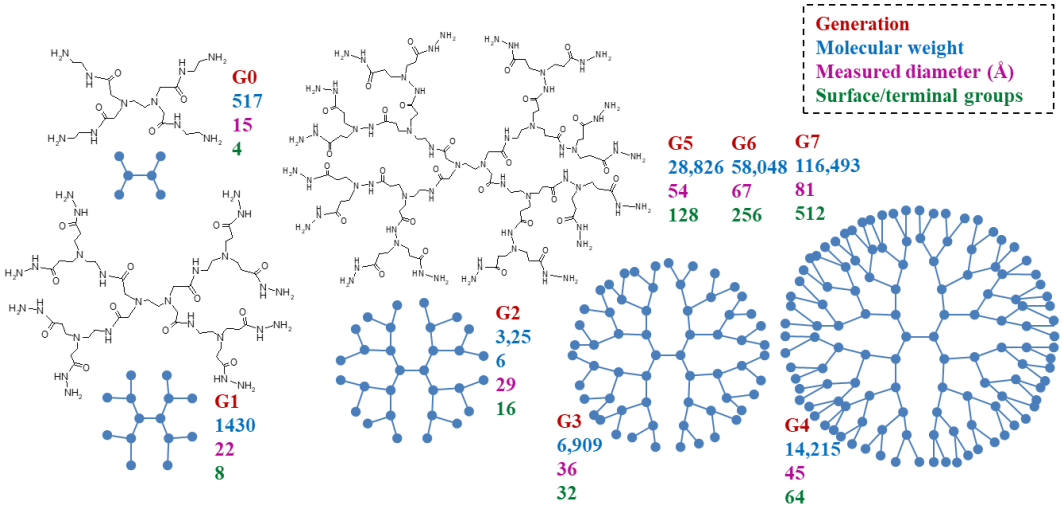

Figure 2-6 Structure of PAMAM dendrimers and their generation comparison.

2.6 Different types of microfluidic systems for rapid and ultra-sensitive detection methods

Miniaturized microfluidic devices include a wide variety of devices of different appearance and with different structures, and most of them are based on lateral flow devices and microfluidic channels. Those devices are designed to be portable and cost-effective with outstanding benefits of high sensitivity and rapid speed. In this section, we categorize MMDs -- according to their structures and functions -- into test strips (*i.e.* lateral flow testing) and microfluidic channels. Furthermore, we will discuss the most recent platforms for detection of foodborne pathogens in several hours with a LOD below 10^3 cells/mL.

2.6.1 Test strips or lateral flow biosensing systems

Test strips or lateral-flow tests have been successfully developed since the 1990s [159]. Test strips rely on capillary forces or wicking action of water through the paper to drive

fluids in one direction [160], and they are essentially the simplest microfluidic systems that are designed to detect a variety of targets and give detection results in minutes. Compared to microfluidic channels, testing strips are generally convenient and inexpensive to fabricate, but the performance is compromised because fluid handling capability is limited. Some strips, such as pregnancy and diabetic test strips, have already been successfully commercialized [29]; it should also be mentioned that some other test strips specifically designed for the detection of foodborne bacteria are also commercially available. For instance, Quick™ 15-minute bacteria test strips by Carolina Biological Supply are commercially available for rapid detection of certain bacteria species, such as *E. coli*, *Salmonella*, and *Shigella* in drinking water with a claimed LOD of 10^3 CFU/mL [161]. Furthermore, a variety of paper-based test strips for foodborne pathogenic bacteria detection have been reported in the literature [76, 162]. Typically, test strips provide only qualitative (presence/absence), not quantitative results; however, some recent strips are designed to be quantitative. For example, Blaskoza *et al*. used a combination of nucleic acid amplification and immunoassay-based lateral flow to detect *Listeria* spp. and *Listeria monocytogenes* [163]. The researchers showed that they were able to detect about 10 cells (*i.e*. *Listeria* spp. and *Listeria monocytogenes*) in 25 mL milk. The detection process took 5 - 15 min to get final results. However, it should be noted that it took 24 h for sample pre-treatment, including cell enrichment and target DNA isolation prior to testing.

More recently, test strips have been further improved by either employing nanoparticles or combining with different types of biosensors. For example, a disposable immuno-sensing strip was developed by Lin *et al*. to detect *E. coli* O157:H7 using screen-printed carbon

electrodes (SPCE) [164]. This detection strip was modified with AuNPs and the detection principle is illustrated in Figure 2-7. The immuno-recognition occurred when the SPCE strip, coated with primary antibodies, was immersed into samples containing *E. coli* O157:H7 cells. Secondary antibodies conjugated with horseradish peroxidase (HRP) were then introduced to form a sandwich structure. Finally, H_2O_2 was used to react with the HRP on the electrodes and the signal was detected as a current response. The detection process from sample-in to answer-out took only 1 h, and the LODs were 6 CFU/strip for *E. coli* in PBS buffer or milk.

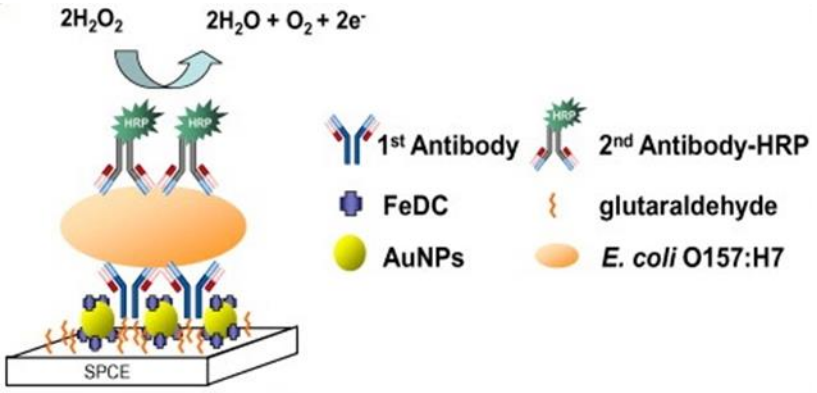

Figure 2-7 Microstructure of the immuno-sensing strip modified with Au nanoparticles and ferrocenedicarboxylic acid (FeDC) for detection of *E. coli* O157:H7. Reprinted from Ref. [164] with permission from Elsevier.

In another piece of work by Wu *et al.*, an aptamer-based lateral flow biosensor was developed to detect *E. coli* O157:H7 [25]. Two aptamers were employed to bind to *E. coli* O157:H7 cell membrane via different membrane proteins. As shown in Figure 2-8A, one aptamer (shown in red) was biotinlated and bound to streptavidin-modified magnetic beads

for target bacterial cell separation and enrichment; the other aptamer (shown in blue) was used as an amplification template for an isothermal DNA amplification method (strand displacement amplification, SDA). The SDA products were ssDNAs which were subsequently cut by a nicking enzyme at specific sites to produce a large number of short ssDNAs. As shown in Figure 2-8B, the resulting short ssDNAs were subsequently introduced into a lateral flow sensor and migrated along a strip where the short ssDNAs were captured by AuNP conjugated with complementary probes (stored on a conjugate pad). The complexed ssDNA-AuNP continued to move to the test zone and eventually gave a characteric red band "T" to indicate the presence of *E. coli* O157:H7 in the sample, as shown in Figure 2-8C. In contrast, a control band (at a different location, "C") would always be present regardless of the presence of *E. coli* O157:H7 cells to indicate the migration of AuNPs along the strip. This assay showed a LOD of 10 CFU/mL.

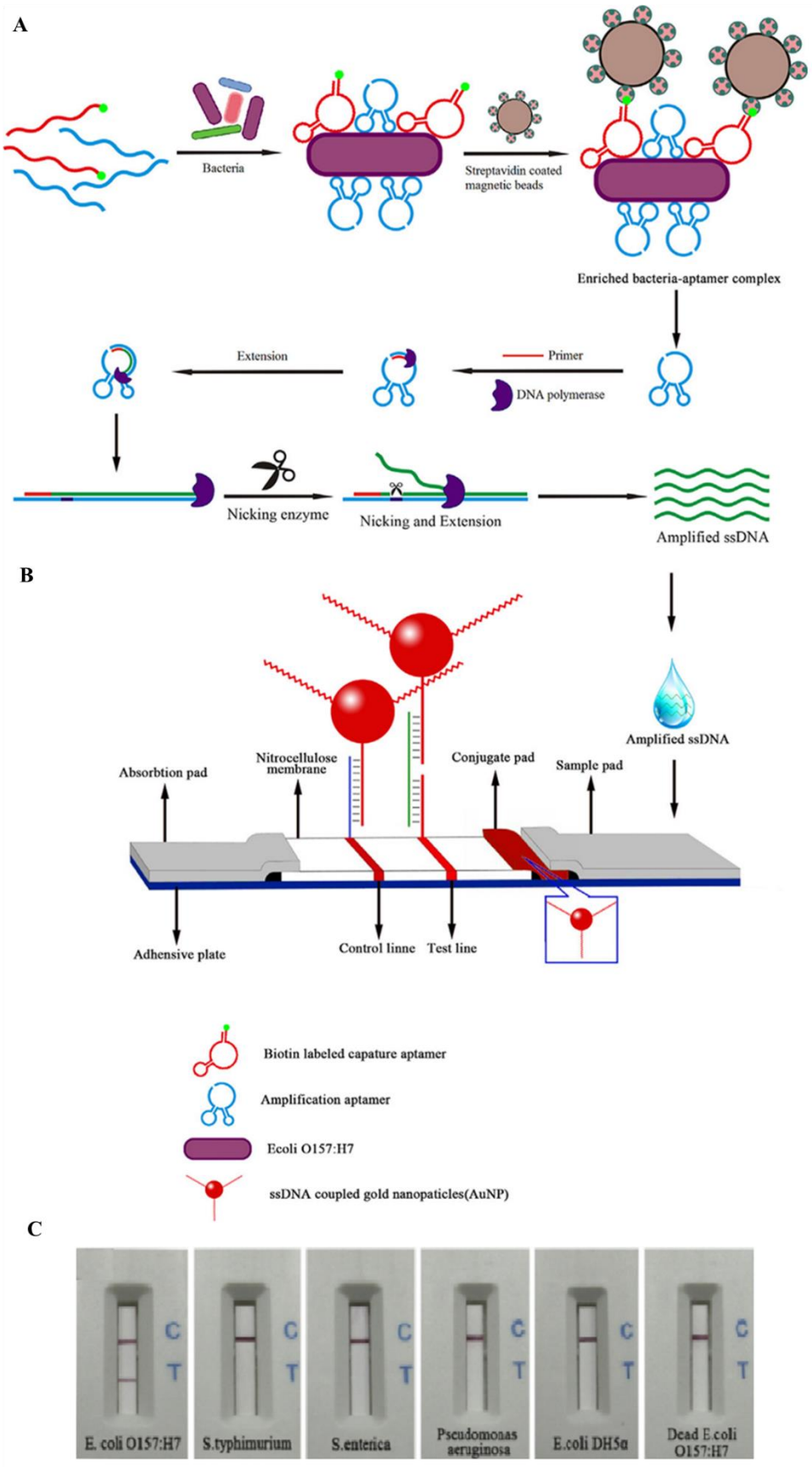
A
Bacteria
Streptavidin coated magnetic beads
Enriched bacteria-aptamer complex
Extension
Primer
DNA polymerase
Nicking enzyme
Nicking and Extension
Amplified ssDNA
B
Amplified ssDNA
Absorbtion pad
Nitrocellulose membrane
Conjugate pad
Sample pad
Adhensive plate
Control linne
Test line
Biotin labeled capature aptamer
Amplification aptamer
Ecoli O157:H7
ssDNA coupled gold nanopaticles(AuNP)
C
C
T
E. coli O157:H7
S.typhimurium
S.enterica
Pseudomonas aeruginosa
E.coli DH5α
Dead E.coli O157:H7

Figure 2-8 Aptamer-based lateral flow biosensor for the detection of *E. coli* O157:H7: A. Bacterial cells were captured by aptamers, concentrated by magnetic microbeads, and the capture event amplified by SDA. SDA products were then cut by specific enzyme; B. the resulting cut ssDNAs were further detected by lateral flow biosensor; and C. typical images of test results for the detection of *E. coli* O157:H7 versus non-target bacterial cells. Images adapted from Ref. [25] with permission from Elsevier.

2.6.2 Microfluidic channels and biochips

Microfluidic channels are always contained in chip-based microfluidic devices and the diameters of the channels are tens to hundreds of micrometers [165]. Biochips contain either microchannels and/or microwells to provide a space for bio-reactions. According to the liquid propulsion principles, microfluidic platforms can be subdivided into the following categories: capillary, pressure driven, centrifugal, eletrokinetic and acoustic systems [29]. The advantages of these microfluidic devices include the capability of handling sophisticated fluids and integration of sample clean-up, preparation and separation, and target detection. However, fabrication of highly integrated microfluidic devices can be complicated and expensive [166].

Sensitive ELISA assays have recently been combined with microfluidics for bacterial cell detection. For example, Song and Vo-Dinh developed a platform (shown in Figure 2-9) using an ELISA biochip with an array of capillary sensors that was modified with antibodies to detect *E. coli* O157:H7 [38]. The high sensitivity was due to the high affinities of the antibody-antigen interactions and the amplification of signals from reactions

between enzyme-conjugated secondary antibodies and substrates. The LODs of this device for detecting *E. coli* O157:H7 were reported to be 3 and 230 cells for the ELISA-based microfluidic system (Figure 2-9A) and the immuno-labelling based (Figure 2-9B) system, respectively.

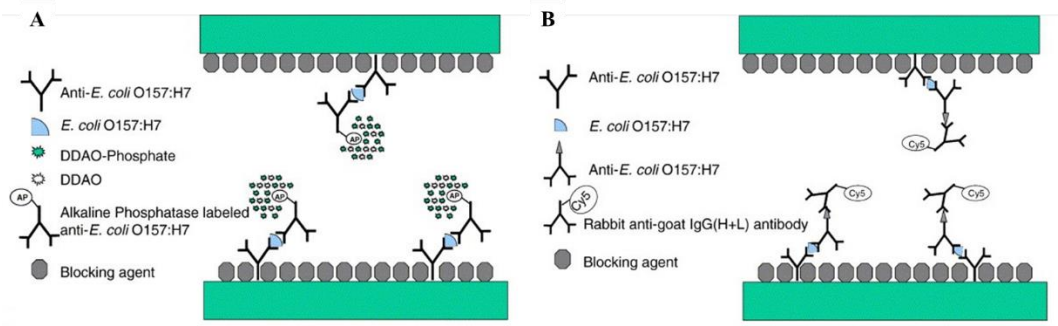

Figure 2-9 Illustration of *E. coli* O157:H7 detection by immunoassay in capillary sensors: A. ELISA and B. Cy5 labeled sandwich immunoassay. Figures were adapted from Ref. [38] with permission from Elsevier.

One of the most significant advantages of microfluidic devices is their ability to integrate different functionalities to carry out complex tasks [30, 137]. Kim *et al*. developed a highly integrated and automated microfluidic device to detect *Salmonella* [167]. This system integrated DNA extraction and isothermal amplification, as well as pathogen detection onto a single miniaturized disc (Figures 2-10A and B). A laser diode was employed to wirelessly adjust a valve control and provide required heating in the isothermal amplification step (Figure 2-10C). The entire detection process from cell lysis and DNA extraction to the final results was automatically controlled and was completed within 30 min. The LOD of this highly integrated disc method was 10 CFU/mL in PBS and 100 CFU/mL in milk samples.

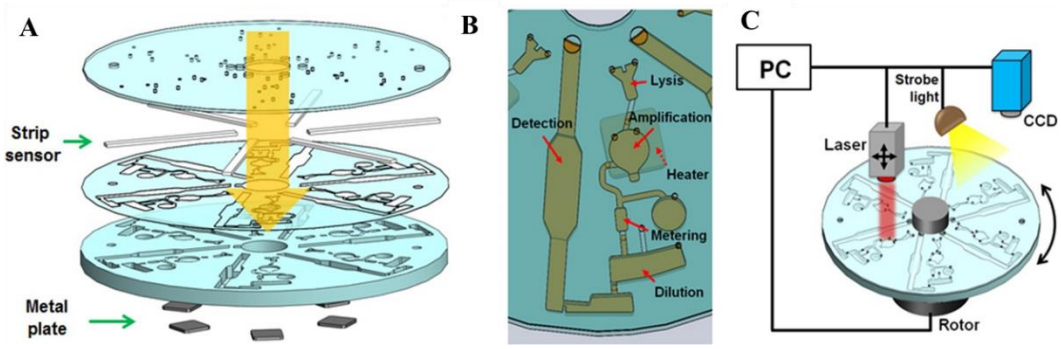

Figure 2-10 Fully integrated lab-on-a-disc for the detection of foodborne pathogens. A. Structure of the lab-on-a-disc with top and bottom plates made of polycarbonate, strip sensors, adhesive layer, and the metal heater; B. Top view of a section of the disc featuring the chambers for cell lysis, isothermal amplification, metering, dilution, and detection; C. Schematic illustration of the experimental setup. Adapted with permission from Ref. [167] Copyright (2014) American Chemical Society.

2.7 New trends in microfluidic detection

2.7.1 Smartphones

Smartphones, as highly integrated devices, contain cameras, batteries, displaying screens, and installed applications. Moreover, smartphones can easily connect to sensing devices and transfer data wirelessly [168]. For example, Zhu *et al.* reported a smartphone based platform to detect *E. coli* O157:H7 in liquid samples [169]. As shown in Figure 2-11A, a sandwich format bioassay using primary and secondary antibodies was conducted inside of a glass capillary. In particular, QD-conjugated secondary antibodies were used, and the fluorescence intensity emitted from the QDs was measured by a smartphone that acted as an integrated module for data collection, storage and processing. The LOD was reported to

be as low as 5 - 10 CFU/mL in both buffer solutions and fat-free milk samples. Another smartphone-based platform was reported by Park *et al.* to detect *Salmonella* [170]. A paper strip modified with polystyrene microparticles and antibodies against *Salmonella* was prepared, as shown in Figure 2-11B. The presence of *Salmonella* in the sample would cause the antibodies and the particles to agglutinate. The extent of agglutination was directly proportional to the concentration of *Salmonella* in the sample and could be detected by light-scattering of the paper strip when viewed at specific viewing angles by a smartphone. This information could be further processed using an application installed on the smartphone (see Figure 2-11C). The platform was reported to be able to complete a detection in 1 min and achieved a LOD of 10 CFU/mL cells in buffer [170]. Similarly, Rajendran *et al*. described an immuno-chromatographic test strip that combined fluorescent nanoparticles with a smartphone (Figure 2-11D) to detect *Salmonella* and *E. coli* bacteria [171]. Specifically, silica nanoparticles (SiNPs) doped with FITC and Ru(bpy) were conjugated with antibodies. The fluorescence images, captured by a smartphone camera upfitted with additional filter and lens, were processed by an application installed on the smartphone (Figure 2-11E). Other examples involving smartphones in foodborne pathogen detection include detection of *Listeria monocytogenes* using a portable platform with the assistance of a smartphone to enable quick data interpretation with the naked eye having a LOD of 20 CFU/mL [172]; in addition, a smartphone was also used to allow quick detection of pathogens in ground beef with a low LOD of 10 CFU/mL [173].

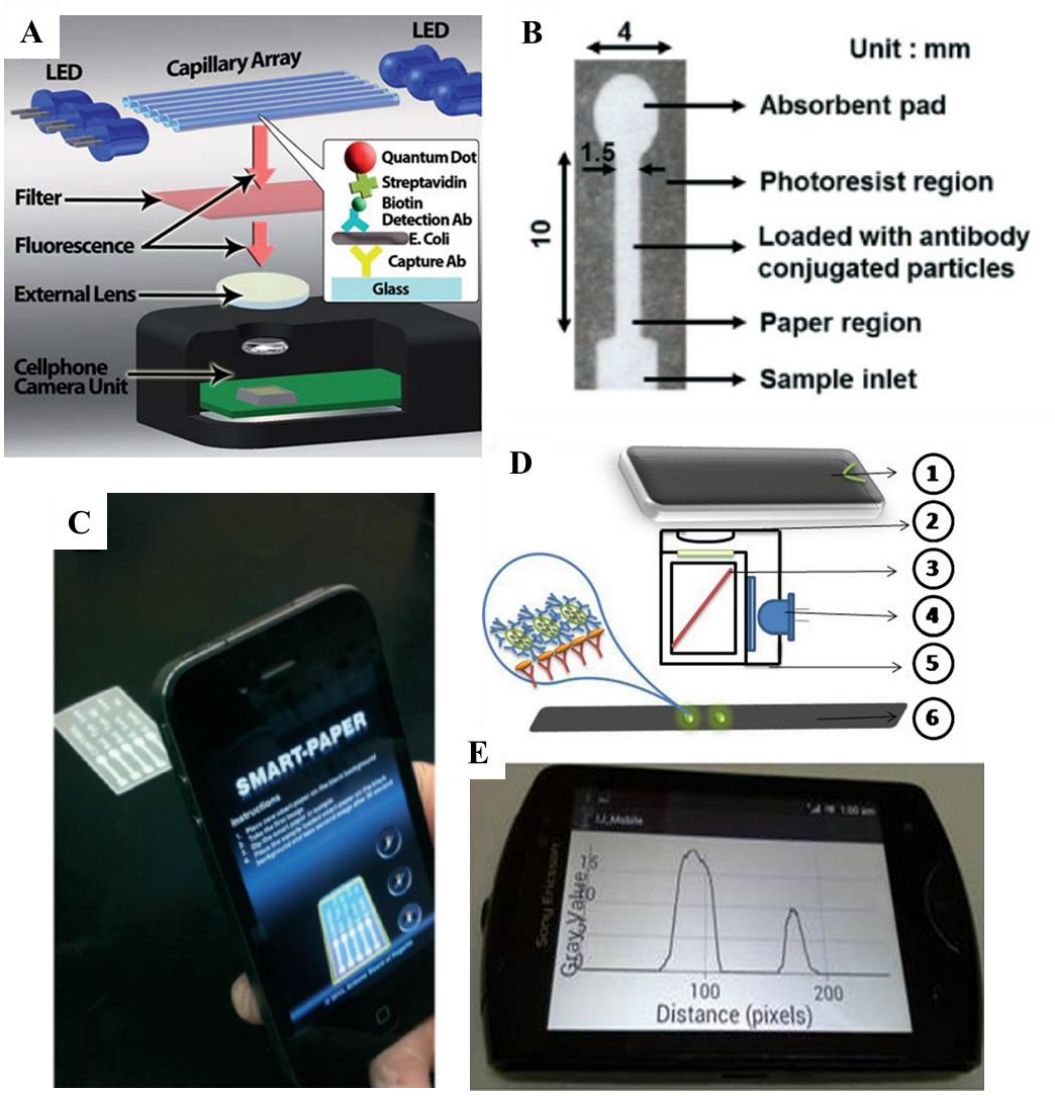

Figure 2-11 A. Schematic diagram of the *E. coli* detection on a cell-phone using the quantum dot based sandwich assay in glass capillary tubes; Adapted from Ref. [169] with permission from The Royal Society of Chemistry; B. Diagram of a single-channel paper microfluidic device; C. Smartphone application for *Salmonella* detection from a multi-channel microfluidic device; In part from Ref. [170] with permission from The Royal Society of Chemistry; D. Optical layout and E. Representative image showing the readout

of the LFIA strip from the smartphone application; Adapted from Ref. [171] with permission of Springer.

The combination of MMDs and smartphones for foodborne pathogen detection emerged in the last several years and is gradually becoming a new trend. With the rapid development of camera quality and other hardware capabilities, it is certain that smartphones will provide more possibilities in pathogen detection.

2.7.2 3-D printing

Fabrication of microfluidic devices is primarily based on soft lithography, a well-established process that is also followed by replica molding and device sealing steps [139]. This process is complicated and time consuming. In addition, soft lithography is only used to fabricate MMDs having relatively simple structures because the pattern features are needed to be printed on a flat photomask for photolithography [174, 175]. To fabricate microchannels with secondary patterns, multi-steps are needed, making the fabrication even more complicated. For example, two-level soft lithography and replica molding were used to fabricate a microchannel with secondary lower-relief structure [176]. In comparison, as an alternative method, the 3-D printing technique creates micro-structures directly from CAD software rather than depending on masks [177]. This reduces the time from device design to the first device in hand [175]. A 3-D structure is built on a layer-by-layer basis using materials as “ink” to “print” [178]. One advantage of 3-D printing over traditional soft photolithography is that it can produce an enclosed structure of MMDs, while the molded elastomer from soft lithography involves manual operations of

assembling and bonding steps (for example, the sealing procedure to enclose the microchannel) [175, 179]. Another advantage of 3-D printing is that it does not require a cleanroom environment [175]. Furthermore, 3-D printing is capable of building specialized 3-D structures with topography flexibility that cannot be otherwise built by soft lithography. For instance, Lee *et al.* produced a microfluidic device containing a 10-loop helical microchannel with trapezoidal cross section (250 and 500 μm, with width of 1000 μm, Figure 2-12A and B) using a 3-D printer to detect pathogenic *E. coli* bacterial cells [180]. This 3-D printed device integrated sample separation and detection processes. 3-D printing technology has developed rapidly in recent years, and its application in microfluidic detection will enable easy and cost-effective fabrication of MMDs [178].

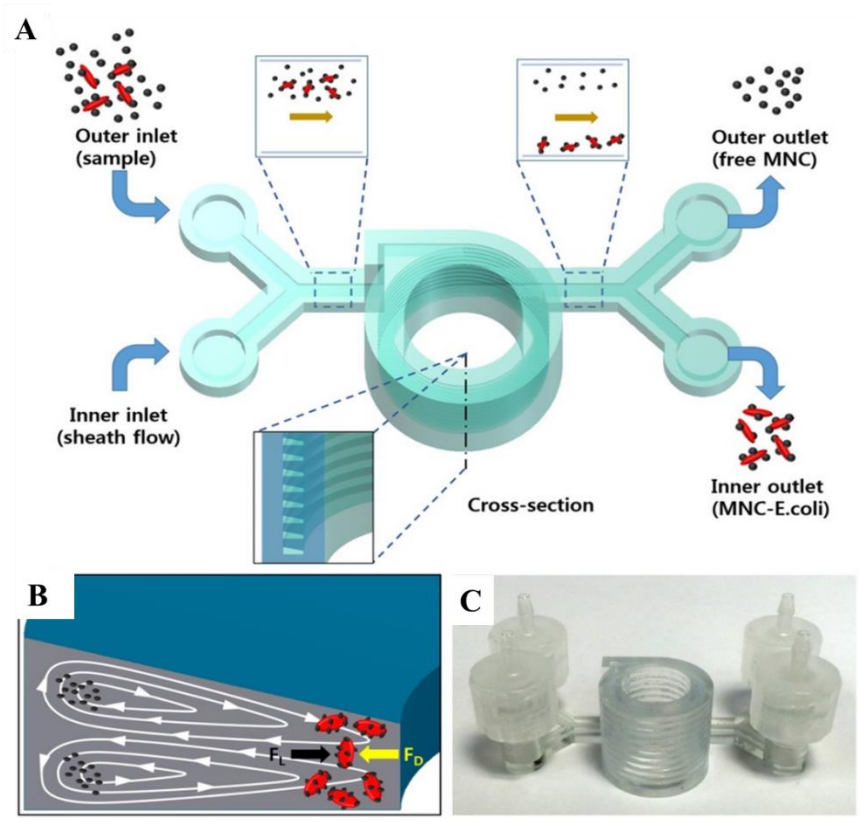

Figure 2-12 A 3-D printed microfluidic device for the detection of *E. coli*: A. Schematic illustration of device design and detection procedure; B. Trapezoidal cross section of the helical microchannel; C. Photograph of the 3-D printed device. Reproduced from Ref. [180] with permission of Nature Publishing Group.

2.8 Summary

Miniaturized microfluidic devices can detect foodborne pathogens at a rapid speed of several hours or less (enrichment procedures are not included) with LODs ranging from several cells/mL to 10^3 cells/mL. To further improve the detection performance, both nanoparticles and magnetic microbeads have been employed. In addition, there is an emerging trend to apply 3-D printing technique to fabricate microfluidic channels,

particularly for channels with complex geometries for potentially better detection performance. To develop more rapid and sensitive detection platform for foodborne pathogens, researchers have started to employ smartphones as a potential tool to substitute computers. The trends of MMDs lie in multiplexing or simultaneous detection of different bacteria as food could be contaminated by various pathogens. One possible approach is to use multiple probes for different pathogens, or use different tagging primers to initiate separate amplifications and achieve simultaneous detection of several foodborne pathogens [181-183]. As the target bacteria from food samples require sequential cultural enrichment steps which accounts for the whole detection time, high sensitivity detection methods in combination with robust and rapid sample concentration methods should be further developed to eventually abolish the need for enrichment steps, thereby producing truly rapid detection.

2.9 References

1. Mead, P.S., et al., *Food-related illness and death in the United States.* Emerging Infectious Diseases, 1999. **5**(5): p. 607.
2. Sharma, H. and R. Mutharasan, *Review of biosensors for foodborne pathogens and toxins.* Sensors and Actuators B: Chemical, 2013. **183**: p. 535-549.
3. Oliver, S., et al., *ASAS Centennial Paper: Developments and future outlook for preharvest food safety.* Journal of Animal Science, 2009. **87**(1): p. 419-437.
4. Henson, S. and J. Caswell, *Food safety regulation: an overview of contemporary issues.* Food Policy, 1999. **24**(6): p. 589-603.
5. Garcia Martinez, M., et al., *Co-regulation as a possible model for food safety governance: Opportunities for public–private partnerships.* Food Policy, 2007. **32**(3): p. 299-314.
6. Gracias, K.S. and J.L. McKillip, *A review of conventional detection and enumeration methods for pathogenic bacteria in food.* Canadian Journal of Microbiology, 2004. **50**(11): p. 883-890.

7. López Campos, G., et al., *Detection, Identification, and analysis of foodborne pathogens*, in *Microarray Detection and Characterization of Bacterial Foodborne Pathogens*. 2012, Springer: Berlin.
8. Arora, P., et al., *Biosensors as innovative tools for the detection of food borne pathogens.* Biosensors and Bioelectronics, 2011. **28**(1): p. 1-12.
9. https://www.foodsafety.gov/poisoning/causes/bacteriaviruses/index.html
10. de Boer, E. and R.R. Beumer, *Methodology for detection and typing of foodborne microorganisms.* International Journal of Food Microbiology, 1999. **50**(1): p. 119-130.
11. Mairhofer, J., K. Roppert, and P. Ertl, *Microfluidic systems for pathogen sensing: a review.* Sensors, 2009. **9**(6): p. 4804-4823.
12. Lin, F.Y., P.M. Sherman, and D. Li, *Development of a novel hand-held immunoassay for the detection of enterohemorrhagic Escherichia coli O157: H7.* Biomedical Microdevices, 2004. **6**(2): p. 125-130.
13. Cevallos Cevallos, J.M., M.D. Danyluk, and J.I. Reyes De Corcuera, *GC-MS based metabolomics for rapid simultaneous detection of Escherichia coli O157: H7, Salmonella Typhimurium, Salmonella Muenchen, and Salmonella Hartford in ground beef and chicken.* Journal of Food Science, 2011. **76**(4): p. M238-M246.
14. You, D.J., K.J. Geshell, and J.Y. Yoon, *Direct and sensitive detection of foodborne pathogens within fresh produce samples using a field-deployable handheld device.* Biosensors and Bioelectronics, 2011. **28**(1): p. 399-406.
15. Lazcka, O., F. Campo, and F.X. Munoz, *Pathogen detection: A perspective of traditional methods and biosensors.* Biosensors and Bioelectronics, 2007. **22**(7): p. 1205-1217.
16. Liu, F., et al., *Multiplex detection and genotyping of pathogenic bacteria on paper-based biosensor with a novel universal primer mediated asymmetric PCR.* Biosensors and Bioelectronics, 2015. **74**: p. 778-785.
17. Silk, T.M. and C.W. Donnelly, *Increased detection of acid-injured Escherichia coli O157: H7 in autoclaved apple cider by using nonselective repair on trypticase soy agar.* Journal of Food Protection, 1997. **60**(12): p. 1483-1486.
18. Heijnen, L. and G. Medema, *Quantitative detection of E. coli, E. coli O157 and other shiga toxin producing E. coli in water samples using a culture method combined with real-time PCR.* Journal of Water and Health, 2006. **4**: p. 487-498.
19. Daly, P., T. Collier, and S. Doyle, *PCR-ELISA detection of Escherichia coli in milk.* Letters in Applied Microbiology, 2002. **34**(3): p. 222-226.

20. Blais, B., et al., *Comparison of fluorogenic and chromogenic assay systems in the detection of Escherichia coli O157 by a novel polymyxin-based ELISA.* Letters in Applied Microbiology, 2004. **39**(6): p. 516-522.
21. Sapsford, K.E., et al., *Detection of Campylobacter and Shigella Species in Food Samples Using an Array Biosensor.* Analytical Chemistry, 2004. **76**(2): p. 433-440.
22. Perelle, S., et al., *Comparison of PCR-ELISA and LightCycler real-time PCR assays for detecting Salmonella spp. in milk and meat samples.* Molecular and Cellular Probes, 2004. **18**(6): p. 409-420.
23. Wang, S., et al., *Portable microfluidic chip for detection of Escherichia coli in produce and blood.* International Journal of Nanomedicine, 2012. **7**: p. 2591.
24. Ohk, S.H. and A.K. Bhunia, *Multiplex fiber optic biosensor for detection of Listeria monocytogenes, Escherichia coli O157: H7 and Salmonella enterica from ready-to-eat meat samples.* Food Microbiology, 2013. **33**(2): p. 166-171.
25. Wu, W., et al., *A sensitive lateral flow biosensor for Escherichia coli O157: H7 detection based on aptamer mediated strand displacement amplification.* Analytica Chimica Acta, 2015. **861**: p. 62-68.
26. Regulation, E., *1441/2007.(2007). Commission regulation on microbiological criteria for foodstuffs.* Official Journal of the European Union. **32**: p. 12-29.
27. Zhang, J. and H.F. Ji, *An anti E. coli O157: H7 antibody-immobilized microcantilever for the detection of Escherichia coli (E. coli).* Analytical Sciences, 2004. **20**(4): p. 585-588.
28. Tourlousse, D.M., et al., *A polymer microfluidic chip for quantitative detection of multiple water-and foodborne pathogens using real-time fluorogenic loop-mediated isothermal amplification.* Biomedical Microdevices, 2012. **14**(4): p. 769-778.
29. Mark, D., et al., *Microfluidic lab-on-a-chip platforms: requirements, characteristics and applications.* Chemical Society Reviews, 2010. **39**(3): p. 1153-1182.
30. Melin, J. and S.R. Quake, *Microfluidic large-scale integration: the evolution of design rules for biological automation.* Annual Review of Biophysics and Biomolecular Structure, 2007. **36**: p. 213-231.
31. Heo, J. and S.Z. Hua, *An overview of recent strategies in pathogen sensing.* Sensors, 2009. **9**(6): p. 4483-4502.
32. Singh, R., et al., *Biosensors for pathogen detection: A smart approach towards clinical diagnosis.* Sensors and Actuators B: Chemical, 2014. **197**: p. 385-404.

33. Atalay, Y.T., et al., *Microfluidic analytical systems for food analysis.* Trends in Food Science & Technology, 2011. **22**(7): p. 386-404.
34. Hall, R.H., *Biosensor technologies for detecting microbiological foodborne hazards.* Microbes and Infection, 2002. **4**(4): p. 425-432.
35. Perumal, V. and U. Hashim, *Advances in biosensors: principle, architecture and applications.* Journal of Applied Biomedicine, 2014. **12**(1): p. 1-15.
36. Gizeli, E. and C.R. Lowe, *Immunosensors.* Current Opinion in Biotechnology, 1996. **7**(1): p. 66-71.
37. Saerens, D., et al., *Antibody fragments as probe in biosensor development.* Sensors, 2008. **8**(8): p. 4669-4686.
38. Song, J.M. and T. Vo Dinh, *Miniature biochip system for detection of Escherichia coli O157: H7 based on antibody-immobilized capillary reactors and enzyme-linked immunosorbent assay.* Analytica Chimica Acta, 2004. **507**(1): p. 115-121.
39. Sheehan, A.D., et al., *The development of novel miniaturized immuno-sensing devices: a review of a small technology with a large future.* Analytical Letters, 2003. **36**(3): p. 511-537.
40. Sapsford, K.E., et al., *Sensors for detecting biological agents.* Materials Today, 2008. **11**(3): p. 38-49.
41. Cho, I.H., A. Bhunia, and J. Irudayaraj, *Rapid pathogen detection by lateral-flow immunochromatographic assay with gold nanoparticle-assisted enzyme signal amplification.* International Journal of Food Microbiology, 2015. **206**: p. 60-66.
42. Li, Z., et al., *Electrochemical impedance immunosensor based on self-assembled monolayers for rapid detection of Escherichia coli O157: H7 with signal amplification using lectin.* Sensors, 2015. **15**(8): p. 19212-19224.
43. Kim, G., et al., *A microfluidic nano-biosensor for the detection of pathogenic Salmonella.* Biosensors and Bioelectronics, 2015. **67**: p. 243-247.
44. Charlermroj, R., et al., *Validation of a high-throughput immunobead array technique for multiplex detection of three foodborne pathogens in chicken products.* International Journal of Food Microbiology, 2016. **224**: p. 47-54.
45. Song, C., et al., *Simple sensitive rapid detection of Escherichia coli O157: H7 in food samples by label-free immunofluorescence strip sensor.* Talanta, 2016. **156**: p. 42-47.

46. Day, J. and U. Basavanna, *Magnetic bead based immuno-detection of Listeria monocytogenes and Listeria ivanovii from infant formula and leafy green vegetables using the Bio-Plex suspension array system.* Food Microbiology, 2015. **46**: p. 564-572.
47. Wang, R., et al., *Immuno-capture and in situ detection of Salmonella typhimurium on a novel microfluidic chip.* Analytica Chimica Acta, 2015. **853**: p. 710-717.
48. Yang, Z., et al., *Ultrasensitive detection and quantification of E. coli O157: H7 using a giant magnetoimpedance sensor in an open-surface microfluidic cavity covered with an antibody-modified gold surface.* Microchimica Acta, 2016: p. 1-7.
49. Zhu, L., et al., *Development of a double-antibody sandwich ELISA for rapid detection of Bacillus Cereus in food.* Scientific Reports, 2016. **6**: p. 16092.
50. Mun, S. and S.J. Choi, *Detection of Salmonella typhimurium by antibody/enzyme-conjugated magnetic nanoparticles.* BioChip Journal, 2015. **9**(1): p. 10-15.
51. Famulok, M., G. Mayer, and M. Blind, *Nucleic acid aptamers from selection in vitro to applications in vivo.* Accounts of Chemical Research, 2000. **33**(9): p. 591-599.
52. Wilson, D.S. and J.W. Szostak, *In vitro selection of functional nucleic acids.* Annual Review of Biochemistry, 1999. **68**(1): p. 611-647.
53. Joshi, R., et al., *Selection, characterization, and application of DNA aptamers for the capture and detection of Salmonella enterica serovars.* Molecular and Cellular Probes, 2009. **23**(1): p. 20-28.
54. Schachermeyer, S., J. Ashby, and W. Zhong, *Aptamer–protein binding detected by asymmetric flow field flow fractionation.* Journal of Chromatography A, 2013. **1295**: p. 107-113.
55. Nutiu, R. and Y. Li, *Structure-switching signaling aptamers.* Journal of the American Chemical Society, 2003. **125**(16): p. 4771-4778.
56. Song, S., et al., *Aptamer-based biosensors.* TrAC Trends in Analytical Chemistry, 2008. **27**(2): p. 108-117.
57. Tan, W., M.J. Donovan, and J. Jiang, *Aptamers from cell-based selection for bioanalytical applications.* Chemical Reviews, 2013. **113**(4): p. 2842-2862.
58. Toh, S.Y., et al., *Aptamers as a replacement for antibodies in enzyme-linked immunosorbent assay.* Biosensors and Bioelectronics, 2015. **64**: p. 392-403.
59. Huang, A., et al., *High-throughput detection of food-borne pathogenic bacteria using oligonucleotide microarray with quantum dots as fluorescent labels.* International Journal of Food Microbiology, 2014. **185**: p. 27-32.

60. Ma, K., et al., *Rapid and simultaneous detection of Salmonella, Shigella, and Staphylococcus aureus in fresh pork using a multiplex real-time PCR assay based on immunomagnetic separation.* Food Control, 2014. **42**: p. 87-93.
61. Wu, S., et al., *Simultaneous aptasensor for multiplex pathogenic bacteria detection based on multicolor upconversion nanoparticles labels.* Analytical Chemistry, 2014. **86**(6): p. 3100-3107.
62. Wang, L., et al., *Rapid and accurate detection of viable Escherichia coli O157: H7 in milk using a combined IMS, sodium deoxycholate, PMA and real-time quantitative PCR process.* Food Control, 2014. **36**(1): p. 119-125.
63. Liu, K., et al., *Aptamer-based detection of Salmonella enteritidis using double signal amplification by Klenow fragment and dual fluorescence.* Microchimica Acta, 2015: p. 1-7.
64. Duan, N., et al., *Salmonella typhimurium detection using a surface-enhanced Raman scattering-based aptasensor.* International Journal of Food Microbiology, 2016. **218**: p. 38-43.
65. Van Dorst, B., et al., *Recent advances in recognition elements of food and environmental biosensors: a review.* Biosensors and Bioelectronics, 2010. **26**(4): p. 1178-1194.
66. Balasubramanian, S., et al., *Lytic phage as a specific and selective probe for detection of Staphylococcus aureus—a surface plasmon resonance spectroscopic study.* Biosensors and Bioelectronics, 2007. **22**(6): p. 948-955.
67. Nanduri, V., et al., *Phage as a molecular recognition element in biosensors immobilized by physical adsorption.* Biosensors and Bioelectronics, 2007. **22**(6): p. 986-992.
68. Archer, M.J. and J.L. Liu, *Bacteriophage T4 nanoparticles as materials in sensor applications: variables that influence their organization and assembly on surfaces.* Sensors, 2009. **9**(8): p. 6298-6311.
69. Van der Merwe, R., et al., *Phage-based detection of bacterial pathogens.* Analyst, 2014. **139**(11): p. 2617-2626.
70. Xu, X. and Y. Ying, *Microbial biosensors for environmental monitoring and food analysis.* Food Reviews International, 2011. **27**(3): p. 300-329.
71. Smartt, A.E., et al., *Pathogen detection using engineered bacteriophages.* Analytical and Bioanalytical Chemistry, 2012. **402**(10): p. 3127-3146.
72. Smietana, M., et al., *Detection of bacteria using bacteriophages as recognition elements immobilized on long-period fiber gratings.* Optics Express, 2011. **19**(9): p. 7971-7978.

73. Tawil, N., et al., *Surface plasmon resonance detection of E. coli and methicillin-resistant S. aureus using bacteriophages.* Biosensors and Bioelectronics, 2012. **37**(1): p. 24-29.
74. Jung, L.S. and J. Ahn, *Evaluation of bacteriophage amplification assay for rapid detection of Shigella boydii in food systems.* Annals of Microbiology, 2015: p. 1-6.
75. Sharp, N.J., et al., *Rapid detection of Bacillus anthracis in complex food matrices using phage-mediated bioluminescence.* Journal of Food Protection, 2015. **78**(5): p. 963-968.
76. Jokerst, J.C., et al., *Development of a paper-based analytical device for colorimetric detection of select foodborne pathogens.* Analytical Chemistry, 2012. **84**(6): p. 2900-2907.
77. Arshak, K., et al., *Conducting polymers and their applications to biosensors: emphasizing on foodborne pathogen detection.* IEEE Sensors Journal, 2009. **9**(12): p. 1942-1951.
78. Ramesh, A., et al., *Application of a convenient DNA extraction method and multiplex PCR for the direct detection of Staphylococcus aureus and Yersinia enterocolitica in milk samples.* Molecular and Cellular Probes, 2002. **16**(4): p. 307-314.
79. Quigley, L., et al., *A comparison of methods used to extract bacterial DNA from raw milk and raw milk cheese.* Journal of Applied Microbiology, 2012. **113**(1): p. 96-105.
80. Wang, X., N. Jothikumar, and M.W. Griffiths, *Enrichment and DNA extraction protocols for the simultaneous detection of Salmonella and Listeria monocytogenes in raw sausage meat with multiplex real-time PCR.* Journal of Food Protection, 2004. **67**(1): p. 189-192.
81. Mori, Y. and T. Notomi, *Loop-mediated isothermal amplification (LAMP): a rapid, accurate, and cost-effective diagnostic method for infectious diseases.* Journal of Infection and Chemotherapy, 2009. **15**(2): p. 62-69.
82. Demidov, V.V., *Rolling-circle amplification in DNA diagnostics: the power of simplicity.* Expert Review of Molecular Diagnostics, 2002. **2**(6): p. 542-548.
83. Fischer, N.O., T.M. Tarasow, and J.B.H. Tok, *Protein detection via direct enzymatic amplification of short DNA aptamers.* Analytical Biochemistry, 2008. **373**(1): p. 121-128.
84. Schweitzer, B. and S. Kingsmore, *Combining nucleic acid amplification and detection.* Current Opinion in Biotechnology, 2001. **12**(1): p. 21-27.
85. Schweitzer, B., et al., *Immunoassays with rolling circle DNA amplification: a versatile platform for ultrasensitive antigen detection.* Proceedings of the National Academy of Sciences, USA, 2000. **97**(18): p. 10113-10119.
86. Kingsmore, S.F. and D.D. Patel, *Multiplexed protein profiling on antibody-based microarrays by rolling circle amplification.* Current Opinion in Biotechnology, 2003. **14**(1): p. 74-81.

87. Zhao, Y., et al., *Isothermal Amplification of Nucleic Acids.* Chemical Reviews, 2015. **115**(22): p. 12491-12545.
88. Uddin, S.M., et al., *A Portable Automatic Endpoint Detection System for Amplicons of Loop Mediated Isothermal Amplification on Microfluidic Compact Disk Platform.* Sensors, 2015. **15**(3): p. 5376-5389.
89. Sayad, A.A., et al., *A microfluidic lab-on-a-disc integrated loop mediated isothermal amplification for foodborne pathogen detection.* Sensors and Actuators B: Chemical, 2016. **227**: p. 600-609.
90. Sun, Y., et al., *A lab-on-a-chip system with integrated sample preparation and loop-mediated isothermal amplification for rapid and quantitative detection of Salmonella spp. in food samples.* Lab on a Chip, 2015. **15**(8): p. 1898-1904.
91. Mikš-Krajnik, M., et al., *Loop-mediated isothermal amplification (LAMP) coupled with bioluminescence for the detection of Listeria monocytogenes at low levels on food contact surfaces.* Food Control, 2016. **60**: p. 237-240.
92. Zhang, J., et al., *A gold nanoparticle-based chronocoulometric DNA sensor for amplified detection of DNA.* Nature Protocols, 2007. **2**(11): p. 2888-2895.
93. Mao, X., et al., *A nanoparticle amplification based quartz crystal microbalance DNA sensor for detection of Escherichia coli O157: H7.* Biosensors and Bioelectronics, 2006. **21**(7): p. 1178-1185.
94. Sanvicens, N., et al., *Nanoparticle-based biosensors for detection of pathogenic bacteria.* TrAC Trends in Analytical Chemistry, 2009. **28**(11): p. 1243-1252.
95. So, H.M., et al., *Single-walled carbon nanotube biosensors using aptamers as molecular recognition elements.* Journal of the American Chemical Society, 2005. **127**(34): p. 11906-11907.
96. Tully, E., et al., *The development of rapid fluorescence-based immunoassays, using quantum dot-labelled antibodies for the detection of Listeria monocytogenes cell surface proteins.* International Journal of Biological Macromolecules, 2006. **39**(1): p. 127-134.
97. García Aljaro, C., et al., *Carbon nanotubes-based chemiresistive biosensors for detection of microorganisms.* Biosensors and Bioelectronics, 2010. **26**(4): p. 1437-1441.
98. Zhao, X., et al., *A rapid bioassay for single bacterial cell quantitation using bioconjugated nanoparticles.* Proceedings of the National Academy of Sciences, USA, 2004. **101**(42): p. 15027-15032.

99. Chung, H.J., et al., *A magneto-DNA nanoparticle system for rapid detection and phenotyping of bacteria.* Nature Nanotechnology, 2013. **8**(5): p. 369-375.

100. Hahn, M.A., J.S. Tabb, and T.D. Krauss, *Detection of single bacterial pathogens with semiconductor quantum dots.* Analytical Chemistry, 2005. **77**(15): p. 4861-4869.

101. Edgar, R., et al., *High-sensitivity bacterial detection using biotin-tagged phage and quantum-dot nanocomplexes.* Proceedings of the National Academy of Sciences, USA, 2006. **103**(13): p. 4841-4845.

102. Zuo, P., et al., *A PDMS/paper/glass hybrid microfluidic biochip integrated with aptamer-functionalized graphene oxide nano-biosensors for one-step multiplexed pathogen detection.* Lab on a Chip, 2013. **13**(19): p. 3921-3928.

103. Naja, G., et al., *Detection of bacteria aided by immuno-nanoparticles.* Journal of Raman Spectroscopy, 2007. **38**(11): p. 1383-1389.

104. Gu, L., et al., *Single-walled carbon nanotubes displaying multivalent ligands for capturing pathogens.* Chemical Communications, 2005(7): p. 874-876.

105. Gu, L., et al., *Single-walled carbon nanotube as a unique scaffold for the multivalent display of sugars.* Biomacromolecules, 2008. **9**(9): p. 2408-2418.

106. van Reenen, A., et al., *Integrated lab-on-chip biosensing systems based on magnetic particle actuation–a comprehensive review.* Lab on a Chip, 2014. **14**: p. 1966-1986.

107. Wright, D., P. Chapman, and C. Siddons, *Immunomagnetic separation as a sensitive method for isolating Escherichia coli O157 from food samples.* Epidemiology and Infection, 1994. **113**(01): p. 31-39.

108. Lee, J., et al., *Diffractometric detection of proteins using microbead-based rolling circle amplification.* Analytical Chemistry, 2009. **82**(1): p. 197-202.

109. Qiu, J., et al., *Immunomagnetic separation and rapid detection of bacteria using bioluminescence and microfluidics.* Talanta, 2009. **79**(3): p. 787-795.

110. Ozalp, V.C., et al., *Pathogen detection in complex samples by quartz crystal microbalance sensor coupled to aptamer functionalized core–shell type magnetic separation.* Analytica Chimica Acta, 2015. **853**: p. 533-540.

111. Viswanathan, S., C. Rani, and J.-a.A. Ho, *Electrochemical immunosensor for multiplexed detection of food-borne pathogens using nanocrystal bioconjugates and MWCNT screen-printed electrode.* Talanta, 2012. **94**: p. 315-319.

112. Xu, M., R. Wang, and Y. Li, *Rapid detection of Escherichia coli O157: H7 and Salmonella Typhimurium in foods using an electrochemical immunosensor based on screen-printed*

interdigitated microelectrode and immunomagnetic separation. Talanta, 2016. **148**: p. 200-208.

113. Chen, Y., et al., *One-step detection of pathogens and viruses: combining magnetic relaxation switching and magnetic separation.* ACS Nano, 2015. **9**(3): p. 3184-3191.
114. Zhu, M., et al., *Construction of Fe3O4/Vancomycin/PEG magnetic nanocarrier for highly efficient pathogen enrichment and gene sensing.* ACS Applied Materials & Interfaces, 2015. **7**(23): p. 12873-12881.
115. Friend, J. and L. Yeo, *Fabrication of microfluidic devices using polydimethylsiloxane.* Biomicrofluidics, 2010. **4**(2): p. 026502.
116. Prakash, S. and S. Kumar, *Fabrication of microchannels: A review.* Proceedings of the Institution of Mechanical Engineers, Part B: Journal of Engineering Manufacture, 2015. **229**(8): p. 1273-1288.
117. McDonald, J.C. and G.M. Whitesides, *Poly (dimethylsiloxane) as a material for fabricating microfluidic devices.* Accounts of Chemical Research, 2002. **35**(7): p. 491-499.
118. Li, W., et al., *Squeeze-chip: a finger-controlled microfluidic flow network device and its application to biochemical assays.* Lab on a chip, 2012. **12**(9): p. 1587-1590.
119. Kovarik, M.L., et al., *Micro total analysis systems for cell biology and biochemical assays.* Analytical Chemistry, 2011. **84**(2): p. 516-540.
120. Liu, R., et al., *Microfluidic CODES: a scalable multiplexed electronic sensor for orthogonal detection of particles in microfluidic channels.* Lab on a Chip, 2016. **16**(8): p. 1350-1357.
121. Sanjay, S.T., et al., *Biomarker detection for disease diagnosis using cost-effective microfluidic platforms.* Analyst, 2015. **140**(21): p. 7062-7081.
122. Dou, M., et al., *A versatile PDMS/paper hybrid microfluidic platform for sensitive infectious disease diagnosis.* Analytical Chemistry, 2014. **86**(15): p. 7978-7986.
123. Matos Pires, N.M. and T. Dong, *Microfluidic biosensor array with integrated poly (2, 7-carbazole)/fullerene-based photodiodes for rapid multiplexed detection of pathogens.* Sensors, 2013. **13**(12): p. 15898-15911.
124. Kim, G., et al., *A microfluidic nano-biosensor for the detection of pathogenic Salmonella.* Biosensors and Bioelectronics, 2015. **67**: p. 243-247.
125. Shin, Y., et al., *Microfluidic assay for simultaneous culture of multiple cell types on surfaces or within hydrogels.* Nature Protocols, 2012. **7**(7): p. 1247.

126. Mehling, M. and S. Tay, *Microfluidic cell culture.* Current Opinion in Biotechnology, 2014. **25**: p. 95-102.

127. Dieguez, L., et al., *Efficient microfluidic negative enrichment of circulating tumor cells in blood using roughened PDMS.* Analyst, 2015. **140**(10): p. 3565-3572.

128. Mazutis, L., et al., *Single-cell analysis and sorting using droplet-based microfluidics.* Nature Protocols, 2013. **8**(5): p. 870.

129. Xiong, B., et al., *Recent developments in microfluidics for cell studies.* Advanced Materials, 2014. **26**(31): p. 5525-5532.

130. Dugan, C.E., et al., *Monitoring cell secretions on microfluidic chips using solid-phase extraction with mass spectrometry.* Analytical and Bioanalytical Chemistry, 2017. **409**(1): p. 169-178.

131. Schmid, L., D.A. Weitz, and T. Franke, *Sorting drops and cells with acoustics: acoustic microfluidic fluorescence-activated cell sorter*. Lab on a Chip, 2014. **14**(19): p. 3710-3718.

132. Headen, D.M., et al., *Microfluidic-Based Generation of Size-Controlled, Biofunctionalized Synthetic Polymer Microgels for Cell Encapsulation.* Advanced Materials, 2014. **26**(19): p. 3003-3008.

133. Novo, P., et al., *Control of sequential fluid delivery in a fully autonomous capillary microfluidic device*. Lab on a Chip, 2013. **13**(4): p. 641-645.

134. Wang, S., et al., *Controlling flow behavior of water in microfluidics with a chemically patterned anisotropic wetting surface.* Langmuir, 2015. **31**(13): p. 4032-4039.

135. Zhou, B., et al., *Design and fabrication of magnetically functionalized flexible micropillar arrays for rapid and controllable microfluidic mixing*. Lab on a Chip, 2015. **15**(9): p. 2125-2132.

136. You, J.B., et al., *PDMS-based turbulent microfluidic mixer*. Lab on a Chip, 2015. **15**(7): p. 1727-1735.

137. Erickson, D. and D. Li, *Integrated microfluidic devices.* Analytica Chimica Acta, 2004. **507**(1): p. 11-26.

138. Dittrich, P.S., K. Tachikawa, and A. Manz, *Micro total analysis systems. Latest Advancements and Trends.* Analytical Chemistry, 2006. **78**(12): p. 3887-3908.

139. Anderson, J.R., et al., *Fabrication of microfluidic systems in poly (dimethylsiloxane).* Electrophoresis, 2000. **21**(1): p. 27-40.

140. Qin, D., Y. Xia, and G.M. Whitesides, *Soft lithography for micro-and nanoscale patterning.* Nature Protocols, 2010. **5**(3): p. 491.

141. Young, R.J. and P.A. Lovell, *Introduction to polymers*. 2011: CRC press.
142. Tomalia, D.A., et al., *Dendritic macromolecules: synthesis of starburst dendrimers.* Macromolecules, 1986. **19**(9): p. 2466-2468.
143. Bosman, A., H. Janssen, and E. Meijer, *About dendrimers: structure, physical properties, and applications.* Chemical Reviews, 1999. **99**(7): p. 1665-1688.
144. Tomalia, D. and R. Esfand, *Dendrons, dendrimers and dendrigrafts.* Chemistry and Industry, 1997(11): p. 416-420.
145. Esfand, R. and D.A. Tomalia, *Poly (amidoamine)(PAMAM) dendrimers: from biomimicry to drug delivery and biomedical applications.* Drug Discovery Today, 2001. **6**(8): p. 427-436.
146. Lee, C.C., et al., *Designing dendrimers for biological applications.* Nature Biotechnology, 2005. **23**(12): p. 1517.
147. Wang, E.C. and A.Z. Wang, *Nanoparticles and their applications in cell and molecular biology.* Integrative Biology, 2014. **6**(1): p. 9-26.
148. Liu, Z.-M., et al., *A hydrogen peroxide biosensor based on nano-Au/PAMAM dendrimer/cystamine modified gold electrode.* Sensors and Actuators B: Chemical, 2005. **106**(1): p. 394-400.
149. Cavaye, H., et al., *Solid-state dendrimer sensors: probing the diffusion of an explosive analogue using neutron reflectometry.* Langmuir, 2009. **25**(21): p. 12800-12805.
150. Kavosi, B., et al., *A highly sensitive prostate-specific antigen immunosensor based on gold nanoparticles/PAMAM dendrimer loaded on MWCNTS/chitosan/ionic liquid nanocomposite.* Biosensors and Bioelectronics, 2014. **52**: p. 20-28.
151. Twyman, L.J., et al., *The synthesis of water soluble dendrimers, and their application as possible drug delivery systems.* Tetrahedron Letters, 1999. **40**(9): p. 1743-1746.
152. Liu, M. and J.M. Fréchet, *Designing dendrimers for drug delivery.* Pharmaceutical science & Technology Today, 1999. **2**(10): p. 393-401.
153. Hudde, T., et al., *Activated polyamidoamine dendrimers, a non-viral vector for gene transfer to the corneal endothelium.* Gene Therapy, 1999. **6**(5).
154. Eichman, J.D., et al., *The use of PAMAM dendrimers in the efficient transfer of genetic material into cells.* Pharmaceutical Science & Technology today, 2000. **3**(7): p. 232-245.
155. Sanvicens, N., et al., *Nanoparticle-based biosensors for detection of pathogenic bacteria.* TrAC Trends in Analytical Chemistry, 2009. **28**(11): p. 1243-1252.

156. Qin, Y., et al., *Developing an ultra non-fouling SU-8 and PDMS hybrid microfluidic device by poly (amidoamine) engraftment.* Colloids and Surfaces B: Biointerfaces, 2015. **127**: p. 247-255.
157. Chang, A.-C., J.B. Gillespie, and M.B. Tabacco, *Enhanced detection of live bacteria using a dendrimer thin film in an optical biosensor.* Analytical Chemistry, 2001. **73**(3): p. 467-470.
158. Ji, J., J.A. Schanzle, and M.B. Tabacco, *Real-time detection of bacterial contamination in dynamic aqueous environments using optical sensors.* Analytical Chemistry, 2004. **76**(5): p. 1411-1418.
159. Ngom, B., et al., *Development and application of lateral flow test strip technology for detection of infectious agents and chemical contaminants: a review.* Analytical and Bioanalytical Chemistry, 2010. **397**(3): p. 1113-1135.
160. Haeberle, S. and R. Zengerle, *Microfluidic platforms for lab-on-a-chip applications.* Lab on a Chip, 2007. **7**(9): p. 1094-1110.
161. http://www.carolina.com/environmental-science-water-quality/quick-18-minute-bacteria-test-strips/652711.pr?question=bacteria+test+strips
162. Sithigorngul, P., et al., *A simple and rapid immunochromatographic test strip for detection of pathogenic isolates of Vibrio harveyi.* Journal of Microbiological Methods, 2007. **71**(3): p. 256-264.
163. Blažková, M., et al., *Development of a nucleic acid lateral flow immunoassay for simultaneous detection of Listeria spp. and Listeria monocytogenes in food.* European Food Research and Technology, 2009. **229**(6): p. 867-874.
164. Lin, Y.H., et al., *Disposable amperometric immunosensing strips fabricated by Au nanoparticles-modified screen-printed carbon electrodes for the detection of foodborne pathogen Escherichia coli O157: H7.* Biosensors and Bioelectronics, 2008. **23**(12): p. 1832-1837.
165. Stone, H.A., A.D. Stroock, and A. Ajdari, *Engineering flows in small devices: microfluidics toward a lab-on-a-chip.* Annual Review of Fluid Mechanics, 2004. **36**: p. 381-411.
166. Baker, C.A., et al., *Recent advances in microfluidic detection systems.* Bioanalysis, 2009. **1**(5): p. 967-975.
167. Kim, T.H., et al., *Fully integrated lab-on-a-disc for nucleic acid analysis of food-borne pathogens.* Analytical Chemistry, 2014. **86**(8): p. 3841-3848.

168. Liu, X., T.Y. Lin, and P.B. Lillehoj, *Smartphones for cell and biomolecular detection.* Annals of Biomedical Engineering, 2014. **42** (11): p. 2205-2217.

169. Zhu, H., U. Sikora, and A. Ozcan, *Quantum dot enabled detection of Escherichia coli using a cell-phone.* Analyst, 2012. **137**(11): p. 2541-2544.

170. San Park, T., et al., *Smartphone quantifies Salmonella from paper microfluidics.* Lab on a Chip, 2013. **13**(24): p. 4832-4840.

171. Rajendran, V.K., P. Bakthavathsalam, and B.M.J. Ali, *Smartphone based bacterial detection using biofunctionalized fluorescent nanoparticles.* Microchimica Acta, 2014. **181**(15-16): p. 1815-1821.

172. Liu, H., et al., *Visual and sensitive detection of viable pathogenic bacteria by sensing of RNA markers in gold nanoparticles based paper platform.* Biosensors and Bioelectronics, 2014. **62**: p. 38-46.

173. Liang, P.-S., T. San Park, and J.Y. Yoon, *Rapid and reagentless detection of microbial contamination within meat utilizing a smartphone-based biosensor.* Scientific Reports, 2014. **4**.

174. Rogers, J.A. and R.G. Nuzzo, *Recent progress in soft lithography.* Materials Today, 2005. **8**(2): p. 50-56.

175. Rogers, C.I., et al., *3D printed microfluidic devices with integrated valves.* Biomicrofluidics, 2015. **9**(1): p. 016501.

176. Anderson, J.R., et al., *Fabrication of topologically complex three-dimensional microfluidic systems in PDMS by rapid prototyping.* Analytical Chemistry, 2000. **72**(14): p. 3158-3164.

177. Ho, C.M.B., et al., *3D printed microfluidics for biological applications.* Lab on a Chip, 2015. **15**(18): p. 3627-3637.

178. Berman, B., *3-D printing: The new industrial revolution.* Business Horizons, 2012. **55**(2): p. 155-162.

179. Jo, B.H., et al., *Three-dimensional micro-channel fabrication in polydimethylsiloxane (PDMS) elastomer.* Journal of Microelectromechanical Systems, 2000. **9**(1): p. 76-81.

180. Lee, W., et al., *3D-printed microfluidic device for the detection of pathogenic bacteria using size-based separation in helical channel with trapezoid cross-section.* Scientific Reports, 2015. **5**: p. 7717.

181. Zhang, H., et al., *Ultrasensitive detection and rapid identification of multiple foodborne pathogens with the naked eyes.* Biosensors and Bioelectronics, 2015. **71**: p. 186-193.

182. Brandão, D., et al., *Simultaneous electrochemical magneto genosensing of foodborne bacteria based on triple-tagging multiplex amplification.* Biosensors and Bioelectronics, 2015. **74**: p. 652-659.
183. Wang, B., et al., *Simultaneous, rapid and sensitive detection of three food-borne pathogenic bacteria using multicolor quantum dot probes based on multiplex fluoroimmunoassay in food samples.* LWT-Food Science and Technology, 2015. **61**(2): p. 368-376.

Chapter 3 A simple dendrimer-aptamer based microfluidic platform for *E. coli* O157:H7 detection and signal intensification by rolling circle amplification

Chapter 3

A simple dendrimer-aptamer based microfluidic platform for *E. coli* O157:H7 detection and signal intensification by rolling circle amplification

Yuqian Jiang [a, b], Shan Zou [b], Xudong Cao [a, *]

A literature review on sensitive and rapid microfluidic detection platforms was discussed in Chapter 2. As a continuation of research work in our group on aptamer-dendrimer coated PDMS microchannels for detecting *E. coli* O157:H7, rolling circle amplification (RCA) was further applied to intensify the fluorescence detection signals of the established system. This dendrimer-aptamer-RCA detection system for *E. coli* O157:H7 was described in Chapter 3.

Abstract

Pathogenic bacteria in food cause a large number of foodborne illnesses and deaths. Therefore there is an increasingly urgent need for rapid, sensitive and cost-effective detection methods in order to avoid or to respond to contamination events and outbreaks in a timely manner. In an attempt to develop a simple and sensitive fluorescence intensity based microfluidic detection platform, poly(amidoamine) (PAMAM) dendrimer was immobilized onto a polydimethyl siloxane (PDMS) microchannel that was further modified with DNA aptamers for detections of *E. coli* O157:H7 cells. To further improve detection performance, rolling circle amplification (RCA) was employed to enhance the fluorescence signals. In addition, RCA products were characterized by both agarose gel electrophoresis and atomic force microscopy. Our results showed that RCA was able to enhance detection signals by up to 50 times and that the limit of detection of the system was reduced to 10^2 cells/mL with excellent detection specificities. Therefore, it can be concluded that this simple dendrimer-aptamer based microfluidic detection platform with RCA signal enhancement is a promising method for rapid and sensitive detection for foodborne pathogenic bacteria.

Keywords: signal amplification, lab-on-a-chip, microfluidic device, dendrimer, aptamer, AFM.

3.1 Introduction

Rapid and sensitive detection of foodborne pathogenic bacteria is of great importance to the food industry and public health since foodborne bacteria cause a large number of foodborne disease cases [1-3]. *E. coli* O157:H7 is an important type of pathogenic bacteria that is associated with foodborne illnesses, and its infective dose is estimated to be only as low as 10 cells [4-6]. It was reported that a high number of hospitalization and mortality resulted from *E. coli* O157:H7 infections in food products [7]. Therefore, it has been recognized as a highly threatening pathogen [8, 9]. To date, the most commonly used detection methods for *E. coli* O157:H7 include plate culture, enzyme-linked immunosorbent assay (ELISA) and polymerase chain reaction (PCR). While plate culture is a conventional method to detect bacteria, it takes several days to get results and involves laborious procedures [10, 11]. Molecular approaches such as ELISA and PCR are sensitive and give fast result turn-around; however sample pre-treatment steps such as cell enrichment and DNA extraction are often required, significantly increasing the overall detection time and complexity [12, 13]. Since the late 1980s, lab-on-a-chip (LOC) techniques that offer portability, high sensitivity, low cost and reduced reagent consumption have attracted growing research interests [13-17]. In addition, aptamers have emerged as a new type of recognition element in detection and gained growing attention [18]. Aptamers are *in vitro* selected single-stranded DNA/RNA oligonucleotides that can recognize and bind to specific targets, including metal ions, proteins and cells with high affinities, through folding into defined tertiary structures [19-21]. Recently, aptamers have found many applications in foodborne pathogen detection due to many of their advantages,

including ease of synthesis and modification, good reproducibility, and high sensitivity [22-27]. For example, an aptamer-based biosensor was developed to detect *E. coli* O157:H7 at concentrations ranging from 10^4 to 10^8 CFU/mL with a high specificity [28]. In another study, aptamers were conjugated to quantum dots for *E. coli* O157:H7 detection and showed a detection limit of 10^2 CFU/mL [29]. Furthermore, an interesting study reported an aptamer-based biosensor that was designed to detect *Salmonella paratyphi A*. In this study, graphene oxide (GO) was employed in combination with aptamers to achieve a detection limit of 10^2 cells/mL [30]. While exciting, these methods are still far away from real applications since they are based on the use of well plates that require laborious sample pre-treatment steps and careful handling procedures. In comparison, microfluidics based detection platforms that feature high throughput, intrinsic ability to integrate with other on-chip functionalities have recently attracted a significant amount of attention [13].

To improve detection sensitivities, signal amplification techniques are required. Currently, the most commonly used signal amplification approaches include nucleic acid amplification, nanoparticles or magnetic microbeads, and substrate-enzyme amplification [31]. Amongst these techniques, nucleic acid amplification techniques have been widely used. In particular, rolling circle amplification (RCA) has attracted growing attention due to its high efficiencies and single reaction temperature requirements. RCA is a robust isothermal DNA amplification technique that utilizes DNA or RNA polymerases to generate long single stranded RCA products (RCAPs) consisting of hundreds to thousands of tandem repeats complementary to a circular template, thereby achieving massive signal amplifications [32]. While many studies have used RCA techniques to enhance signals in

various detection systems, most of them are focused on detection of nucleic acids, proteins, and other biomolecules [33-38]. In fact, few studies have used RCA for whole-cell detections [39, 40].

In this study, we employed RCA in a novel dendrimer-aptamer coated microfluidic device. Specifically, a PDMS microchannel was initially modified with PAMAM dendrimers, which rendered the microchannel non-fouling and provided multiple binding sites for subsequent aptamer conjugation. The RCA was carried out in the presence of captured *E. coli* O157:H7 cells in the microfluidic channels. To confirm the RCA reaction, RCAPs were characterized by both agarose gel electrophoresis (AGE) and atomic force microscopy (AFM). Finally, the dendrimer-aptamer-RCA microfluidic system was used to detect *E. coli* O157:H7 cells. Our results showed that the LOD of this system was 10^2 cells/mL with excellent specificity, and that the detection signals were significantly enhanced by up to 50 times under RCA conditions when compared with detections without RCA.

3.2 Experimental

3.2.1 Overall design of the dendrimer-aptamer based detection system

The overall designs of the dendrimer-aptamer microfluidic system and dendrimer-aptamer-RCA detection system are shown in Figure 3-1. The capturing aptamer – immobilized on the inner surface of the PDMS microchannel via pre-conjugated PAMAM dendrimers – was employed to recognize and capture the target *E. coli* O157:H7 cells in samples. The dendrimer modification was optimized previously and generation 7 of PAMAM was

chosen as the optimal dendrimer, which showed remarkably non-fouling properties [40, 44]. Herein, the functions of PAMAM dendrimer are: 1) to prevent non-specific adsorption of non-target particles, and 2) to provide multiple binding sites and to maximize subsequent aptamer bindings [41]. In this study, we employed RCA to further improve the fluorescence detection signals. The principles of RCA are shown in Figure 3-1B, where the designed padlock probe and aptamer-primer specifically hybridize with each other and are further ligated to form a circular template. As shown in Figure 3-1C, the RCA process is incorporated into a capturing aptamer|bacterium|aptamer-primer sandwich structure with a free primer "tail" that serves as a hybrid binding site for padlock probe and RCA reaction initiation. RCA produces single-stranded repeating copies of DNA molecules complementary to the circular template that is extended from the end of the surface-bound aptamer-primer. At the end of the RCA, the RCAPs will hybrid with appropriately designed complementary fluorescent probes that give off quantitative signals for detection. As a result of the RCA reaction, the detection signals are significantly enhanced. In contrast, in the absence of target bacteria, the aptamer-primer will be washed away from the microchannel and no signals will be detected.

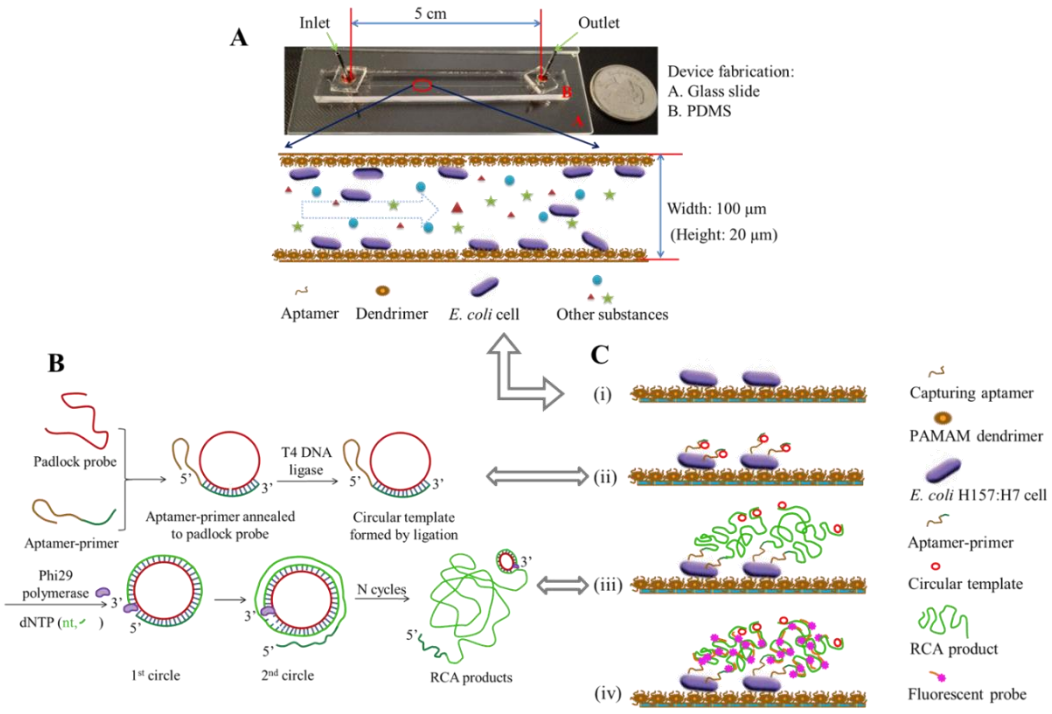

Figure 3-1 Schematic drawing of the dendrimer-aptamer-RCA detection system: A. image of the microfluidic device and illustration of target bacteria captured by dendrimer-aptamer modified PDMS detection system; B. schematic representation of RCA based on a padlock probe-ligated circular template; C. signal enhancement by RCA: (i) target bacterial cells are captured by the modified microchannel; (ii) aptamer-primer and padlock probe are sequentially introduced and circular template is formed via ligation; (iii) RCA is initiated and long tandem-repeat single strands are generated; (iv) fluorescent probes are added to visualize the detection signals.

3.2.2 Materials

Poly(amido amine) (PAMAM) dendrimers with ethylenediamine core (generation seven) were purchased from Sigma-Aldrich (Oakville, ON), and the surface amino groups were

further modified to carboxyl groups based on a previous report [41]. 1-(3-dimethylaminopropyl)-3-ethylcarbodiimide (EDC) was obtained from Alfa Aesar (Ward Hill, MA). (3-aminopropyl)-trimethoxysilane (APTMS) and N-hydroxysuccinimide (NHS) were purchased from Thermo Fisher Scientific (Rockford, IL). Nuclease-free water, IDTE buffer and DNA oligonucleotides (sequence shown below) capped with either amine or Cy3 were obtained from Integrated DNA Technologies (IDT) (Coralville, IA). Phi29 DNA polymerase, T4 DNA ligase and deoxynucleotide (dNTP) solution mix, Tris/Boric Acid/EDTA (TBE) buffer mix for electrophoresis, agarose (genetic analysis grade for DNA/RNA separation with broad range from 500 bp to 25 kb), promega blue/orange loading dye, DNA ladders and ethidium bromide were purchased from Fisher Scientific (Ottawa, ON). Sylgard 184 poly(dimethyl siloxane) (PDMS) kit was purchased from Dow Corning (Midland, MI). All other chemicals were obtained from Sigma-Aldrich and used as received unless indicated otherwise. Formalin-killed fluorescein isothiocyanate (FITC) labeled and non-labeled *E. coli* O157: H7 cells were generous gifts from Canada Food Inspection Agency (Ottawa, ON).

Table 3-1 Sequences of DNA oligonucleotides

Sequence name	Sequence
Capturing aptamer	5'-NH_2-ATCCG TCACA CCTGC TCTAT CAAAT GTGCA GATAT CAAGA CGATT TGTAC AAGAT GGTGT TGGCT CCCGT AT-3'
Designed aptamer-primer	5'-*ATCCG TCACA CCTGC TCTAT CAAAT GTGCA GATAT CAAGA CGATT TGTAC AAGAT GGTGT TGGCT CCCGT AT*TTT TTTTT GTCCG TGCTA GAAGG AAACA GTTAC-3'
Designed padlock probe	5'-TAGCA CGGAC ATATA TGATG GACCG CAGTA TGAGT ATCTC CTATC ACTAC TAAGT GGAAG AAATG TAACT GTTTC CTTC-3'

Designed Cy3 fluorescently labelled complementary probe	5'-Cy3-GTTTC CTTCT AGCAC-3'

Note: the capturing aptamer was selected from an approved patent, which is reported to bind with the lipopolysaccharide (LPS) on the cell membrane of *E. coli* O157:H7 with good specificity [28, 42]. Other reported aptamer candidates for *E. coli* O157:H7 are summarized in Appendix A. The italic portion of aptamer-primer sequence had the same sequence as the capturing aptamer as shown above; the underlined portion was the primer [43] where single and double underlined sequences were complementary to the sequences respectively underlined in the padlock probe, see Figure 3-2.

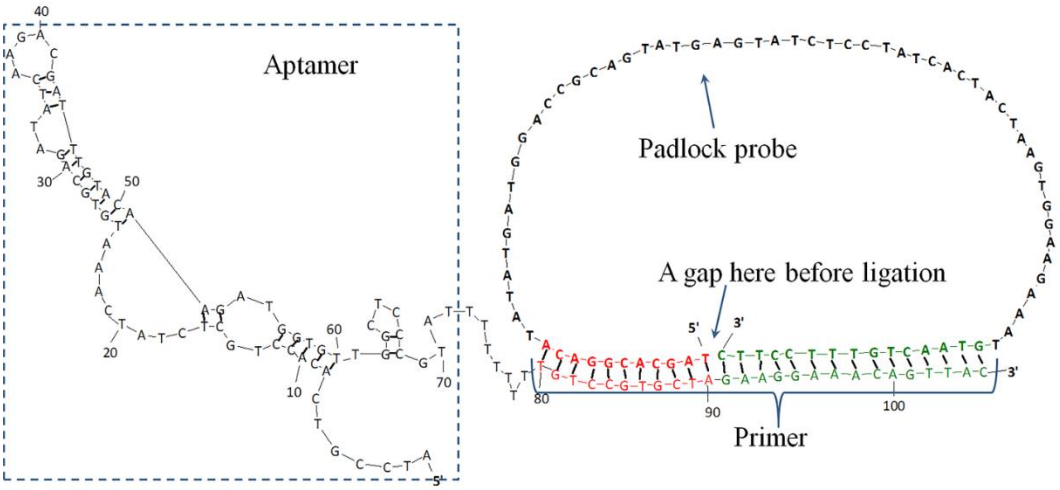

Figure 3-2 Schematic drawing of oligonucleotides sequences showing aptamer-primer and padlock probe. Note that the gap shown in the sequence is to be linked to form a circular template via DNA ligation; the single and double underlined sequences described in the text above are shown in red and green, respectively.

3.2.3 Fabrication and modification of PDMS microfluidic device

3.2.3.1 PDMS microfluidic channel preparation

PDMS stamps were prepared using a standard lithography process [41]. To seal the microchannel, PDMS stamp and glass slide (as substrate) were first treated by oxygen plasma with a plasma cleaner before joining the two treated surfaces. Subsequently the bonded surfaces were heated at 100 °C for 30 min to make a permanent bond, as we have previously reported [41, 44]. Figure 3-1A shows a photograph of the resulting microfluidic device.

3.2.3.2 Surface amination and PAMAM dendrimer engraftment

To introduce amino groups to the inner surfaces of a PDMS microchannel and its glass substrate, a silane coupling method was employed, as we have demonstrated elsewhere [44]. To conjugate PAMAM dendrimer to the amine functionalized inner surfaces of the microchannel, PAMAM-NH_2 was modified to obtain PAMAM dendrimer functionalized with carboxyl groups (*i.e.* PAMAM-COOH) using a previously reported method [41]. Subsequently, the microchannel was extensively washed and stored in PBS for future use.

3.2.3.3 Immobilization of capturing aptamers

To immobilize capturing aptamers to the inner surfaces of the resulting PAMAM-COOH modified microchannel surfaces, capturing aptamers capped with -NH_2 was used to react with PAMAM-COOH surfaces [45]. Immediately prior to the reaction, capturing aptamers were denatured at 95 °C for 5 min and cooled on ice for 1 min. After the modification reaction, the microchannel was extensively washed and stored in PBS for future use. To

further confirm and characterize the capturing aptamer immobilizations on the PDMS-dendrimer surface, Cy3 functionalized capturing aptamers (Cy3-aptamer) capped with -NH_2 were used to modify the dendrimer coated PDMS surfaces. Therefore the amount of Cy3-aptamers immobilized on the surface could be estimated by the relative fluorescence intensity. The significance of fluorescence intensity changes was analyzed by one way ANOVA test.

3.2.3.4 Aptamer *E. coli* O157:H7 capturing performance

To confirm *E. coli* bacterial cell capturing performance of the aptamers, aptamers and *E. coli* O157:H7 cells were fluorescently labelled with Cy3 and FITC, respectively. The fluorescently labelled aptamers and *E. coli* O157:H7 cells were incubated together at 37 ºC for 30 min, after which unreacted aptamers were washed away by centrifugation (14,000 × g for 5 min). The washing step was repeated 3 times to ensure that all unreacted aptamers were removed. Finally, the cells were collected, re-suspended in PBS (pH 7.4), and observed using both phase contrast and fluorescence microscopy. To further test the capturing ability of the dendrimer-aptamer functionalized microchannels, FITC labelled *E. coli* O157:H7 cells were injected into fully functionalized microchannels at a flow rate of 0.05 mL/h for 1 h. The total injection volume of *E. coli* O157:H7 cells was 150 µl (the volume of microchannel plus the injection volume of sample solution) per channel. The microchannels were subsequently washed with PBS (pH 7.4), and the captured cells were observed under fluorescence microscope along the microchannels under fluorescence modes (Olympus IX81, Richmond Hill, ON).

3.2.4 RCA reaction conditions and characterization of RCAPs

3.2.4.1 RCA reaction

To prepare circular templates for RCA reaction, 50 μL hybrid solution containing 2 μM of both aptamer-primer and padlock probe were incubated at 37 °C for 30 min to allow hybridization between aptamer-primer and padlock probe. This was followed by ligation reaction catalyzed by 10 U T4 DNA ligase in 10 × T4 ligation buffer (400 mM Tris-HCl, 100 mM $MgCl_2$, 100 mM DTT, 5 mM ATP, pH 7.8) at room temperature for 30 min, after which the ligation mixture was heated at 65 °C for 10 min to deactivate the T4 DNA ligase in order to stop the ligation reaction. RCA reaction was subsequently performed by adding phi29 DNA polymerase into the ligation reaction mixture. Specifically, for a 100 μL RCA reaction mixture, 10 U of phi29 DNA polymerase was used. After the reaction mixture was allowed to react at 37 °C for 2 h, it was heated at 65 °C for 10 min to deactivate the phi29 DNA polymerase in order to stop the RCA reaction. It should be noted that oligonucleotides were denatured by heating at 95 °C for 5 min and cooled on ice for 1 min to obtain conformational equilibrium to ensure desired intramolecular folding [43].

3.2.4.2 Characterization of RCAPs

To characterize the RCA products, both agarose gel electrophoresis (AGE) and atomic force microscopy (AFM) were used. For AGE characterizations, RCAPs were first denatured at 95 °C for 5 min and ice-cooled prior to loading the samples into 2% agarose gel. After the gel electrophoresis, gel images were obtained using an AlphaImager (HP Imaging System, San Jose, CA). Original oligonucleotides, *i.e*. aptamer-primer and

padlock probe were used as controls. For AFM characterizations, diluted DNA solutions were carefully dropped onto a freshly cleaved mica surface (V-1 Grade, SPI Supplies Division of Structure Probe Inc., West Chester, PA) pre-treated by 5 mM $NiCl_2$ and incubated at room temperature for 20 min. Subsequently the coated mica surface was carefully rinsed by filtered Milli-Q water and dried by pure nitrogen [46]. The MultiMode AFM with the NanoScope V controller (Bruker Nano Surfaces Division, Santa Barbara, CA, USA), in Bruker's ScanAsyst or PeakForce QNM modes. The peak force with which the tip taps the sample surface was always kept at the lowest stable imaging level of 20 mV (this is the raw signal measured by the 4 quadrant photodiode that corresponds approximately to 0.5 nN based on the nominal spring constant of the cantilevers used and on the typical photodiode sensitivity when the tip is properly aligned on our AFM). ScanAsyst-Air AFM probes (0.4 N/m, f_0:50-90 kHz, Bruker AFM Probes, Camarillo, CA), which are made of silicon nitride, were used. The typical tip diameter is 2 nm according to the manufacturer's specifications. While images of sizes of up to 20 × 20 μm^2 were acquired to insure good homogeneity of the samples, all the images that are shown in the thesis and that were used to measure heights were 1 × 1 μm^2 in size, acquired with the 512 × 512 pixels resolution, and at a scan rate of 1 Hz. In this way the pixel size is approximately 2 × 2 nm^2. The diameters or heights of all the DNAs were in the range from 1.2 to 2 nm. Based on manufacturer's specifications and on our own tests, the radii of AFM tips used were 3 to 15 nm, and the tips with larger radii were replaced. Based on the combination of the tip and nanotube radii, the pixel size of 2 × 2 nm^2 was chosen as sufficient to have reliable nanotube height measurements, where larger images or less pixels would lead to underestimation of the diameter. The obtained AFM images were

processed using open access software Gwyddion (http://gwyddion.net/). The height distributions were obtained by measuring 500 locations of strands from more than ten AFM images.

3.2.4.3 Signal amplification by RCA

To investigate signal enhancement by RCA, the following experiment was carried out. Unlabeled *E. coli* O157:H7 cell suspension at concentrations of 10^2, 10^3, 10^4 and 10^5 cells/mL were individually injected into fully functionalized microchannels at a flow rate of 0.05 mL/h for 1 h. The total injection volume of *E. coli* O157:H7 cells was 150 µl (the volume of microchannel plus the injection volume) per channel; subsequently the ligation products of aptamer-primer and padlock probes (1 µM) was introduced at the same flow rate for 1 h. After washing with PBS buffer, Cy3 labeled fluorescent probes were injected into the channel and incubated with the RCAPs at 37 °C for 30 min to allow hybridization, after which the unbound probes were washed with PBS (pH 7.4). Fluorescent images of the microchannels were captured under a 10 × objective using an inverted fluorescence microscope (Olympus X70) equipped with a high-resolution camera (QIC-F-CLR-12, QImaging). Fluorescence intensities of the images were analyzed using Image J and the fluorescence detection signals were the measured average intensity of the microchannel after subtraction of background intensity (*i. e.* the fluorescence intensity of the non-target microchannel) [47]. A total number of 20 images were captured from random positions of each microchannels using 1000 ms as the exposure time. The original fluorescence images are 1392 × 1040 pixels, 16-bit. The histogram was analyzed after selecting the microchannel area by selection tools in ImageJ. The mean value of the analyzed area was

used as the fluorescence intensity of each images. Images obtained from negative controls were used as background for subtraction. The tests were repeated in triplicates and error bars represent standard deviations of measurements (n=3).

3.3 Results and discussion

3.3.1 Immobilization of capturing aptamer on dendrimer modified PDMS microchannel

In a previous study, we successful demonstrated the immobilization of dendrimers on PDMS surfaces (*i.e.* microchannel inner surface) [41], as shown in Steps (i)→(ii)→(iii) in Figure 3-3A. In this study, we further modified the PDMS-dendrimer surfaces with capturing aptamers against *E. coli* O157:H7. To confirm that the capturing aptamers were successfully immobilized, Cy3 modified aptamer (*i.e*. Cy3-aptamer) was used, as shown in Step (iv) in Figure 3-3A. The fluorescence intensities of the modified surfaces are shown in Figure 3-3B. It is clear that the fluorescence intensities on the surfaces of interest increased significantly ($p < 0.01$, $n=10$, $\alpha=0.05$) from 49.6 ± 33.6 a.u. before the Cy3-aptamer modification, to 590.1 ± 102.7 a.u. after Cy3-aptamer modification. It is noted that the background fluorescence observed in samples before modification is mainly due to PDMS auto-fluorescence, as reported previously [48]. This more than 10-fold fluorescence intensity increase in comparison with the original PDMS-dendrimer surface strongly suggests that the aptamers were successfully immobilized on the dendrimer modified PDMS microchannel surfaces. Moreover, the fluorescence intensity increased minimally when the Cy3-aptamer was introduced to the dendrimer PDMS surface without the

catalysis of NHS/EDC as shown in Fig. 3.3 B (b), which further confirmed the successful bonding between Cy3-aptamer and dendrimer-PDMS.

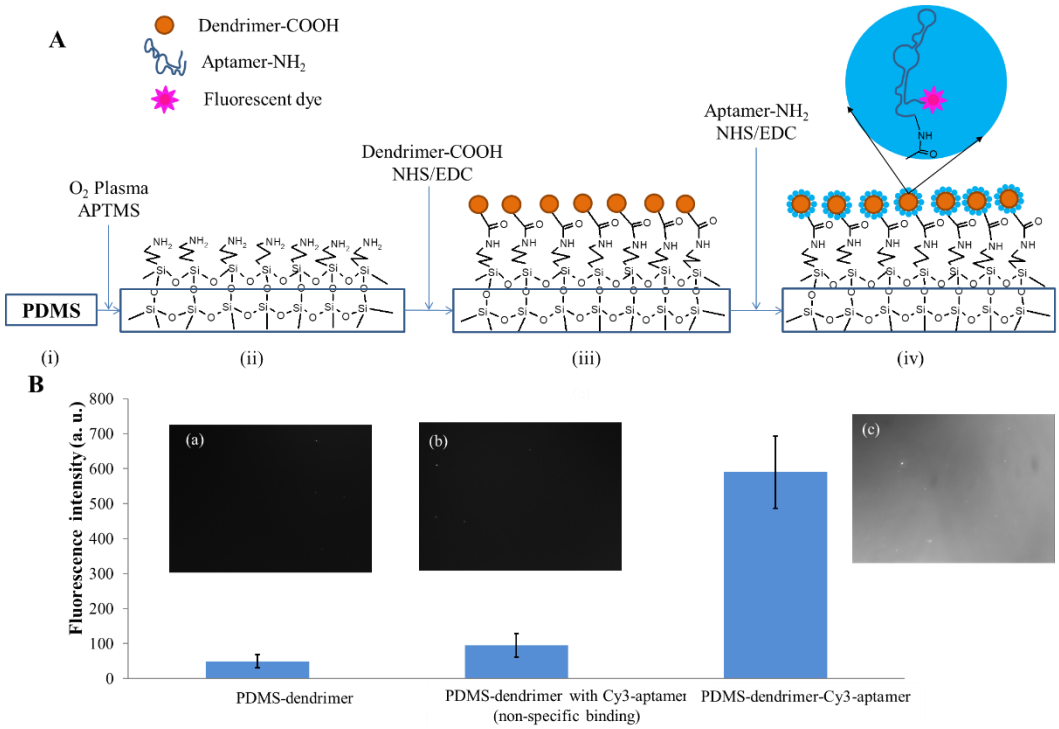

Figure 3-3 Illustration of PDMS surface modifications: A. schematic drawing of PDMS surface modification steps (i) native PDMS surface; (ii) PDMS surface amination by O_2 plasma activation and APTMS treatment; (iii) PAMAM surface dendrimer modification by NHS/EDC chemistry; (iv) fluorescently labeled capturing aptamer immobilized to the surface via PAMAM dendrimer; and B. fluorescence signal intensities of PDMS-dendrimer surfaces before and after aptamer conjugation. Insets: fluorescence micrographs of each surface of interest.

3.3.2 Recognition of *E. coli* O157:H7 by aptamers and device performance

To verify recognitions between aptamers and *E. coli* O157:H7 bacterial cells, FITC labeled *E. coli* O157:H7 were incubated with Cy3 labeled aptamer. After removing the unbound Cy3-aptamers, the centrifugated bacteria cells were observed under phase contrast microscope as shown in Figure 3.4A. The fluorescence spots were imaged when switched to FITC and Cy3 modes of microscope, which were further merged and showed in Figure 3.4D. Our results indicate that the aptamers, both in solution and PDMS surface immobilized, were able to effectively recognize and bind to the *E. coli* O157:H7 cells (see Figure 3-4).

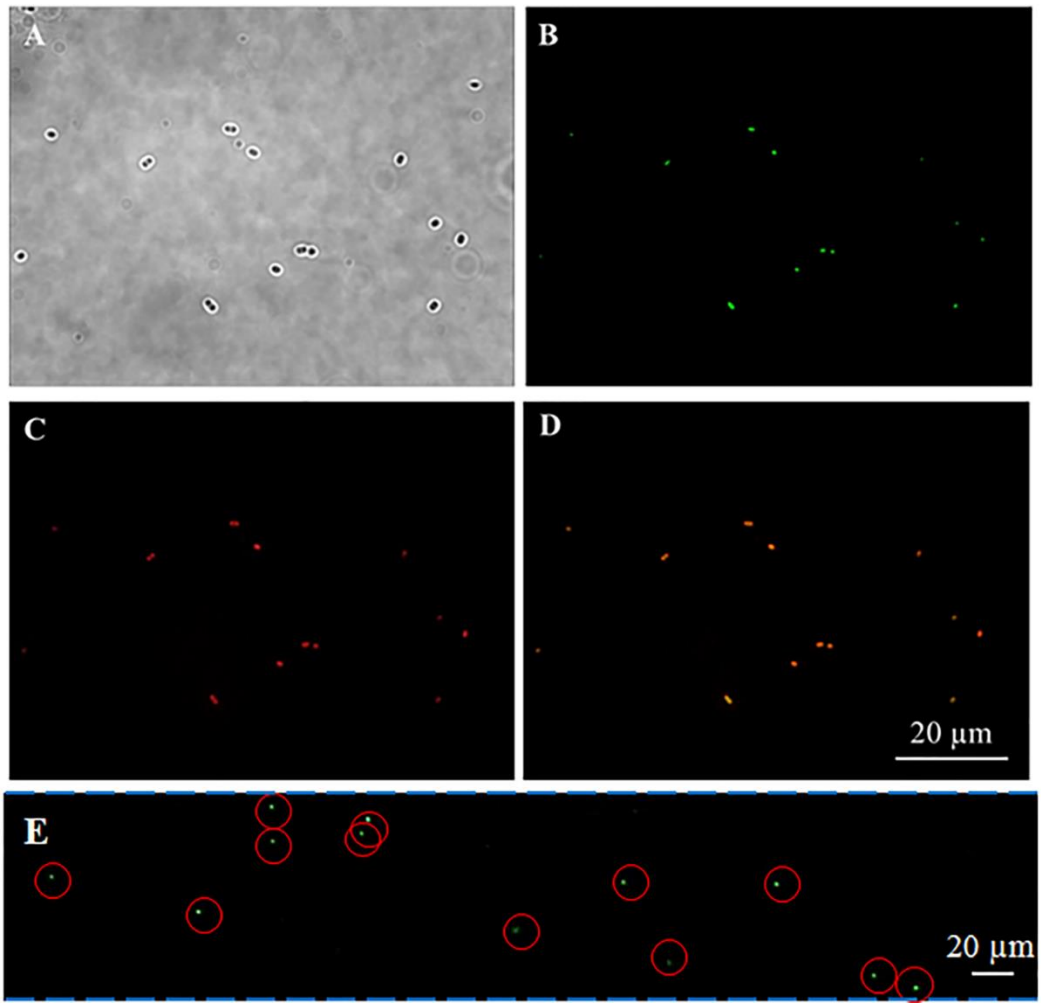

Figure 3-4 Micrographs of FITC labeled *E. coli* O157:H7 cells: A. *E. coli* O157:H7 cells observed under phase contrast microscope; B. FITC labeled *E. coli* O157:H7 cells observed under fluorescence microscope; C. Cy3 labeled aptamer observed under fluorescence microscope; D. merged image of B and C; and E. FITC labeled *E. coli* cells captured by dendrimer-aptamer PDMS microchannel.

3.3.3 Characterization of RCAPs

To confirm RCA reactions, RCA products were characterized by both AGE and AFM. Figure 3-5 shows gel images of the original aptamer-primer (Lane 1), padlock probe (Lane 2) and RCA products (Lane 3). As expected, each of Lane 1 and Lane 2 showed one band that indicated low molecular weight (*i.e*. less than 100 bp), whereas Lane 3 showed DNA products with extremely low mobility and high molecular weights exceeding 10, 000 bp. This provides a clear evidence to confirm RCA reactions. It is worthwhile mentioning that DNA markers used in this experiment were designed for double stranded DNAs; therefore discrepancies between the real molecular weights for single stranded DNAs and those derived using the DNA markers were expected [43].

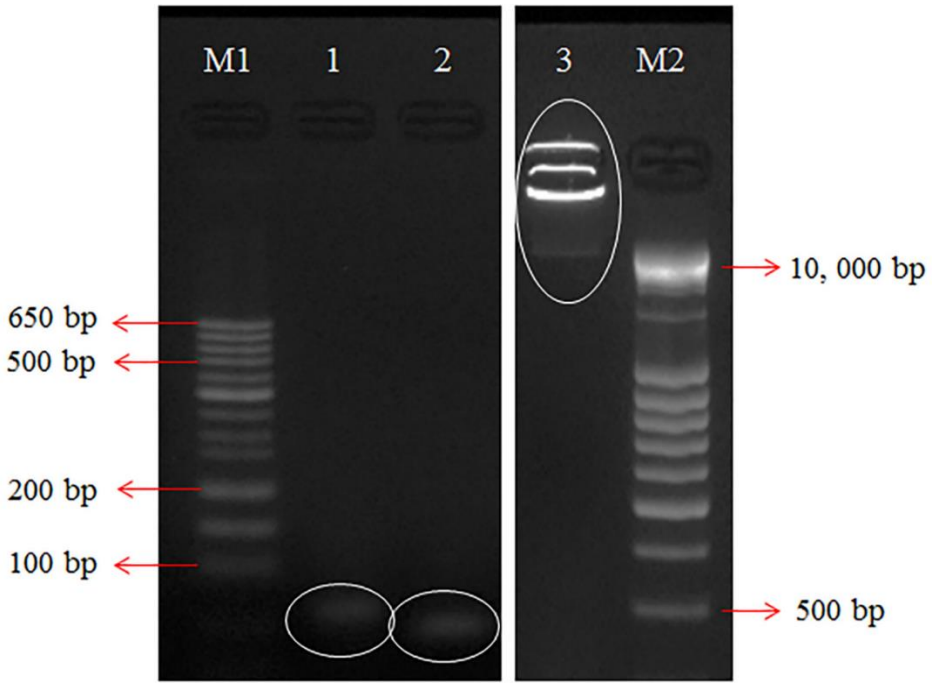

Figure 3-5 Agarose gel (2%) electrophoresis images of RCA products: Lane 1: aptamer-primer; Lane 2: padlock probe; and Lane 3: RCA products.

Furthermore, RCA products were also characterized by AFM. In comparison with the aptamer-primer (Figure 3-6A and 6B) and padlock probe (Figure 3-6C and 6D) that showed small DNA segments, the RCAPs showed clear and long chains of DNA molecules (Figure 3-6E), suggesting a significant growth in molecular size, as expected. This result also supports the AGE results as shown in Figure 3-5. The AFM image of RCAPs after conjugation with complementary fluorescent probes is shown in Figure 3-6G. In addition, DNA molecule profile heights and height distributions for both RCAPs and RCAPs conjugated with complementary probes are shown in Figure 3-6F and 6H, respectively. It is interesting to note that for RCAPs, the height distribution histogram shows a unimodal distribution with a peak value of 0.8 nm (Figure 3-6F). However, after hybridization with complementary fluorescent probes, the height distribution histogram shows a clear bimodal distribution with two peak values at 0.8 nm and 1.1 nm (Figure 3-6H). This change in height distribution after probe conjugation is most likely because of formations of double stranded DNA segments along the long single stranded RCAP molecular chains. In fact, single stranded DNA has a reported height of 0.4-0.6 nm while double stranded DNA has a reported height of 0.7-2.0 nm [49-51]. Taken together, the results discussed above strongly indicate that complementary probes were successfully conjugated to the long RCAP molecular chains.

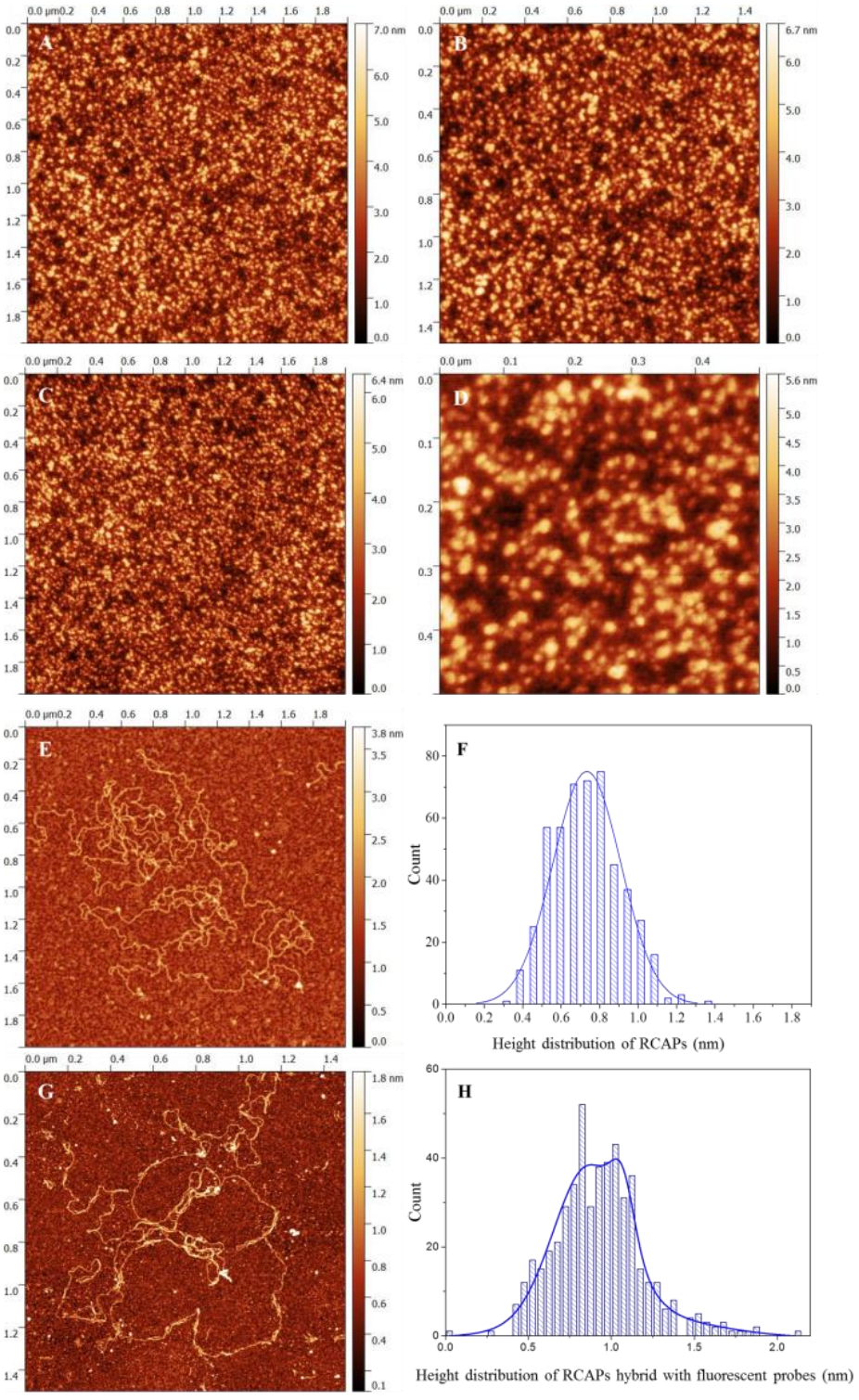
A
B
C
D
E
F
G
H
Count
Height distribution of RCAPs (nm)
Height distribution of RCAPs hybrid with fluorescent probes (nm)

Figure 3-6 AFM measurements of different samples: A. AFM image of aptamer-primer; B. zoomed-in image of A; C. AFM image of padlock probe; D. zoomed-in image of B; E. AFM image of RCA products; F. measured strand height distribution of RCA products (n=500 measurements); G. AFM image of RCA products conjugated with complementary fluorescent probes; and H. measured strand height distribution of RCA products conjugated with complementary fluorescent probes (n=500 measurements).

3.3.4 *E. coli* O157:H7 detection with RCA signal enhancement

To investigate the efficacy of the detection system in detecting *E. coli* O157:H7 cells, we compared detections of *E. coli* O157:H7 cell with and without RCA signal enhancements at different cell concentrations. The fluorescence images of the detection results are shown in Figure 3-7A. It is clear that as the concentration of target cells increased, signal intensities also increased for detections both with and without RCA signal enhancement. It is also evident that for a given cell concentration, the detection signals with RCA enhancement (R1-R4) were always greater than those without (C1-C4); in fact, a closer look at Figure 3-7B reveals that detections with RCA resulted in approximately 30-50 folds increases in signal intensities, suggesting a significant signal enhancement by RCA for detections. As seen in Figure 3-7A, C1-C4 show detection singals without RCA enhancement, *i.e*. fluorescent probes were directly introduced to the capturing aptamer|bacterial cell|aptamer-primer sandwich detection system without the RCA -- this is in comparison with R1-R4, detections with the RCA. The reason why there are signals for C1-C4 is because the fluorescent probes have complementary sequences with a portion of the aptamer-primer complex. This design is done on purpose to show differences

between detection signals with and without RCA. As a result of the design, C1 – C4 still show fluorescence signals –albeit much weaker -- in comparison with the RCA group as can be seen in Figure 3-7A. As a result of the significant signal enhancement by RCA (see Figure 3-7A), the LOD was 10^3 cells/mL for detections without RCA while the LOD was 10^2 cells/mL for detections with RCA. The limit of detection is defined as the lowest bacterial concentration that can provide fluorescence signals at least three standard deviations greater than those from the negative control [52-54]. Furthermore, the linear relationship shown between signal intensities (with RCA) and cell concentrations ranging from 10^2 to 10^5 cells/mL (inset in Figure 3-7B) strongly suggests the current detection system with RCA signal enhancement will detect *E. coli* O157:H7 cell concentrations at as low as 10^2 cells/mL. It should be mentioned that microchannels modified with dendrimers and without capturing aptamers (*i.e*. blanks, B1-B4) showed minimal background signals at all cell concentrations studied (Figure 3-7A). The minimal background noises obtained might due to surface modifications with PAMAM dendrimers by decreasing surface non-specific adsorptions, thus further increasing detection sensitivities.

In an attempt to incorporate RCA approach with microfluidic channels, Sato *et al*. successfully detected *Salmonella enterica* by means of detecting the extracted genomic DNA from the target bacteria with RCA enhancement in microfluidic devices. This approach achieved high detection sensitivity due to the application of RCA [55]. In the current study, we also combine the RCA with microfluidic devices with the focus on developing a whole cell assay without the need to extract DNA molecules from the target samples. This could be advantageous for fast detection. We demonstrate that RCA signal

enhancement can significantly increase detection signals, thereby decreasing LOD by 10 folds from 10^3 cells/mL (*i.e.* without RCA) to 10^2 cells/mL (*i.e.* with RCA). Using an aptamer based biosensing system without RCA, Wu and colleagues [28] reported a LOD 10^4 cells/mL in their efforts to detect *E. coli* O157:H7 cells. The significant differences in LODs between the two studies strongly indicate the effectiveness of RCA in signal enhancement. It is also interesting to note that in this study, the LOD without RCA is 10^3 cells/mL, about 10 times more sensitive than the reported LOD of 10^4 cells/mL. This difference can be attributed to the use of PAMAM dendrimers in this study to 1) reduce background signals since PAMAM dendrimer modified microfluidic system has been shown to suppress up to 99% of non-specific particle/cell adhesions to PDMS microfluidic channel surfaces [41]; and 2) attach multiple copies of aptamers to the microchannel for detection by using PAMAM dendrimers as multifunctional templates to further conjugate capturing aptamers to provide more capturing surface areas and to achieve enhanced target capturing probabilities [56], both of which will enhance target capturing efficiency for detection, particularly in low concentration detections.

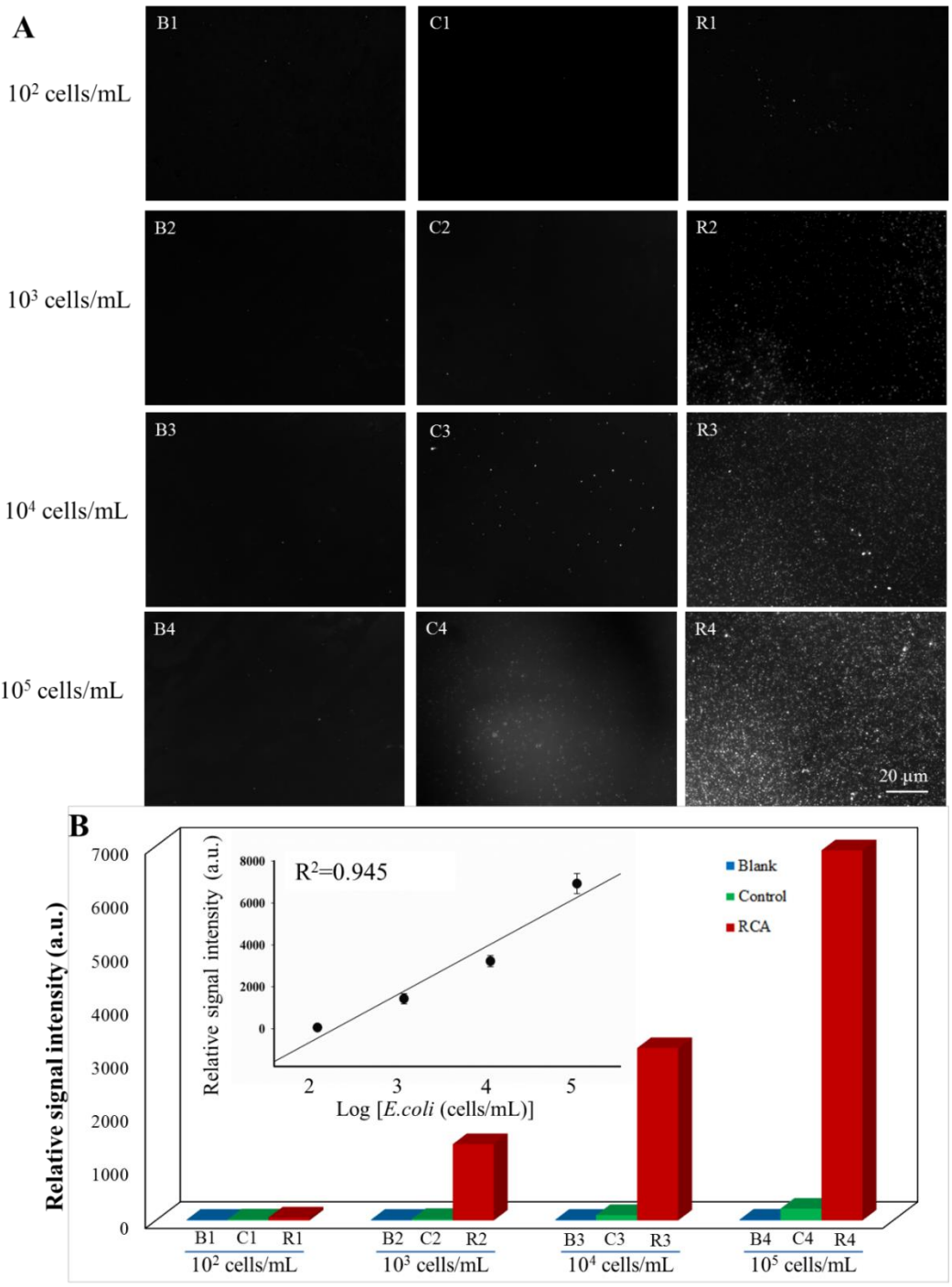

Figure 3-7 Detection of *E. coli* O157:H7 cells with and without RCA signal enhancement at different cell concentrations. A. Fluorescence images of detection results at different bacteria concentrations; B1 to B4 represent blank controls (channel surface with dendrimer

modification + bacteria + RCA, *i.e*. no capturing aptamers) at different cell concentrations; C1 to C4 represent detection without RCA at different detection concentrations; R1 to R4 represent detection with RCA groups. Note signal intensities comparisons between detections with and without RCA; B. signal intensities of different detections at different bacteria concentrations; Inset: relationship between RCA signal intensities and different bacteria concentrations.

3.3.5 Detection specificities

The specificity of the new microfluidic dendrimer-aptamer PDMS system for the detection of *E. coli* O157:H7 was investigated using non-target cells, including *Listeria innocua*, *E. coli* K12 and *E. coli* ER2420 at two different cell concentrations, *i.e.* 1×10^3 and 1×10^4 cells/mL. After RCA signal enhancement and fluorescence probe hybridization, fluorescence signals were measured. As shown in Figure 3-8, for both cell concentrations, the current simple microfluidic system demonstrates excellent specificities for *E. coli* O157:H7, the target bacterial cell, as the fluorescence signals from all non-target samples are minimal.

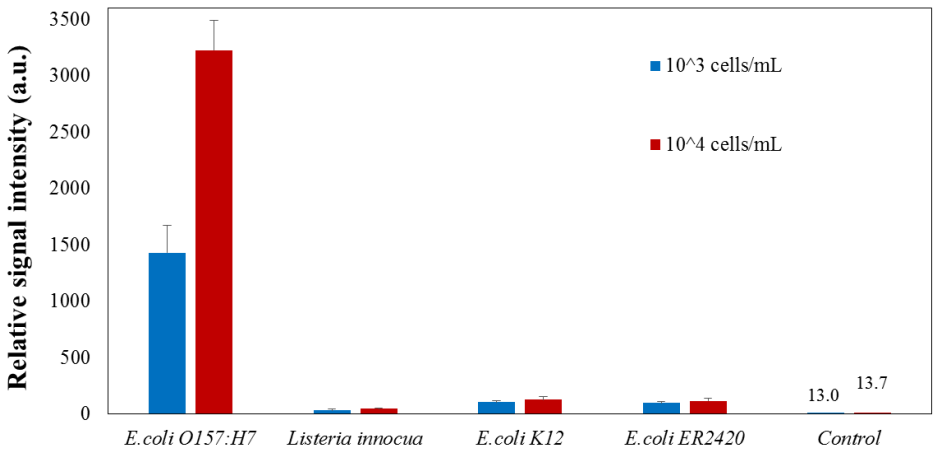

Figure 3-8 Detection specificities of the new dendrimer-aptamer-RCA detection system as demonstrated by detections of both target *E. coli* O157:H7 cells and non-target cells at concentrations of 10^3 and 10^4 cells/mL. Error bars represent standard deviations (n=9).

In addition, the detection performances of the current dendrimer-aptamer system with RCA signal enhancement was compared with those of recently reported methods (see supporting information Table 3-2). In particular, it is evident that whole cell assays are more advantageous as they do not require laborious DNA extraction procedures and therefore allow fast detection result turn-around. Furthermore, in comparison with other detection methods, the current method offers relatively high detection sensitivities with a LOD at 10^2 cells/mL. To the best of our knowledge, this is the best detection sensitivity achieved using simple microfluidic channels for bacterial detection to date. The simplicity of this design and the possibilities to integrate it with other on-chip microfluidic functionalities, such as sample preparations [13, 57], make this reported microchannel a powerful tool for bacteria detection by microfluidic devices.

Table 3-2 Comparisons on detection sensitivity of different methods for E. coli O157:H7 cells

Method	Sample type	Limit of detection (LOD)	Enrichment steps or DNA extraction	Overall detection time	Ref.
Multiplex Polymerase Chain Reaction (mPCR)	Purified DNA extracted from bacteria	0.45 to 0.05 pM/μl	Yes	More than 28 h	[58]
Real time PCR	Artificially contaminated meat products	10^3 to 10^4 CFU/g	Yes	More than 24 h	[59]
Multiplex PCR	Meat sample	10^3 CFU/ml	Yes	More than 30 h	[60]
Surface plasmon resonance (SPR) immunosensor	Bacteria in buffer	3.0×10^5 CFU/mL	No	Less than 2 h, excluding sample preparations	[61]
Fiber optic based biosensor	Ready-to-eat meat samples	~ 10^3 CFU/mL	No	More than 24 h, including cell enrichment culture	[62]
Lateral flow immunoassay	bacterial cells in PBS buffer and milk samples	1.14×10^3 CFU/mL and 1.14×10^4 CFU/mL, respectively.	No	< 1 h	[63]
Dendrimer-aptamer biosensing with RCA signal enhancement	Bacteria in PBS buffer	10^2 cells/mL	No	4 - 5 h	Current study

3.4 Conclusions

In this study, we designed a simple and highly sensitive dendrimer-aptamer-RCA microfluidic detection system to detect *E. coli* O157:H7 cells. To increase the detection sensitivity, PAMAM dendrimer was used to reduce background signals and at the same time used as a multi-handled template to subsequently conjugate multiple aptamers for greater probability and more surface area for target bacteria capturing. The design was advanced by the application of RCA to enhance detection signals to allow detection sensitivities to be further enhanced. The resulting microfluidic detection device showed an impressive LOD of 10^2 cells/mL with high specificity, which is a highly sensitive detection performance in the field of whole bacterial cell detection by simple microfluidic devices. Therefore, it is expected that its simple design and intrinsic possibilities to integrate with other on-chip functionality modules, such as sample separation and concentration, will make this novel microchannel a promising tool for pathogenic bacteria detection.

3.5 References

1. Scallan, E., et al., *Foodborne illness acquired in the United States—major pathogens.* Emerging Infectious Diseases, 2011. **17**(1).
2. Tauxe, R.V., *Emerging foodborne pathogens.* International Journal of Food Microbiology, 2002. **78**(1): p. 31-41.
3. Painter, J.A., et al., *Attribution of foodborne illnesses, hospitalizations, and deaths to food commodities by using outbreak data, United States, 1998–2008.* Emerging Infectious Diseases, 2013. **19**(3): p. 407.
4. Jalalpour, S., *Food borne diseases bacteria; frequency antibiotic resistance bacteria in Iranian foods.* African Journal of Microbiology Research, 2012. **6**(4): p. 719-723.
5. Sharma, H. and R. Mutharasan, *Review of biosensors for foodborne pathogens and toxins.* Sensors and Actuators B: Chemical, 2013. **183**: p. 535-549.
6. Radke, S.M. and E.C. Alocilja, *A high density microelectrode array biosensor for detection of E. coli O157: H7.* Biosensors and Bioelectronics, 2005. **20**(8): p. 1662-1667.

7. Mead, P.S., et al., *Food-related illness and death in the United States.* Emerging Infectious Diseases, 1999. **5**(5): p. 607.
8. Neil, K.P., et al., *A novel vehicle for transmission of Escherichia coli O157: H7 to humans: multistate outbreak of E. coli O157: H7 infections associated with consumption of ready-to-bake commercial prepackaged cookie dough—United States, 2009.* Clinical Infectious Diseases, 2012. **54**(4): p. 511-518.
9. Banatvala, N., et al., *The United States national prospective hemolytic uremic syndrome study: microbiologic, serologic, clinical, and epidemiologic findings.* Journal of Infectious Diseases, 2001. **183**(7): p. 1063-1070.
10. Gracias, K.S. and J.L. McKillip, *A review of conventional detection and enumeration methods for pathogenic bacteria in food.* Canadian Journal of Microbiology, 2004. **50**(11): p. 883-890.
11. de Boer, E. and R.R. Beumer, *Methodology for detection and typing of foodborne microorganisms.* International Journal of Food Microbiology, 1999. **50**(1): p. 119-130.
12. Lazcka, O., F.J. Del Campo, and F.X. Munoz, *Pathogen detection: a perspective of traditional methods and biosensors.* Biosensors and Bioelectronics, 2007. **22**(7): p. 1205-1217.
13. Jiang, Y., S. Zou, and X. Cao, *Rapid and ultra-sensitive detection of foodborne pathogens by miniaturized microfluidic devices: a review.* Analytical Methods, 2016. **8**(37): p. 6668-6681.
14. Chin, C.D., V. Linder, and S.K. Sia, *Lab-on-a-chip devices for global health: past studies and future opportunities.* Lab on a Chip, 2007. **7**(1): p. 41-57.
15. Yoon, J.Y. and B. Kim, *Lab-on-a-chip pathogen sensors for food safety.* Sensors, 2012. **12**(8): p. 10713-10741.
16. Mairhofer, J., K. Roppert, and P. Ertl, *Microfluidic systems for pathogen sensing: a review.* Sensors, 2009. **9**(6): p. 4804-4823.
17. Foudeh, A.M., et al., *Microfluidic designs and techniques using lab-on-a-chip devices for pathogen detection for point-of-care diagnostics.* Lab on a Chip, 2012. **12**(18): p. 3249-3266.
18. Jayasena, S.D., *Aptamers: an emerging class of molecules that rival antibodies in diagnostics.* Clinical Chemistry, 1999. **45**(9): p. 1628-1650.
19. Zhou, W., et al., *Aptamer-based biosensors for biomedical diagnostics.* Analyst, 2014. **139**(11): p. 2627-2640.

20. Nutiu, R. and Y. Li, *Structure-switching signaling aptamers.* Journal of the American Chemical Society, 2003. **125**(16): p. 4771-4778.
21. Cho, E.J., J.W. Lee, and A.D. Ellington, *Applications of aptamers as sensors.* Annual Review of Analytical Chemistry, 2009. **2**: p. 241-264.
22. Lee, H.J., et al., *A sensitive method to detect Escherichia coli based on immunomagnetic separation and real-time PCR amplification of aptamers.* Biosensors and Bioelectronics, 2009. **24**(12): p. 3550-3555.
23. Queirós, R.B., et al., *A label-free DNA aptamer-based impedance biosensor for the detection of E. coli outer membrane proteins.* Sensors and Actuators B: Chemical, 2013. **181**: p. 766-772.
24. Wu, W., et al., *A sensitive lateral flow biosensor for Escherichia coli O157: H7 detection based on aptamer mediated strand displacement amplification.* Analytica Chimica Acta, 2015. **861**: p. 62-68.
25. Ma, X., et al., *An aptamer-based electrochemical biosensor for the detection of Salmonella.* Journal of Microbiological Methods, 2014. **98**: p. 94-98.
26. Fang, Z., et al., *Lateral flow biosensor for DNA extraction-free detection of salmonella based on aptamer mediated strand displacement amplification.* Biosensors and Bioelectronics, 2014. **56**: p. 192-197.
27. Yuan, J., et al., *A visual detection method for Salmonella typhimurium based on aptamer recognition and nanogold labeling.* Food Control, 2014. **37**: p. 188-192.
28. Wu, W., et al., *An aptamer-based biosensor for colorimetric detection of Escherichia coli O157: H7.* PloS One, 2012. **7**(11): p. e48999.
29. Demirkol, D.O. and S. Timur, *A sandwich-type assay based on quantum dot/aptamer bioconjugates for analysis of E. Coli O157: H7 in microtiter plate format.* International Journal of Polymeric Materials and Polymeric Biomaterials, 2016. **65**(2): p. 85-90.
30. Yan, X., et al., *Highly sensitive fluorescent aptasensor for Salmonella paratyphi A via DNase I-mediated cyclic signal amplification.* Analytical Methods, 2015. **7**(24): p. 10243-10250.
31. Giri, B., et al., *Signal amplification strategies for microfluidic immunoassays.* TrAC Trends in Analytical Chemistry, 2016. **79**: p. 326-334.
32. Lee, J., et al., *Diffractometric detection of proteins using microbead-based rolling circle amplification.* Analytical Chemistry, 2009. **82**(1): p. 197-202.

33. Lizardi, P.M., et al., *Mutation detection and single-molecule counting using isothermal rolling-circle amplification.* Nature Genetics, 1998. **19**(3): p. 225-232.
34. Nallur, G., et al., *Signal amplification by rolling circle amplification on DNA microarrays.* Nucleic Acids Research, 2001. **29**(23): p. e118-e118.
35. Najafzadeh, M., et al., *Rapid identification of fungal pathogens by rolling circle amplification using Fonsecaea as a model.* Mycoses, 2011. **54**(5): p. e577-e582.
36. Wu, Z., et al., *Electrochemical aptameric recognition system for a sensitive protein assay based on specific target binding-induced rolling circle amplification.* Analytical Chemistry, 2010. **82**(6): p. 2282-2289.
37. Cheng, W., et al., *Cascade signal amplification strategy for subattomolar protein detection by rolling circle amplification and quantum dots tagging.* Analytical Chemistry, 2010. **82**(8): p. 3337-3342.
38. Tong, P., et al., *Double-probe signal enhancing strategy for toxin aptasensing based on rolling circle amplification.* Biosensors and Bioelectronics, 2012. **33**(1): p. 146-151.
39. Guo, Y., et al., *Label-free and highly sensitive electrochemical detection of E. coli based on rolling circle amplifications coupled peroxidase-mimicking DNAzyme amplification.* Biosensors and Bioelectronics, 2016. **75**: p. 315-319.
40. Bi, S., et al., *A chemiluminescence imaging array for the detection of cancer cells by dual-aptamer recognition and bio-bar-code nanoprobe-based rolling circle amplification.* Chemical Communications, 2013. **49**(33): p. 3452-3454.
41. Qin, Y., et al., *Developing an ultra non-fouling SU-8 and PDMS hybrid microfluidic device by poly (amidoamine) engraftment.* Colloids and Surfaces B: Biointerfaces, 2015. **127**: p. 247-255.
42. Bruno, J. and J. Chanpong, *Methods of producing competitive aptamer fret reagents and assays*. 2009, US Application. Patent No. US20090186342A1.
43. Zhou, L., et al., *Aptamer-based rolling circle amplification: a platform for electrochemical detection of protein.* Analytical Chemistry, 2007. **79**(19): p. 7492-7500.
44. Yeh, P.Y., et al., *Nonfouling hydrophilic poly (ethylene glycol) engraftment strategy for PDMS/SU-8 heterogeneous microfluidic devices.* Langmuir, 2012. **28**(46): p. 16227-16236.
45. Hao, X., *Detection of foodborne pathogens using microfluidic channels*, in *Chemical and Biochemical Engineering*. 2015, University of Ottawa.

46. Bußkamp, H., et al., *A new building block for DNA network formation by self-assembly and polymerase chain reaction.* Beilstein Journal of Organic Chemistry, 2014. **10**(1): p. 1037-1046.
47. Collins, T.J., *ImageJ for microscopy.* Biotechniques, 2007. **43**(1 Suppl): p. 25-30.
48. Cesaro-Tadic, S., et al., *High-sensitivity miniaturized immunoassays for tumor necrosis factor α using microfluidic systems.* Lab on a Chip, 2004. **4**(6): p. 563-569.
49. Xu, W., et al., *Ultrasensitive colorimetric DNA detection using a combination of rolling circle amplification and nicking endonuclease-assisted nanoparticle amplification (NEANA).* Small, 2012. **8**(12): p. 1846-1850.
50. Cheglakov, Z., et al., *Increasing the complexity of periodic protein nanostructures by the rolling-circle-amplified synthesis of aptamers.* Angewandte Chemie International Edition, 2008. **47**(1): p. 126-130.
51. Lyubchenko, Y.L., et al., *Atomic force microscopy imaging of double stranded DNA and RNA.* Journal of Biomolecular Structure and Dynamics, 1992. **10**(3): p. 589-606.
52. Shrivastava, A. and V. Gupta, *Methods for the determination of limit of detection and limit of quantitation of the analytical methods.* Chronicles of Young Scientists, 2011. **2**(1): p. 21-21.
53. Chen, C.-S. and R.A. Durst, *Simultaneous detection of Escherichia coli O157: H7, Salmonella spp. and Listeria monocytogenes with an array-based immunosorbent assay using universal protein G-liposomal nanovesicles.* Talanta, 2006. **69**(1): p. 232-238.
54. Waswa, J., J. Irudayaraj, and C. DebRoy, *Direct detection of E. coli O157: H7 in selected food systems by a surface plasmon resonance biosensor*. LWT-Food Science and Technology, 2007. **40**(2): p. 187-192.
55. Sato, K., et al., *Microbead-based rolling circle amplification in a microchip for sensitive DNA detection.* Lab on a Chip, 2010. **10**(10): p. 1262-1266.
56. Esfand, R. and D.A. Tomalia, *Poly (amidoamine)(PAMAM) dendrimers: from biomimicry to drug delivery and biomedical applications.* Drug Discovery Today, 2001. **6**(8): p. 427-436.
57. Mu, C., et al., *Development of a highly effective multi-stage surface acoustic wave SU-8 microfluidic concentrator.* Sensors and Actuators B: Chemical, 2015. **215**: p. 77-85.
58. Park, Y.S., S.R. Lee, and Y.G. Kim, *Detection of Escherichia coli O157: H7, Salmonella spp., Staphylococcus aureus and Listeria monocytogenes in kimchi by multiplex polymerase chain reaction (mPCR).* Journal of Microbiology-Seoul, 2006. **44**(1): p. 92.

59. Nguyen, L., et al., *Detection of Escherichia coli O157: H7 and Listeria monocytogenes in beef products by real-time polymerase chain reaction.* Foodbourne Pathogens & Disease, 2004. **1**(4): p. 231-240.
60. Kawasaki, S., et al., *Multiplex PCR for simultaneous detection of Salmonella spp., Listeria monocytogenes, and Escherichia coli O157: H7 in meat samples.* Journal of Food Protection, 2005. **68**(3): p. 551-556.
61. Wang, Y., et al., *Subtractive inhibition assay for the detection of E. coli O157: H7 using surface plasmon resonance.* Sensors, 2011. **11**(3): p. 2728-2739.
62. Ohk, S.H. and A.K. Bhunia, *Multiplex fiber optic biosensor for detection of Listeria monocytogenes, Escherichia coli O157: H7 and Salmonella enterica from ready-to-eat meat samples.* Food Microbiology, 2013. **33**(2): p. 166-171.
63. Chen, M., et al., *Dual gold nanoparticle lateflow immunoassay for sensitive detection of Escherichia coli O157: H7.* Analytica Chimica Acta, 2015. **876**: p. 71-76.

Chapter 4 A study on rolling circle amplification and its signal enhancing application in a dendrimer-PDMS microfluidic system

Chapter 4

A study on rolling circle amplification and its signal enhancing application in a dendrimer-PDMS microfluidic system

Yuqian Jiang, Shan Zou, Xudong Cao

In Chapter 3, a dendrimer-aptamer-RCA detection system for *E. coli* O157:H7 was developed and showed up to 50-fold signal enhancement compared with non-RCA dendrimer-aptamer detection system. In this chapter, to further investigate effects of the RCA reaction time on the detection signal intensification, the morphological changes of RCA products were characterized by atomic force microscopy. Different RCA reaction times were applied to enhance fluorescence detection signals and results indicated that 2 h was the optimal reaction time.

Abstract

Rolling circle amplification (RCA) has been used to enhance detection signals as its long single stranded RCA products can provide multiple binding sites for signal probes for detection. Therefore formations and morphologies of the RCA products are important to study in order to optimize such signal amplifications. However, molecular chain growth of the RCA products has not been particularly explored in the literature. In the current study, we employ atomic force microscopy (AFM) to monitor the RCA products during the course of the RCA process over time. Subsequently the results of the RCA obtained from the AFM study are combined with those from the conventional electrophoresis method to optimize RCA reactions for rapid and sensitive detection. We show that there appears to be an non-homogeneous RCA initiation phase in early to mid stage of the RCA reaction where some chains grow faster while others grow slower or even remain dormant, an observation that has not been reported in the literature. Furthermore, to demonstrate the efficacy of RCA signal enhancement in detection, RCA is used in a dendrimer-aptamer modified microfluidic whole-cell detection system to detect samples spiked with *E. coli* O157:H7 cells at concentrations ranging from 10^2 to 10^5 cells/mL. Our results show that there is a linear relationship between detection signals and *E. coli* O157:H7 cell concentrations after RCA signal intensification. Our results also indicate that the RCA is able to enhance detection signals by around 100 folds and that the observed signal enhancement and detection sensitivity increase with increasing RCA reaction time. Taken together, these results suggest that a properly configured RCA reaction in combination with dendrimer-

aptamer surface modified microfluidic channel is a promising approach to simple and sensitive whole-cell detection.

Keywords: Rolling circle amplification; Pathogen detection; Aptamers; Biosensing; Atomic force microscopy; Agarose gel electrophoresis.

4.1 Introduction

Sensitive detections of foodborne pathogenic bacteria are important since a large number of food poisoning cases are caused by bacterial pathogens [1]. For example, 353 cases of outbreaks related to foodborne *E. coli* O157:H7 were reported in the United States from 2003 to 2012 [2]. The Canadian Food Inspection Agency (CFIA) issued 9 recalls in 2013, all due to *E. coli* O157:H7 contaminations. Since traditional culture methods for pathogen detection are time-consuming, and molecular methods such as enzyme-linked immunosorbent assay (ELISA) and polymerase chain reaction (PCR) require lengthy and labor-intensive cell enrichment and DNA extraction procedures, developing an efficient and sensitive detection method for *E. coli* O157:H7 represents a pressing issue. Since the late 1980s, lab-on-a-chip (LOC) or microfluidic biosensors have attracted growing research interest [3-8]. In a microfluidic biosensing system, antibodies, nucleic acids, aptamers or bacteriophages are the main recognition elements used to identify target analytes [4]. To further enhance detection sensitivity and signal read-out, signal amplification techniques, such as nucleic acid amplification, antigen-antibody amplification, nanoparticles and magnetic beads have been employed [9-13].

Rolling circle amplification (RCA) has been widely used to enhance detection signals in biosensing systems due to its high efficiency and isothermal reaction temperature requirements. As an isothermal enzymatic DNA/RNA amplification technique, RCA utilizes circular single stranded nucleic acid template (*i.e.* circular template) to generate repetitive and long single stranded DNA/RNA molecular chains under the catalysis of polymerases [14, 15]. Requirements for a RCA reaction include a circular template, a

primer with a free 3'-end, DNA or RNA polymerase and deoxynucleotides (dNTPs) as substrates [16]. In general, a RCA starts with the formation of a circular template from a padlock probe, an originally linear oligonucleotide that can be ligated to form a circular molecule, which can be subsequently used as a template for DNA amplifications [17]. For the DNA amplifications, a properly designed primer is required to anneal to and circularize the padlock probe to form a circular template (under the catalytic action of T4 DNA ligase), after which nucleotides will be continuously added to the 3' end of the primer – based on the circular template, thus growing a long molecular chain from the original primer. This "lock and roll" process can extend a single stranded DNA/RNA molecule hundreds to thousands of times of its original length based on the circular template. In comparison with PCR, RCA does not require expensive equipment for thermal cycling or special laboratory conditions. In fact, RCA can be conducted on any solid supports or in complex biological environments such as on a cell surface or inside of a cell [15], and the reaction temperature for RCA can range from room temperature to 42 ºC [18]. These advantages make the RCA technique versatile and adaptable to low-cost and robust biosensing applications. As a result, RCA has gained considerable attention as an important DNA amplification tool and has been used for ultrasensitive detection of nucleic acids, proteins and other molecules [15, 16, 19-26].

Typically, the long RCA products consist of hundreds to thousands of tandem repeats which act as binding sites for signal elements, such as complementary fluorescent probes. Therefore, knowledge about chain growth of the RCA products is important to optimize their applications in detection. To characterize the RCA products, several methods have

been reported in the literature. Gel electrophoresis (polyacrylamide gel electrophoresis or agarose gel electrophoresis) is one of the most common ways to characterize the RCA products by directly demonstrating the production and relative quantity of high molecular weight RCA products [27, 28]. In addition, SYBR Green I dye has also been used to detect RCA products that would give off fluorescence signals when long strands of RCA products interact with the SYBR Green dye [29]. In comparison with the two above mentioned techniques, AFM has been used to provide a versatile platform for imaging and manipulating molecules at a single-molecule resolution, which has been successfully employed in a number of studies to characterize DNA molecules, including RCA products [30-33]. Generally, RCA products have been characterized by AFM solely for morphology analysis in order to confirm the presence of RCA products (RCAPs) as evidence of successful RCA reactions and only at the end of the RCA reactions [28, 33-36]. In the present study, AFM is used to follow the RCA reaction during the course of the RCA process, including ligation between aptamer-primer complex and padlock probe (*i.e.* formation of circular template), and the "rolling" process for RCA products as a function of reaction time. This new approach to study the RCA reaction, in combination with the gel electrophoresis method, provides new insights into the RCA reaction process over time. In the latter aspects of the study, RCA signal intensification was further explored in a poly(dimethyl siloxane) (PDMS) microfluidic system for application to *E. coli* O157:H7 cell detection. Results from the dendrimer-aptamer modified microfluidic detection system showed that the detection signals of *E. coli* O157:H7 were significantly enhanced by up to 100-fold when RCA was used; moreover, the effect of detection signal enhancement was increased as the RCA reaction time was increased and a linear relationship was observed

between bacterial concentration and detection signal. These results support the concept that RCA can be used as a signal amplification strategy in combination with a microfluidic detection system in a sensitive whole-cell detection assay. As a result, it is concluded that this is a promising new approach to develop a simple and sensitive detection method for foodborne and clinical pathogenic bacteria.

4.2 Experimental

4.2.1 Materials

All DNA oligonucleotides (sequences shown below), nuclease-free water, IDTE buffer were purchased from Integrated DNA Technologies (IDT) (Coralville, IA). Poly(amido amine) (PAMAM) dendrimers with ethylenediamine core (generation seven) (G7) were obtained from Sigma-Aldrich (Oakville, ON). 1-(3-dimethylaminopropyl)-3-ethylcarbodiimide (EDC) was obtained from Alfa Aesar (Ward Hill, MA). (3-aminopropyl)-trimethoxysilane (APTMS) and N-hydroxysuccinimide (NHS) were purchased from Thermo Fisher Scientific (Rockford, IL). Phi29 DNA polymerase, T4 DNA ligase, deoxynucleotide (dNTP) solution mix, Tris/Boric Acid/EDTA (TBE) buffer mix, Promega blue/orange loading dye, DNA ladders, and ethidium bromide for electrophoresis were purchased from Fisher Scientific (Ottawa, ON). Sylgard 184 poly(dimethyl siloxane) (PDMS) kit was purchased from Dow Corning (Midland, MI). All other chemicals were obtained from Sigma-Aldrich (Oakville, ON) and used as received unless indicated otherwise. Formalin killed *E. coli* O157: H7 cells were generously donated by the Canada Food Inspection Agency (Ottawa, ON).

Table 4-1 Oligonucleotide sequences used in this section

Sequence name	Sequence
E. coli O157:H7 capturing aptamer [37, 38]	5'-NH_2-ATCCG TCACA CCTGC TCTAT CAAAT GTGCA GATAT CAAGA CGATT TGTAC AAGAT GGTGT TGGCT CCCGT AT-3'
Aptamer-primer complex	5'-*ATCCG TCACA CCTGC TCTAT CAAAT GTGCA GATAT CAAGA CGATT TGTAC AAGAT GGTGT TGGCT CCCGT AT*TTT TTTTT GTCCG TGCTA GAAGG AAACA GTTAC-3'
Designed padlock probe	5'-TAGCA CGGAC ATATA TGATG GACCG CAGTA TGAGT ATCTC CTATC ACTAC TAAGT GGAAG AAATG TAACT GTTTC CTTC-3'
Designed Cy3 fluorescently labelled complementary probe	5'-Cy3-GTTTC CTTCT AGCAC-3'

Note: the *italic* portion of aptamer-primer complex has the same sequence as the capturing aptamer and that the underlined portion is the primer [25] where the single and double underlined sequences are complementary to the sequences likewise underlined in the padlock probe sequence.

4.2.2 Fabrication and surface modification of PDMS microfluidic device with *E. coli* O157:H7 capturing aptamers

PDMS microfluidic devices were prepared using a standard lithography process. All procedures were based on well-established protocols reported elsewhere [39, 40].

4.2.3 Rolling circle amplification reactions

A typical RCA reaction starts with the formation of circular templates. To prepare the circular templates, 50 μL hybrid solution containing 100 nM of both aptamer-primer complex and padlock probe were incubated at 37 °C for 30 min to allow hybridization

between the aptamer-primer complex and the padlock probe. This was followed by ligation reaction catalyzed by 10 U T4 DNA ligase in 10 × T4 ligation buffer (400 mM Tris-HCl, 100 mM $MgCl_2$, 100 mM DTT, 5 mM ATP, pH 7.8) at room temperature for 30 min, after which the ligation mixture was heated at 65 °C for 10 min to inactivate the T4 DNA ligase in order to stop the ligation reaction. Subsequently, the RCA reaction was performed by adding phi29 DNA polymerase and dNTP into the ligation reaction mixture. Specifically, for a 100 μL RCA reaction mixture, 10 U of phi29 DNA polymerase was used. After the reaction mixture was allowed to react at 37 °C for pre-determined periods of time (*i.e.*, 5, 15, 60, 120, 180, and 600 min), it was heated at 65 °C for 10 min to inactivate the phi29 DNA polymerase in order to stop the RCA reaction. It should be mentioned that all oligonucleotides were denatured by heating at 95 °C for 5 min and quickly cooled on ice for 1 min to ensure desired intramolecular folding immediately prior to RCA reactions [25].

4.2.4 Agarose gel electrophoresis (AGE) analysis of RCA products

To analyze RCA products, AGE was used. Briefly, RCA products were analyzed by 0.5% or 2% agarose gel electrophoresis in TBE buffer (44.5 mM Tris, 44.5 mM H_3BO_3, 1 mM EDTA) (pH 8.5) at room temperature for 30 min at 75 V. Gel images were obtained using an AlphaImager (HP Imaging System, San Jose, CA) and were quantitatively analysed using ImageJ [41, 42].

4.2.5 AFM studies of RCA reactions over time

The RCA reactions were followed over time using AFM. Specifically, RCA product solutions (100 nM) at different RCA reaction time points were drop-cast on freshly cleaved

mica surfaces (V-1 Grade, SPI Supplies Division of Structure Probe Inc., West Chester, PA) pre-treated with 5 mM $NiCl_2$ in order to increase affinities between the negatively charged DNA molecules and the mica surfaces. The coated mica surfaces were then carefully rinsed by filtered Milli-Q water and dried by pure nitrogen. The resulting samples were imaged using a Multimode AFM with NanoScope V controller (Bruker Nano Surfaces Division, Santa Barbara, CA) in either Bruker's ScanAsyst or PeakForce QNM modes. ScanAsyst-Air AFM probes (0.4 N/m, f_0: 50-90 kHz, Bruker AFM Probes, Camarillo, CA) with typical tip diameters of 2-5 nm were used. AFM images were acquired with a scan size between 500 by 500 nm and 10 by 10 μm (512 × 512 pixel) and at a scan rate of 1 Hz. The obtained AFM images were processed using open access software Gwyddion (http://gwyddion.net/).

4.2.6 Dendrimer-aptamer-RCA detection and signal enhancement system

The construction of the dendrimer-aptamer modified PDMS microfluidic devices followed a procedure reported elsewhere with minor modifications [43]. The detection of the *E. coli* O157:H7 was demonstrated using a dendrimer-aptamer (surface bound) | *E. coli* O157:H7 cell | aptamer-primer complex, a sandwich detection system with RCA for signal enhancements, as shown in Figure 4-1. Specifically, highly branched dendrimers were immobilized on the inner surfaces of the PDMS microchannels and the capturing aptamers were consequently conjugated to the dendrimer coated PDMS surfaces via functional groups of the PAMAM dendrimers. The benefits of using the PAMAM dendrimers were twofold as we have demonstrated in our previous work [39, 44]: (1) the dendrimers are shown to render modified surfaces non-fouling to minimize non-specific bindings, thus

reducing background signals; and (2) the immobilized multifunctional dendrimers can provide multiple binding sites for conjugating multiple copies of the *E. coli* O157:H7-capturing aptamer to significantly increase capturing probabilities. Buffer solutions spiked with formalin inactivated *E. coli* O157:H7 cells at different concentrations (*i.e.* 10^2, 10^3, 10^4 and 10^5 cells/mL) were injected into the dendrimer-aptamer modified PDMS devices at a flow rate of 0.05 ml/h for 1 h. Subsequently the devices were washed with PBS (pH 7.4), after which the aptamer-primer complex was introduced to react with the captured *E. coli* O157:H7 cells for 30 min in order to form a sandwich detection format (see Figure 4-1). The resulting devices were carefully washed again with PBS (pH 7.4), and signal enhancements by RCA were initiated on top of the captured *E. coli* O157:H7 cells using procedures described above. Subsequently, complementary fluorescent Cy3 labelled probes (see sequence in Materials section) were used to hybrid with the RCA products at 37 °C for 30 min to give off quantitative signals for detection. The whole system was washed with PBS (pH 7.4) to remove excess probes. Fluorescence images were captured using an inverted Olympus fluorescence microscope (IX81, Richmond Hill, ON) equipped with a high-resolution camera (QImaging, Surrey, BC). Specifically, the images were captured using 1000 ms as the exposure time. At least twenty fluorescence images for each sample were collected from random and different areas of the detection surfaces, and fluorescence signals were analyzed by ImageJ [45]. More details can be found in section 3.2.4.3. PDMS microchannels modified with dendrimers only but not with capturing aptamers were used as controls.

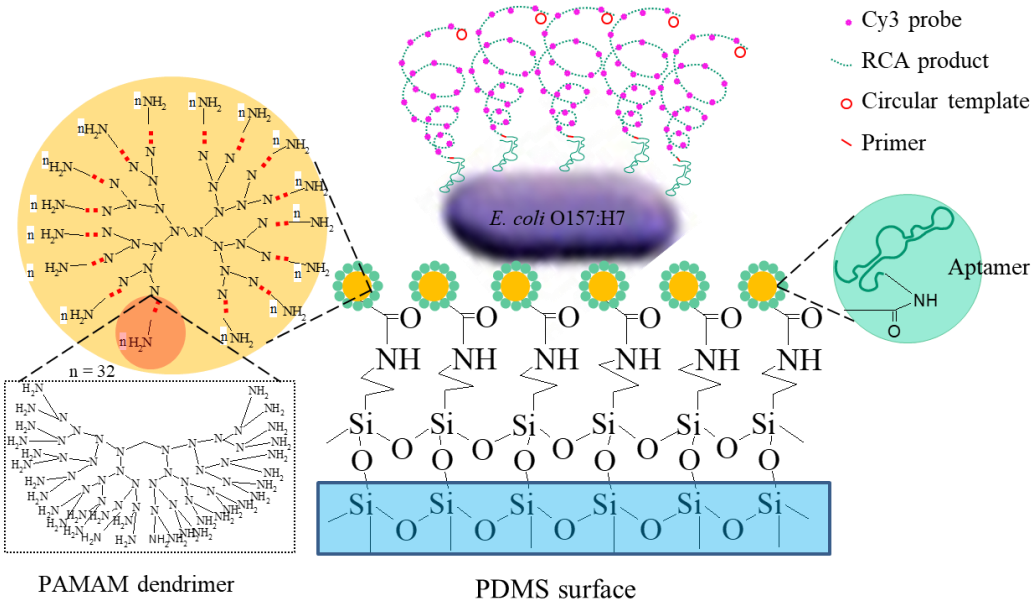

Figure 4-1 Schematic drawing to demonstrate dendrimer-aptamer sandwich detection system with RCA for signal enhancement.

4.3 Results and discussion

PDMS microfluidic channels were successfully prepared and their inner surfaces were modified with *E. coli* O157:H7 capturing aptamers as reported in our previous studies [39, 40].

4.3.1 RCA product characterizations by both AFM and AGE

Products from the RCA reactions were characterized using both AFM and AGE. As shown in Figure 4-2A, a RCA reaction was initiated with the generation of circular DNA molecular chains that were formed by ligating aptamer-primer complexes and padlock probes by T4 DNA ligase. In the presence of the phi29 DNA polymerase, single stranded DNA molecules (*i.e.*, RCA products) were produced using the circular DNA molecular

chains as templates (*i.e.* the process of rolling). AFM was used to study the morphologies of the RCA products throughout the RCA reaction over time. As shown in Figure 4-2, it is evident that circular template DNAs were formed in the ligation procedure. It is interesting to note that the circular templates were indeed circular in shape (see Figure 4-2D). In addition, a closer analysis of these circular templates showed that the sizes of the circular structures were around 15 nm in diameter. This result is in good agreement with a theoretical value of 20-30 nm, considering that the padlock probe is a linear ssDNA of 79 nt [46]. Significantly, although AFM has been used to probe RCA products [31], a "rolling" RCA product has been successfully imaged by AFM (shown in Figure 4-2E) for the first time to the best of our knowledge. This imaged RCA product appeared to have an elongated and coiled molecular chain that exhibited a morphology similar to that of a "lollipop". The contour length of this RCA product was measured to be ~ 1.3 μm, consistent with other published studies reporting that RCA products are usually from hundreds of nanometers to microns in length depending on RCA reaction conditions [14, 47]. It is interesting to note that at the central portion of this lollipop, there was a bright spot that had a greater height (measured at ~ 3 nm) than the RCA product chain (measured at ~ 1 nm); this spot is most likely phi29 polymerase since it is known that during the RCA reactions, phi29 polymerase attaches to a primer-template substrate before the next incoming nucleotide binds the polymerase [48, 49]. This is the first direct evidence in support of this concept. Short ssDNAs of aptamer-primer complex and padlock probes were also imaged by AFM to show small DNA molecules before ligation and RCA reactions, where small molecular spots rather than long DNA strands were observed (Figs. 2b and 2c).

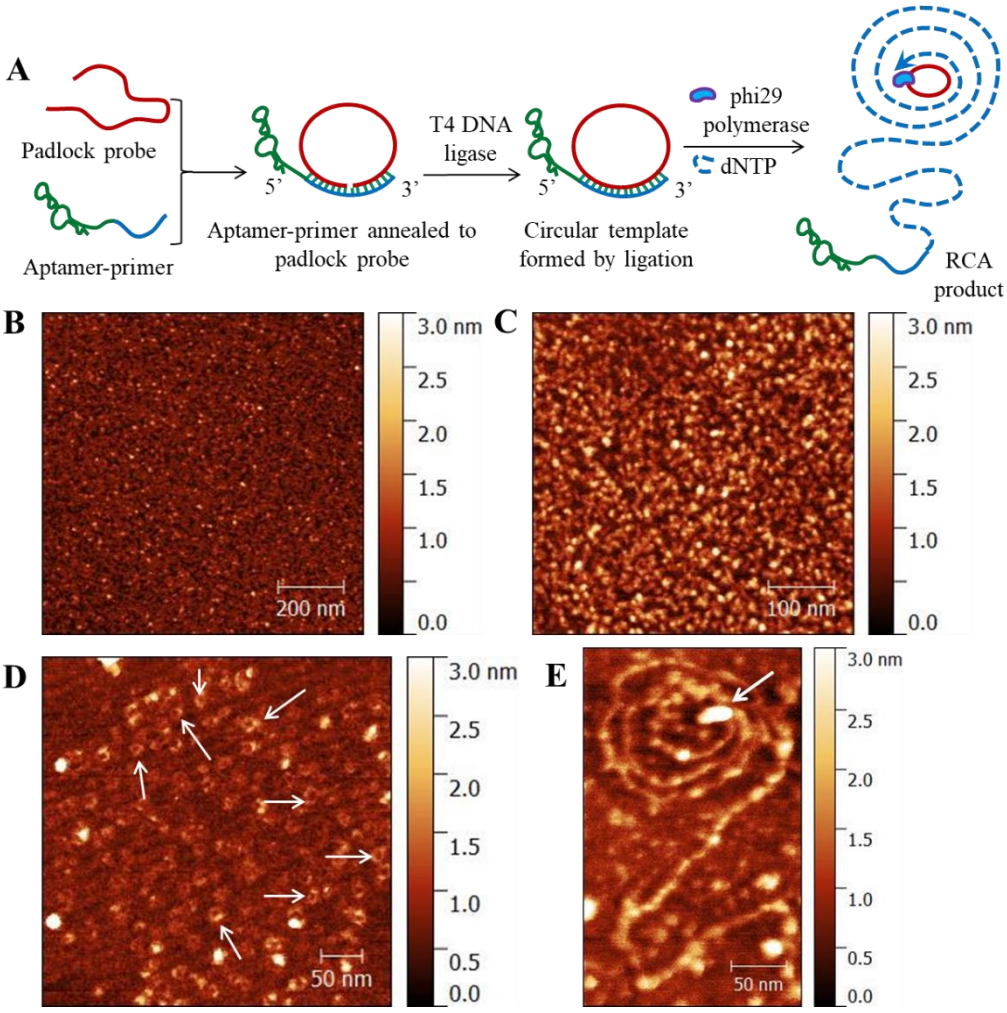

Figure 4-2 RCA reactions as characterized by AFM. A. schematic illustration of padlock-ligated RCA process; B. AFM image of aptamer-primer complex before ligation; C. AFM image of padlock probe before ligation; D. formation of circular templates (arrows) after ligation between aptamer-primer complex and padlock probe; E. RCA product showing a long and coiled ssDNA chain and phi29 polymerase (arrow) at the growing end of the molecular chain.

Agarose gel electrophoresis was also used to confirm the formation of RCA products, and the results are shown in Figure 4-3. It can be seen that both the original aptamer-primer

complex (Lane 1) and the original padlock probe (Lane 2) displayed short DNA molecular chains, as expected. In contrast, after the ligation reactions between the aptamer-primer and the padlock probe, the resulting circular template showed a roughly two-fold increase in molecular weight, as shown in Lane 3. Besides, there are several extra bands in Lane 3 which might be the dimers of aptamer-primer and padlock probes or other by-products of ligation reactions. Likewise, Lane 4 showed RCA products after 2 h of RCA reaction, suggesting the presence of high molecular weight products (>> 10 kbp) with extremely low mobility. This result is in good agreement with previous studies that showed similar gel electrophoresis results [50, 51]. It has been established that the synthesis rate of RCA is around 50 nt/sec along the circular template [52], which translates into the formation of RCA products with molecular weights of more than 300 kbp after 2 h of RCA reaction. This suggests that the RCA products would have too low of a mobility to migrate out of the wells in the electrophoresis experiment, which was confirmed by the AGE results in the current study (Lane 4). It is worthwhile to mention that other than the high molecular weight products, Lane 4 also showed some relatively low molecular weight products, likely explained by the presence of short RCA products and unreacted aptamer-primer complex (*i.e.* circular templates) after 2 h of RCA reaction.

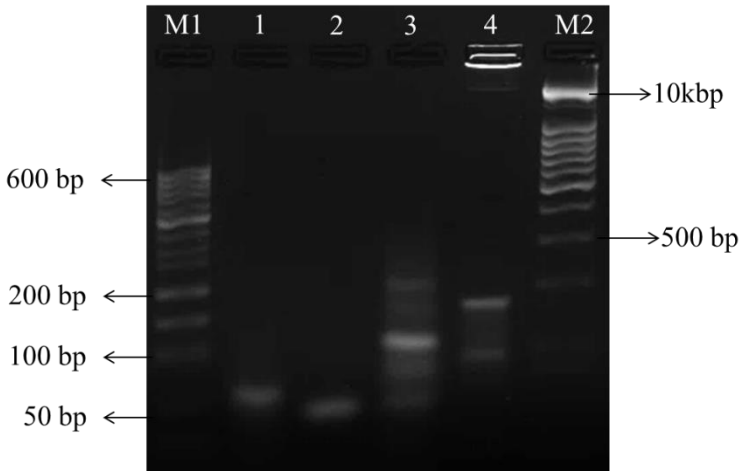

Figure 4-3 RCA reactions as characterized by AGE (2% agarose gel). Lanes shown are original aptamer-primer complex (Lane 1), original padlock probe (Lane 2), ligation product of aptamer-primer complex and padlock probe (Lane 3), and RCA products after 2 h of RCA reaction (Lane 4). Lanes M1 and M2 are DNA markers with top band at 650 bp and 10 kbp, respectively.

4.3.2 RCA reactions followed by AFM over time

RCA reactions were followed over time by AFM. To achieve this, RCA samples were collected at different time points, and their RCA product morphologies were studied using AFM. As shown in Figure 4-4, at 5 min, there were many small round shaped dots, suggesting the formation of many circular templates by ligation reactions between aptamer-primer complexes and padlock probes without obviously observed RCA chains; however, no observable long RCA products were spotted. At 15 min, it was clear that the majority of the dots had - albeit small - “tails”, likely suggesting that initiations of RCA mainly took place within this time frame but there was no significant RCA chain growth during the

same period of time. When reaction time was increased to 60 min, long chains of RCA products were readily identified. However, it was also evident that the initiation of the RCA reaction and the growth of the RCA product were not homogenous as most of the circular templates did not grow into long RCA product chains; in fact, only a very small percentage of the molecules showed long chains after 60 min of RCA reaction while the vast majority of the chains were still short. In contrast, when the reaction time was further increased to 2 h, a greater percentage of long RCA product chains were observed, and these chains appeared to be longer than those at 60 min. However, it is also evident that there were still a significant amount of short molecular chains as indicated by the presence of small dots. When the reaction time was further increased to 3 h, it was clear that the number of the short chains was significantly reduced; however, it was difficult to compare the RCA product chain length due to entanglements of the long chains. Finally, after 10 h of RCA reaction, AFM results demonstrated many extremely extensive and long RCA products. It is also interesting to note that the short DNA strands observed at previous time points completely disappeared, confirming that the low weight products seen in AGE (see Figure 4-3 in Lane 4) were short chain RCA products. Overall, the AFM results appears to suggest that for the given RCA reaction system, there is a non-homogeneous RCA lag phase at the early to mid stage (*i.e.* 0 ~ 60 min) of the RCA reaction where some chains grow faster while others grow slower or even remain dormant. This observation has not been reported in the literature before, likely because AFM has not been used to characterized RCA products over time like the way it was used in the current study. It is not yet known why there are such differences between the chains. However, it is clear that if given enough time (*i.e.* 10 h) all chains will grow into high molecular weight RCA products.

As a signal amplification technique, RCA reaction conditions should be optimized to achieve sufficient signal amplification with reasonable detection time. Based on the results obtained from the AFM study (see Figure 4-4), it can be concluded that a reaction time of 2 h or more should be chosen as optimum RCA reaction time, as our AFM results showed that for RCA reaction for more than 2 h there were many fully developed RCA chains for sufficient signal enhancement; in addition, a much longer reaction time would not be desirable since it would not allow for fast turn-around detection [4]. As a result, a reaction time of 2 h was determined as an optimal RCA reaction time in this study. A closer look at RCA conditions used by previously published studies shows that RCA reactions were carried out using a wide range of reaction times, ranging from 10 min to 6 h [16, 25, 50-58], suggesting that RCA conditions, such as reaction time, should be further investigated for RCA optimizations. It would be particularly interesting to study ways to initiate homogeneous RCA reactions in the initial phase (*i.e*. in the first 1 hour of the RCA reaction as shown in this study) to allow for more effective RCA signal intensifications within a shorter period of time (*i.e.* 1 hour or less).

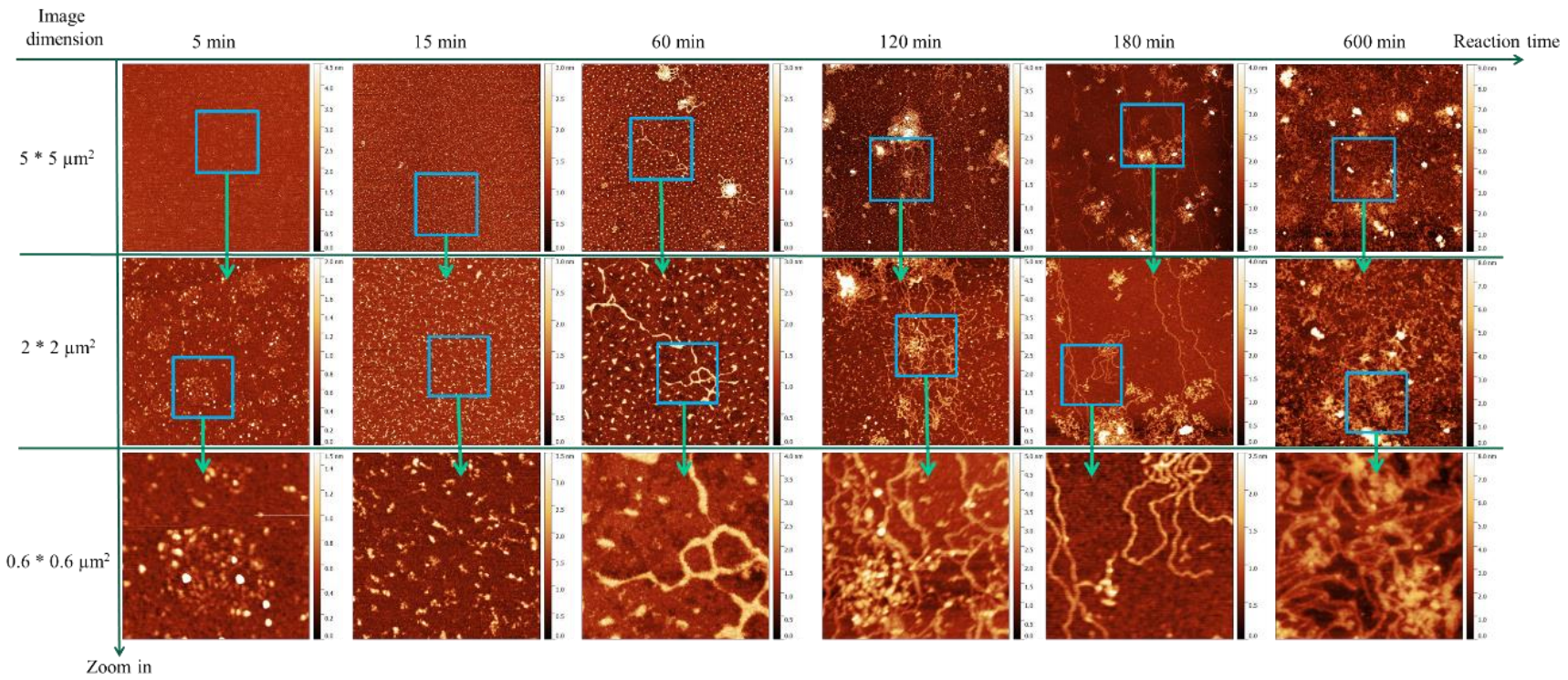

Figure 4-4 Morphological changes of RCA reactions products by AFM from varied reaction time. The downward arrows point different levels of zoom-ins.

The RCA reactions were also studied by AGE. Figure 4-5 shows AGE results of RCA products collected over a range of RCA reaction times (Figure 4-5A) and relative quantities of the high molecular weight molecules in the overall RCA products from all groups (*i.e.* fractions with molecular weights greater than 10 kbp, as shown in the box in Fig 4-5B). The ethidium bromide staining dyes intercalate with nucleic acid RCA products and the relative fluorescence intensity under UV light is positively proportional to the amount of RCA products. It is clear that the fractions of high molecular weight RCA products increased with increasing RCA reaction time. For example, from 5 min to 120 min, high molecular weight RCA products increased dramatically with increasing reaction time. However, when the reaction time was further increased beyond 120 min, the reaction rate appeared to slow down significantly, as additional 60 min reaction time from 120 min to 180 min did not result in as much RCA products as it did from 60 min to 120 min. Therefore, 2 h was used as an optimal reaction time.

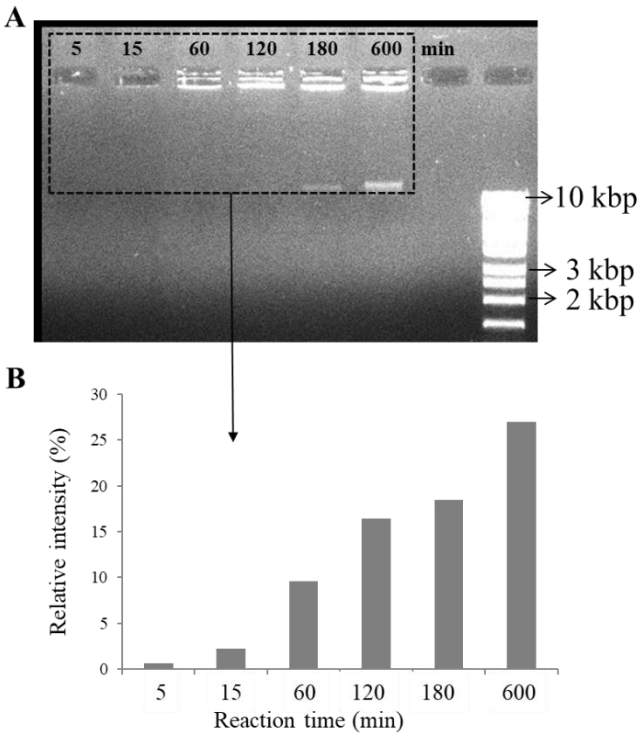

Figure 4-5 RCA products at different reaction time points characterized by AGE. A. AGE image of RCA products at different reaction time points; B. relative quantities of high molecular weight RCA products (*i.e.* molecular weight greater than 10 kbp as shown within the box) as a function of RCA reaction time.

4.3.3 Application of RCA in detection systems for signal intensification

To further investigate the effect of reaction time on detection signal enhancement, a dendrimer-aptamer based microfluidic detection system was used to detect samples spiked with formalin inactivated *E. coli* O157:H7 cells at different concentrations (*i.e.* 10^2 - 10^5 cells/mL) using RCA signal amplification with different reaction times. As shown in Figure 4-6A, there was a linear relationship between detected fluorescence signals and bacterial

concentrations investigated. Furthermore, for a given concentration, the detected fluorescence signals increased with increasing RCA reaction time, as shown in Figure 4-6B. This is expected since increasing RCA reaction time would result in increasing chain length of the RCA products, which in turn resulted in more complementary binding sites for fluorescent probes to conjugate for enhanced signal for detection. A closer analysis of the data reveals that the slope of each of the straight lines increased with increasing RCA reaction time, suggesting an increasingly sensitive detection with longer RCA reaction time, as detection sensitivities are determined by the slope of the response curve [59, 60]. In contrast, detection without RCA signal enhancements (fluorescent probes were directly introduced to the detection systems without RCA reactions) showed significantly less sensitive responses (*i.e.* slope was flat). This demonstrates the benefit of using RCA that enhanced the fluorescence signals by almost 100 folds, when signals from detections with RCA enhancement for 2 h or 10 h were compared with that without RCA at the same concentrations. It is also interesting to note that for detections employing 10 h as RCA reaction time, while the fluorescence signals increased with increasing target concentrations in the sample, it levelled off at 10^5 cells/mL of *E. coli* O157:H7 (see Figure 4-6A); this is likely because at this high concentration and long RCA reaction time, the RCA products formed highly extensive and entangled structures that physically prevented the fluorescent probes to freely (and quantitatively) hybrid with the RCA products. Therefore, it is clear that RCA reactions enhance detection signals and that the extent of enhancement is dependent on the RCA reaction time. Longer RCA reaction times (*e.g.*, 2 h and 10 h) resulted in higher detection sensitivities -- as evidenced by both the greater slopes in the linear relationship seen in Figure 4-6A and more intense signals for a given

concentration -- suggesting that long RCA reaction times are particularly beneficial for low target concentration detection, such as at concentrations of 10^2 cells/mL or lower. However, excessively long RCA reaction time may not be practically feasible as it will significantly slow down the detection process and render the detection method less attractive. Therefore, RCA reaction for 2 h was chosen as the optimal reaction condition for the detection of *E. coli* O157:H7 at the concentration range investigated in this study. It is interesting to note that there is a wide range of RCA reaction conditions used in the literature for detection [16, 25, 51, 55, 61], further suggesting that an appropriate RCA reaction conditions for a particular detection application are dependent on not only factors such as circular template design and RCA reaction temperature, but also the target analyte concentration whose interplay with RCA reaction time is a key factor to be further studied.

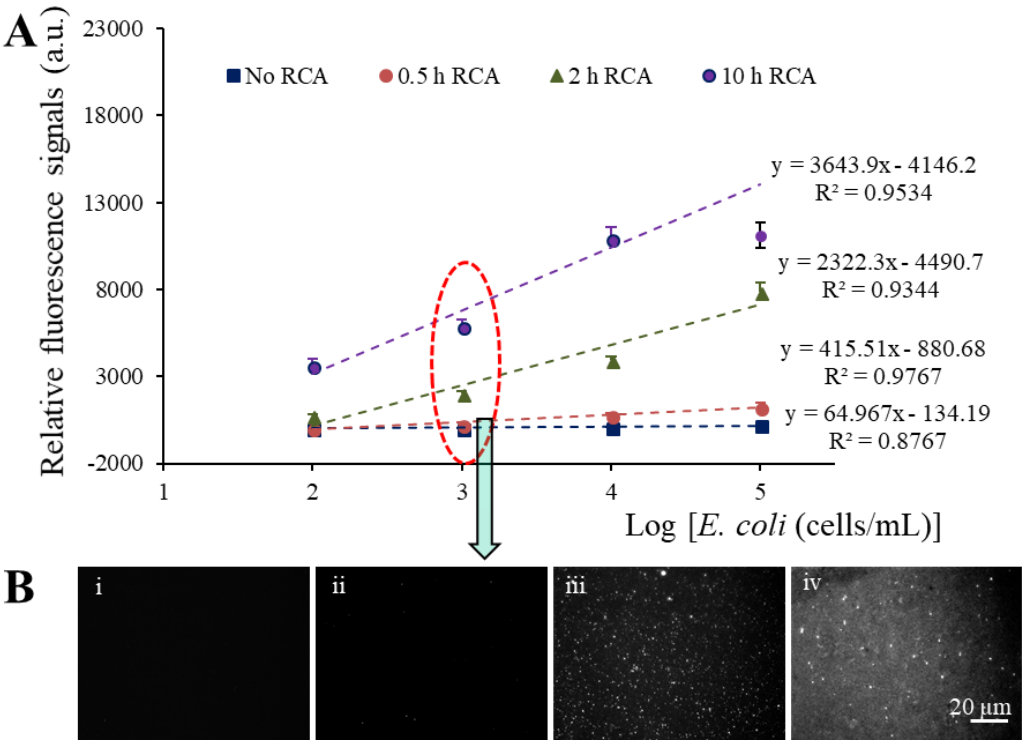

Figure 4-6 Detections of different *E. coli* O157:H7 concentrations using RCA signal enhancement. A. Fluorescence signals of aptamer-RCA detection system with different RCA reaction time when varied *E. coli* O157:H7 concentrations were applied (from 10^2 to 10^5 cells/mL); B. Fluorescence images of detection systems with varied RCA reaction time (i - iv: 0, 0.5, 2, 10 h, respectively) when 10^3 cells/mL *E. coli* O157:H7 were applied.

4.3.4 Detection specificity

The specificity of the current dendrimer-aptamer-RCA microfluidic detection system for *E. coli* O157:H7 was investigated by testing several non-target bacteria including *Listeria innocua*, *E. coli* K12 and *E. coli* ER2420. The detection signals collected after RCA intensification for *E. coli* O157:H7, *Listeria innocua*, *E. coli* K12, *E. coli* ER2420 and

control (*i.e.* without any bacteria) were plotted at different bacteria concentrations (Figure 4-7). It is evident that the fluorescence signals for the target *E. coli* O157:H7 at concentrations of 10^3 and 10^4 cells/ml were significantly higher than those for non-targets and controls, demonstrating excellent specificities of the current detection platform for *E. coli* O157:H7.

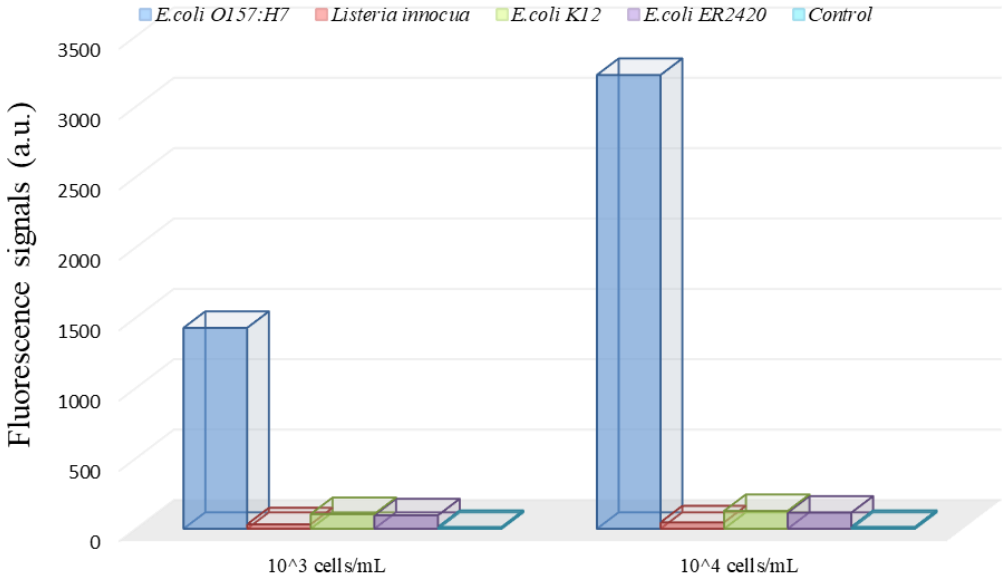

Figure 4-7 Detection specificity of the current dendrimer-aptamer-RCA detection system by a comparison on fluorescence signals on target *E. coli* O157:H7 cells and non-target *Listeria innocua*, *E. coli* K12 and *E. coli* ER2420 cells at different cell concentrations.

To further demonstrate that the detection system is a powerful and sensitive whole-cell detection platform, its detection performance was compared with those of other recently published whole bacterial cell detection systems in Table 4-1. The difference between this

comparison table with the previous Table 3-2 in Chapter 4 is that whole cell detection methods for foodborne bacteria were compared with the work in this chapter. It is evident that the detection results obtained in this study showed lower LOD than other electrochemical, colorimetric and fluorescence biosensors, and that the present dendrimer-aptamer-RCA microfluidic system is a simple and sensitive approach to whole cell detections. The simplicity of this design and the possibilities to integrate with other on-chip microfluidic sample preparation functionalities, such as sample concentration [62] and separation [63], make this reported microfluidic detection method a powerful tool for foodborne pathogen detection.

Table 4-2 A comparison of the current dendrimer-aptamer-RCA approach with other reported methods for whole bacterial cell detection

Target	Method	Sample	Limit of detection (LOD)	Ref.
E. coli O157:H7	Fluorescence immunoassay	Spiked whole milk	5×10^2 CFU/mL	[64]
E. coli O157:H7	Electrochemical	Ground beef	2.05×10^3 CFU/mL	[65]
S. Typhimurium	immunosensor	Chicken rinse water	1.04×10^3 CFU/mL	
E. coli O157:H7	Electrochemical biosensor	Bacteria solution	10^3 CFU/ml	[66]
E. coli O157:H7	Bacteriophage based colorimetric assay	Spiked skim milk	4.9×10^4 CFU/mL	[67]
E. coli O157:H7	Amperometric immunosensor	Bacteria solution	3.6×10^3 CFU/mL	[26]
E. coli O157:H7	Electrochemical impedance immunosensor	Bacteria solution	10^2 CFU/ml	[68]

S. typhimurium	Aptamer-based impedimetric sensor	Bacteria solution	6×10^2 CFU/mL	[69]
L. monocytogenes	Colorimetric sensing platform	Spiked milk	2.17×10^2 CFU/ml	[70]
E. coli O157:H7	Aptamer-based fluorescence biosensor	Bacteria solution	10^2 cells/mL	This study

4.4 Conclusions

In this study, the RCA reaction process and RCA products were investigated by both AFM and gel electrophoresis for a better understanding of RCA reaction and its application in detection signal amplification. For the first time, lollipop-like RCA product morphology was directly documented by AFM, and the development of long strands of RCA products was followed over time. The AFM results revealed a non-homogeneous chain growth especially at the initial stage of the RCA reaction. AFM and gel characterizations were both used to characterize the RCA reaction conditions and RCA signal intensification was used in the dendrimer-aptamer microfluidic system to detect *E. coli* O157:H7 in samples. Our results showed that there was a 100-fold signal enhancement by RCA reaction in comparison with detection without RCA and that with increasing RCA reaction time, both the detection signals and detection sensitivity increased. Given the wide range of RCA reaction conditions employed in the literature, further studies are warranted to investigate optimal RCA conditions such as reaction time, reaction temperature, and interplays between the above mentioned conditions and target analyte concentrations. It is our belief that a properly configured RCA reaction in combination with a dendrimer-aptamer surface-modified microfluidic channel is a promising approach to simple and sensitive bacterial whole-cell detection.

4.5 References

1. Jalalpour, S., *Food borne diseases bacteria; frequency antibiotic resistance bacteria in Iranian foods.* African Journal of Microbiology Research, 2012. **6**(4): p. 719-723.
2. Heiman, K.E., et al., *Escherichia coli O157 outbreaks in the United States, 2003-2012.* Emerging Infectious Diseases, 2015. **21**(8): p. 1293.
3. Foudeh, A.M., et al., *Microfluidic designs and techniques using lab-on-a-chip devices for pathogen detection for point-of-care diagnostics.* Lab on a Chip, 2012. **12**(18): p. 3249-3266.
4. Jiang, Y., S. Zou, and X. Cao, *Rapid and ultra-sensitive detection of foodborne pathogens by using miniaturized microfluidic devices: a review.* Analytical Methods, 2016. **8**(37): p. 6668-6681.
5. Eccleston, J.F., R.G. Messerschmidt, and D.W. Yates, *A simple rapid mixing device.* Analytical Biochemistry, 1980. **106**(1): p. 73-77.
6. Matsumoto, K., S. Katsuyama, and H. Ohya, *Separation of yeast by cross-flow filtration with backwashing.* Journal of Fermentation Technology, 1987. **65**(1): p. 77-83.
7. Dolník, V., M. Deml, and P. Boček, *Large sample volume preseparation for trace analysis in isotachophoresis.* Journal of Chromatography A, 1985. **320**(1): p. 89-97.
8. Whitesides, G.M., *The origins and the future of microfluidics.* Nature, 2006. **442**(7101): p. 368-373.
9. Singh, R., et al., *Biosensors for pathogen detection: A smart approach towards clinical diagnosis.* Sensors and Actuators B: Chemical, 2014. **197**: p. 385-404.
10. Schweitzer, B., et al., *Immunoassays with rolling circle DNA amplification: a versatile platform for ultrasensitive antigen detection.* Proceedings of the National Academy of Sciences, 2000. **97**(18): p. 10113-10119.
11. Hahn, M.A., J.S. Tabb, and T.D. Krauss, *Detection of single bacterial pathogens with semiconductor quantum dots.* Analytical Chemistry, 2005. **77**(15): p. 4861-4869.
12. Qiu, J., et al., *Immunomagnetic separation and rapid detection of bacteria using bioluminescence and microfluidics.* Talanta, 2009. **79**(3): p. 787-795.
13. Arata, H., et al., *Rapid and sensitive microRNA detection with laminar flow-assisted dendritic amplification on power-free microfluidic chip.* PloS One, 2012. **7**(11): p. e48329.

14. Zhao, W., et al., *Rolling circle amplification: applications in nanotechnology and biodetection with functional nucleic acids.* Angewandte Chemie International Edition, 2008. **47**(34): p. 6330-6337.
15. Ali, M.M., et al., *Rolling circle amplification: a versatile tool for chemical biology, materials science and medicine.* Chemical Society Reviews, 2014. **43**(10): p. 3324-3341.
16. Lee, J., et al., *Diffractometric detection of proteins using microbead-based rolling circle amplification.* Analytical Chemistry, 2009. **82**(1): p. 197-202.
17. Kuhnemund, M., et al., *Circle-to-circle amplification on a digital microfluidic chip for amplified single molecule detection.* Lab on a Chip, 2014. **14**(16): p. 2983-2992.
18. Takahashi, H., Y. Okamura, and T. Kobori, *Use of DNA circLigase for direct isothermal detection of microbial mRNAs by RNA-primed rolling circle amplification and preparation of ø29 DNA polymerase not contaminated by amplifiable DNA*, in *Rolling circle amplification (RCA)*. 2016, Springer. p. 37-46.
19. Johne, R., et al., *Rolling-circle amplification of viral DNA genomes using phi29 polymerase.* Trends in Microbiology, 2009. **17**(5): p. 205-211.
20. Shavitt, O. and Z. Livneh, *Rolling-circle replication of UV-irradiated duplex DNA in the phi X174 replicative-form----single-strand replication system in vitro.* Journal of Bacteriology, 1989. **171**(6): p. 3530-3538.
21. Kingsmore, S.F. and D.D. Patel, *Multiplexed protein profiling on antibody-based microarrays by rolling circle amplification.* Current Opinion in Biotechnology, 2003. **14**(1): p. 74-81.
22. Fischer, N.O., T.M. Tarasow, and J.B.H. Tok, *Protein detection via direct enzymatic amplification of short DNA aptamers.* Analytical Biochemistry, 2008. **373**(1): p. 121-128.
23. Nilsson, M., et al., *Analyzing genes using closing and replicating circles.* Trends in Biotechnology, 2006. **24**(2): p. 83-88.
24. Nilsson, M., *Lock and roll: single-molecule genotyping in situ using padlock probes and rolling-circle amplification.* Histochemistry and Cell Biology, 2006. **126**(2): p. 159-164.
25. Zhou, L., et al., *Aptamer-based rolling circle amplification: a platform for electrochemical detection of protein.* Analytical Chemistry, 2007. **79**(19): p. 7492-7500.
26. Cheng, P., et al., *A novel regeneration-free E. coli O157:H7 amperometric immunosensor based on functionalised four-layer magnetic nanoparticles.* Sensors and Actuators B: Chemical, 2014. **204**: p. 561-567.

27. Ali, M.M. and Y. Li, *Colorimetric sensing by using allosteric-DNAzyme-coupled rolling circle amplification and a peptide nucleic acid–organic dye probe.* Angewandte Chemie, 2009. **121**(19): p. 3564-3567.
28. Cheglakov, Z., et al., *Diagnosing viruses by the rolling circle amplified synthesis of DNAzymes.* Organic & Biomolecular Chemistry, 2007. **5**(2): p. 223-225.
29. Rodrigues, A.M., et al., *Rapid identification of emerging human-pathogenic Sporothrix species with rolling circle amplification.* Frontiers in Microbiology, 2015. **6**.
30. Martin, A., et al., *Observation of DNA–polymer condensate formation in real time at a molecular level.* FEBS letters, 2000. **480**(2-3): p. 106-112.
31. Mizuta, R., M. Mizuta, and D. Kitamura, *Atomic force microscopy analysis of rolling circle amplification of plasmid DNA.* Archives of Histology and Cytology, 2003. **66**(2): p. 175-181.
32. Li, Z., et al., *A replicable tetrahedral nanostructure self-assembled from a single DNA strand.* Journal of the American Chemical Society, 2009. **131**(36): p. 13093-13098.
33. Xu, W., et al., *Ultrasensitive colorimetric DNA detection using a combination of rolling circle amplification and nicking endonuclease-assisted nanoparticle amplification (NEANA).* Small, 2012. **8**(12): p. 1846-1850.
34. Beyer, S., P. Nickels, and F.C. Simmel, *Periodic DNA nanotemplates synthesized by rolling circle amplification.* Nano Letters, 2005. **5**(4): p. 719-722.
35. Yata, T., et al., *Efficient amplification of self-gelling polypod-like structured DNA by rolling circle amplification and enzymatic digestion.* Scientific Reports, 2015. **5**: p. 14979
36. Ma, Y., et al., *RCA strands as scaffolds to create nanoscale shapes by a few staple strands.* Journal of the American Chemical Society, 2013. **135**(8): p. 2959-2962.
37. Wu, W., et al., *An aptamer-based biosensor for colorimetric detection of Escherichia coli O157: H7.* PloS One, 2012. **7**(11): p. e48999.
38. Bruno, J. and J. Chanpong, *Methods of producing competitive aptamer fret reagents and assays*. 2009, US Application. Patent No. US20090186342A1.
39. Qin, Y., et al., *Developing an ultra non-fouling SU-8 and PDMS hybrid microfluidic device by poly (amidoamine) engraftment.* Colloids and Surfaces B: Biointerfaces, 2015. **127**: p. 247-255.
40. Yeh, P.Y., et al., *Nonfouling hydrophilic poly (ethylene glycol) engraftment strategy for PDMS/SU-8 heterogeneous microfluidic devices.* Langmuir, 2012. **28**(46): p. 16227-16236.

41. Shoaib, M., et al., *Multiple displacement amplification for complex mixtures of DNA fragments.* BMC Genomics, 2008. **9**(1): p. 415.
42. Abràmoff, M.D., P.J. Magalhães, and S.J. Ram, *Image processing with ImageJ.* Biophotonics International, 2004. **11**(7): p. 36-42.
43. Jiang, Y., S. Zou, and X. Cao, *A simple dendrimer-aptamer based microfluidic platform for E. coli O157: H7 detection and signal intensification by rolling circle amplification.* Sensors and Actuators B: Chemical, 2017. **251**: p. 976-984.
44. Qin, Y., et al., *Developing a non-fouling hybrid microfluidic device for applications in circulating tumour cell detections.* Colloids and Surfaces B: Biointerfaces, 2017. **151**: p. 39-46.
45. Collins, T.J., *ImageJ for microscopy.* Biotechniques, 2007. **43**(1 Suppl): p. 25-30.
46. Pang, D., A.R. Thierry, and A. Dritschilo, *DNA studies using atomic force microscopy: capabilities for measurement of short DNA fragments.* Frontiers in Molecular Biosciences, 2015. **2**: p. 1.
47. Zhao, W., et al., *Bioinspired multivalent DNA network for capture and release of cells.* Proceedings of the National Academy of Sciences, 2012. **109**(48): p. 19626-19631.
48. Berman, A.J., et al., *Structures of phi29 DNA polymerase complexed with substrate: the mechanism of translocation in B-family polymerases.* The EMBO Journal, 2007. **26**(14): p. 3494-3505.
49. Kamtekar, S., et al., *Insights into strand displacement and processivity from the crystal structure of the protein-primed DNA polymerase of bacteriophage φ29.* Molecular Cell, 2004. **16**(4): p. 609-618.
50. Guo, Y., et al., *A functional oligonucleotide probe from an encapsulated silver nanocluster assembled by rolling circle amplification and its application in label-free sensors.* RSC Advances, 2016. **6**(92): p. 88967-88973.
51. Tong, P., et al., *Double-probe signal enhancing strategy for toxin aptasensing based on rolling circle amplification.* Biosensors and Bioelectronics, 2012. **33**(1): p. 146-151.
52. Dean, F.B., et al., *Rapid amplification of plasmid and phage DNA using phi29 DNA polymerase and multiply-primed rolling circle amplification.* Genome Research, 2001. **11**(6): p. 1095-1099.
53. Tang, L., et al., *Colorimetric and ultrasensitive bioassay based on a dual-amplification system using aptamer and DNAzyme.* Analytical Chemistry, 2012. **84**(11): p. 4711-4717.

54. He, Y., B. Jiao, and H. Tang, *Interaction of single-stranded DNA with graphene oxide: fluorescence study and its application for S1 nuclease detection.* Rsc Advances, 2014. **4**(35): p. 18294-18300.
55. Cheng, W., et al., *A facile scanometric strategy for ultrasensitive detection of protein using aptamer-initiated rolling circle amplification.* Chemical Communications, 2010. **46**(36): p. 6720-6722.
56. Hao, L., et al., *An enhanced chemiluminescence resonance energy transfer aptasensor based on rolling circle amplification and WS_2 nanosheet for Staphylococcus aureus detection.* Analytica Chimica Acta, 2017. **959**: p. 83-90.
57. He, Y., et al., *"Off" to "On" surface-enhanced raman spectroscopy platform with padlock probe-based exponential rolling circle amplification for ultrasensitive detection of microRNA 155.* Analytical Chemistry, 2017. **89**(5): p. 2866-2872.
58. Jiang, H., et al., *G-quadruplex fluorescent probe-mediated real-time rolling circle amplification strategy for highly sensitive microRNA detection.* Analytica Chimica Acta, 2016. **943**: p. 114-122.
59. Ingle Jr, J., *Sensitivity and limit of detection in quantitative spectrometric methods.* Journal of Chemical Education, 1974. **51**(2): p. 100.
60. Norrod, K.L., et al., *Quantitative comparison of five SERS substrates: sensitivity and limit of detection.* Applied Spectroscopy, 1997. **51**(7): p. 994-1001.
61. He, P., et al., *Ultrasensitive detection of thrombin using surface plasmon resonance and quartz crystal microbalance sensors by aptamer-based rolling circle amplification and nanoparticle signal enhancement.* Chemical Communications, 2014. **50**(12): p. 1481-1484.
62. Mu, C., et al., *Development of a highly effective multi-stage surface acoustic wave SU-8 microfluidic concentrator.* Sensors and Actuators B: Chemical, 2015. **215**: p. 77-85.
63. Yeh, P., et al., *An Efficient Spiral Microchannel for Continuous Small Particle Separations.* Sensors and Actuators B: Chemical, 2017.
64. Chen, R., et al., *A novel fluorescence immunoassay for the sensitive detection of Escherichia coli O157:H7 in milk based on catalase-mediated fluorescence quenching of CdTe quantum dots.* Analytica Chimica Acta, 2016. **947**: p. 50-57.
65. Xu, M., R. Wang, and Y. Li, *Rapid detection of Escherichia coli O157: H7 and Salmonella Typhimurium in foods using an electrochemical immunosensor based on screen-printed interdigitated microelectrode and immunomagnetic separation.* Talanta, 2016. **148**: p. 200-208.

66. Li, Y., et al., *Impedance based detection of pathogenic E. coli O157: H7 using a ferrocene-antimicrobial peptide modified biosensor*. Biosensors and Bioelectronics, 2014. **58**: p. 193-199.
67. Zhang, Y., et al., *Rapid and selective detection of E. coli O157:H7 combining phagomagnetic separation with enzymatic colorimetry.* Food Chemistry, 2017. **234**: p. 332-338.
68. Li, Z., et al., *Electrochemical Impedance Immunosensor Based on Self-Assembled Monolayers for Rapid Detection of Escherichia coli O157: H7 with Signal Amplification Using Lectin.* Sensors, 2015. **15**(8): p. 19212-19224.
69. Labib, M., et al., *Aptamer-based viability impedimetric sensor for bacteria.* Analytical Chemistry, 2012. **84**(21): p. 8966-8969.
70. Alhogail, S., G.A. Suaifan, and M. Zourob, *Rapid colorimetric sensing platform for the detection of Listeria monocytogenes foodborne pathogen.* Biosensors and Bioelectronics, 2016. **86**: p. 1061-1066.

Chapter 5 Developing a dual-RCA aptamer-based microfluidic platform for sensitive whole-cell detections of *E. coli* O157:H7

Chapter 5

Developing a dual-RCA aptamer-based microfluidic platform for sensitive whole-cell detections of *E. coli* O157:H7

Yuqian Jiang [a, b], Shan Zou [b], Xudong Cao [a, *]

Based on the detection system described in Chapter 3 and Chapter 4, a new RCA sequence set was designed to produce tandem repeated aptamers for *E. coli* O157:H7 in order to improve the capture efficiency of the dendrimer modified PDMS microchannel. In this chapter, cRCA was characterized and used to *in situ* synthesize poly-aptamers, which was verified to perform higher capture efficiency compared with the previous mono-layer aptamers.

Abstract

Aptamer based microfluidic platforms have been developed rapidly and strategies to improve detection sensitivity are highly desired. As capturing agents, aptamers immobilized right into a detection system should improve capture of target bacterial cells. In this study, rolling circle amplification (RCA) was used to produce repeated capture aptamer units (capturing RCA, cRCA) and characterized using atomic force microscopy and gel electrophoresis. *In situ* synthesized cRCA products on a microchannel inner surface composed of long single stranded tandem repeated aptamers (cRCA-aptamers) were used for capturing *E. coli* O157:H7 cells. This cRCA-aptamer-modified microchannel showed more than 3 times higher capture efficiency than the previously constructed microchannel modified using a single layer of *E. coli* O157:H7 aptamers (monolayer aptamers). To transduce and intensify detection signals, a different RCA set (sRCA) was further applied to the detection system after bacterial cells were captured by the cRCA-aptamers. sRCA products were visualized by complementary fluorescent probes to quantitatively determine the number of target cells. Linear relationships between fluorescence signals and *E. coli* O157:H7 concentrations ranging from 10^2 to 10^4 cells/mL were obtained. Results also showed that the cRCA-aptamers increased fluorescence signals up to 5-fold in comparison with the previous monolayer aptamers system. This dual-RCA detection system is a promising approach for sensitive detection of pathogenic bacteria in food, environmental and clinical detection systems.

Keywords: Rolling circle amplification; Bacteria detection; Aptamers; Biosensors; Atomic force microscopy; Microfluidic channels.

5.1 Introduction

Researchers have devoted continuously increasing efforts in the field of "lab on a chip" (LOC), or micro total analysis systems (μTAS), in the past two decades [1-5]. Detection of foodborne pathogenic bacteria, such as *E. coli* O157:H7 and *Salmonella*, using microfluidic analysis systems has developed rapidly and gained growing attention due to the miniaturized sizes of the devices, potential for continuous sampling and reduced costs [6-8]. In a microfluidic detection system, recognition elements are usually immobilized for target identification. Aptamers, as one type of recognition element in microfluidic detection systems, are *in vitro* selected single stranded nucleic acids identified using Systematic Evolution of Ligands by EXponential enrichment (SELEX) [9-11]. Aptamers have been used as sensing agents to recognize and bind to their corresponding targets with high affinities and specificities [12, 13]. As reported, bacterial cells captured by aptamers in microfluidic systems can be subsequently eluted for cell sample purification and enrichment before DNA extraction, followed by PCR based assays for detection [14, 15]. In addition, the captured cells can be further visualized into read-out detection signals by transduction of binding interactions between target cells and corresponding aptamers [16, 17].

Rolling circle amplification (RCA) is an efficient isothermal nucleic acid amplification technique, which extends very short primers (~ 15 mer) into several micrometers of long single stranded products (~ 100,000 mer) [18, 19]. RCA has been exploited in many applications in biosensing and detection. Typically, it has been used for signal amplification to enhance detection sensitivity of systems for detection of nucleic acids,

proteins, and target elements [20-25]. RCA products consist of tandem repeating copies (determined by the designed circular template) acting as multiple binding sites for the complementary signal probes. Generally, the complementary oligonucleotides for RCA products are tagged with fluorescent dyes, magnetic beads, quantum dots or other nanoparticles [26-29]. In this study, RCA was used for intensifying detection signals (signal RCA or sRCA). Essentially, those repeating units of RCA products can be modified into desired sequences by altering the circular template. Taking advantage of this feature, researchers have produced tandem repeating aptamers with high efficiency for a specific target by a specially designed RCA [30-33]. For example, in a study by Zhang and colleagues, multiple leukemia cell-binding aptamers were synthesized by RCA, which were further combined with doxorubicin to form poly-aptamer-drug [30]. The poly-aptamer was produced by RCA, which enhanced more than 40-fold the binding affinity to target leukemia cells. Zhao *et al.* incorporated RCA synthesized aptamers for cancer cells into a microfluidic device and found that the RCA-aptamers showed higher capture ability than regular monolayer aptamers and antibodies [32].

In our previous work, a dendrimer coated PDMS microchannel was further immobilized with *E. coli* O157:H7 capture aptamers and sRCA was utilized to improve the fluorescence detection signals [16]. To further improve the detection sensitivity, a newly designed RCA (for capturing target bacterial cells more efficiently, thus called “cRCA”) which produced tandem repeated *E. coli* O157:H7 aptamers (cRCA-aptamers), was proposed to replace the previous monolayer aptamers. The difference between monolayer aptamers and cRCA-aptamers is that the former has short and single units of *E. coli* O157:H7 aptamer sequence,

while the latter has relatively longer strands containing tandem repeated units of the same aptamer sequences. We speculated that these cRCA-aptamers, whose length would be several micrometers, would be able to specifically capture more target bacterial cells because of the tentacle-like structure produced. In other words, the cRCA-aptamer-modified microchannels would capture more target bacterial cells than those modified using monolayer aptamers, given the equivalent inoculum volume. Overall, dual-RCA reactions can be integrated to develop a sensitive detection system for *E. coli* O157:H7 cells, where the function of cRCA is to produce cRCA-aptamers for enhancing target capture in the modified microchannel, while the previous sRCA will be used for signal amplification to provide increased florescence. This is a novel combination of two different RCA reactions to improve detection performance. As sRCA was developed in our previous work, only cRCA sequence design and reaction condition optimization are required in this work. cRCA products were imaged and analyzed by atomic force microscopy (AFM) and gel electrophoresis. Results showed that the cRCA-aptamer-modified microchannels captured three times more target bacterial cells than those modified with monolayer aptamers at *E. coli* O157:H7 concentrations ranging from 10^2 to 10^4 cells/mL. Moreover, fluorescence detection signals were collected after sRCA intensification, which indicated that detection signals were enhanced by 3-5 times in comparison with monolayer aptamers microchannels. This is the first time that dual-RCA was employed in a whole-cell detection system, which provides a potential application in sensitive whole-cell detection of pathogenic bacteria in food safety, environmental monitoring and clinical diagnosis applications.

5.2 Experimental

5.2.1 Overall design of the aptamer based dual-RCA detection system

The overall design of the dual-RCA microfluidic detection system and schematic representation of the modified inner channel surface are shown in Figure 5-1. Initially, PAMAM dendrimers were immobilized onto the inner surfaces of a PDMS microchannel to render the resulting surfaces nonfouling and to provide multiple handles for conjugation of primer-padlock ligation products for further cRCA reactions [34]. Subsequently, cRCA reactions were carried out in order to produce tandem repeated aptamers that are specific for *E. coli* O157:H7 cells. The products of the cRCA reactions were used - *in situ* - as capturing aptamers to recognize and capture target *E. coli* O157:H7 cells as the first layer of the cRCA | *E. coli* O157:H7 cells | aptamer-primer sandwich detection format. This cRCA layer design is aimed to significantly enhancing surfaces areas for capturing bacteria cells by longer c-RCA aptamers and thus improving capturing probabilities. To further enhance the detection signals, sRCA will be employed to transduce the capturing events and to intensify the fluorescence detection signals, thus allowing sensitive detection [16]. More specifically, to achieve the cRCA, a properly designed padlock probe must first hybridize with its matching primer (capped with $-NH_2$ on the 5' end) to form a circular template (*i.e.* ligation product) that is subsequently immobilized onto the inner surface of the PDMS microchannel. The cRCA reactions are carried out using the immobilized ligation products as templates and result in extended long chains of cRCA products under the catalysis of phi29 DNA polymerase. Each long chain of cRCA product consists of hundreds to thousands copies of *E. coli* O157:H7 aptamers as the sequence of circular

template is designed to be complementary to the sequence of the *E. coli* O157:H7 aptamers. Similarly, the sRCA reactions start with the formations of circular templates by conjugations between the aptamer-primers and the padlock probes. The aptamer-primer complexes serve three purposes: 1) the aptamer-primer sequence is designed to conjugate with the padlock probe to form circular template; 2) the aptamer segment of the aptamer-primer complex recognizes the captured target *E. coli* O157: H7 cells on the microchannel surfaces and attaches to the cells; and 3) the primer segment of the aptamer-primer complex provides binding sequence for sRCA reaction using the padlock probe as a template for strand elongation. The long DNA chains that are produced provide multiple binding sites for complementary fluorescent probes and thus visualizing the target cells by counting the fluorescent signals. In short, cRCA is employed to benefit the capture performance and sRCA is used for signal intensification.

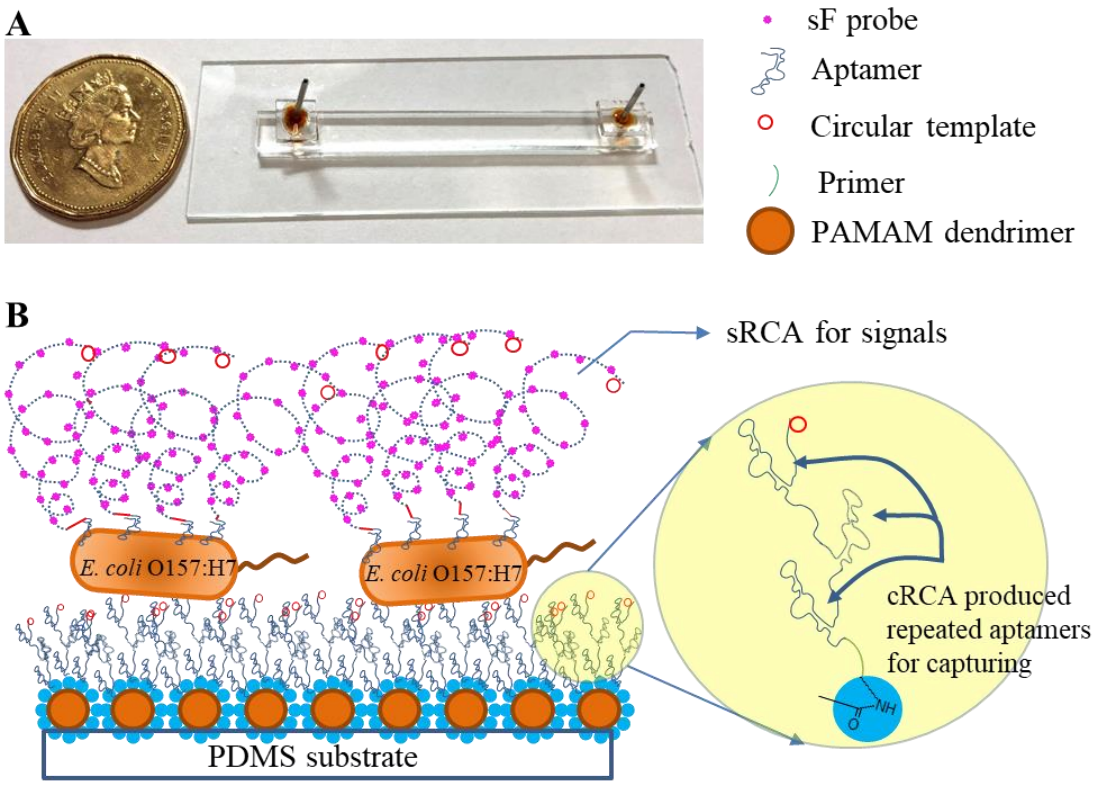

Figure 5-1 Scheme of the aptamer based dual-RCA detection system. A. Photography of the constructed microfluidic device; B. schematic drawing and illustration of microfluidic channel inner surface, where the PDMS surface is modified with PAMAM dendrimers (generation 7) and cRCA (producing repeated aptamers for capturing target bacteria) is subsequently conjugated to form multi layers of aptamers. sRCA is finally introduced for detection signal amplification after target bacteria are captured.

5.2.2 Materials

Sylgard® 184 silicone elastomer kit for poly(dimethyl siloxane) (PDMS) device fabrication was purchased from Dow Corning (Midland, MI). Poly(amido amine) (PAMAM) dendrimer (Generation 7) with ethylenediamine core and carboxyl surface functional

groups was purchased from Sigma-Aldrich (Oakville, ON). All oligonucleotides used in this study were obtained from Integrated DNA Technologies (IDT) (Coralville, IA) and their respective sequences are shown in Table 5-.1. RCA reagents including Phi29 DNA polymerase, T4 DNA ligase, deoxynucleotide (dNTP) solution mix, and electrophoresis related chemicals including Tris/Boric Acid/EDTA (TBE) buffer mix, Promega blue/orange loading dye, DNA ladders, and ethidium bromide (EB) were obtained from Fisher Scientific (Ottawa, ON). 1-(3-dimethylaminopropyl)-3-ethylcarbodiimide (EDC) was obtained from Alfa Aesar (Ward Hill, MA). (3-aminopropyl)-trimethoxysilane (APTMS) and N-hydroxysuccinimide (NHS) were purchased from Thermo Fisher Scientific (Rockford, IL). All other chemicals, unless otherwise stated, were purchased from Sigma-Aldrich (Oakville, ON). Formalin killed *E. coli* O157: H7 cells were generously donated by the Canada Food Inspection Agency (Ottawa, ON).

Table 5-1 Summary of DNA sequences used in the dual-RCA detection system

	Name	**Seq.#**	**Sequences (5'-3')**	**Source**
Capturing-RCA (cRCA)	Primer	S1	5'-NH_2-TTTTT TTTTT GAAGG ACTTA GTTAC TGTCG AGCGA T-3' (36 nt)	This work
	Padlock probe	S2	5'-AACTA AGTCC TTC*AT ACGGG AGCCA ACACC ATCTT GTACA AATCG TCTTG ATATC TGCAC ATTTG ATAGA GCAGG TGTGA CGGAT* ATCGC TCGAC AGT-3' (98 nt)	This work, designed to produce *E. coli* O157:H7 aptamer
	cF probe	S3	5'-Cy3-TTTTC TTGTA CAAAT CGTCT-3' (20 nt)	This work
Signaling-RCA (sRCA)	Aptamer-primer	S4	5'-NH_2-*ATCCG TCACA CCTGC TCTAT CAAAT GTGCA GATAT CAAGA CGATT TGTAC AAGAT GGTGT TGGCT CCCGT AT*TTT TTTTT GTCCG TGCTA GAAGG AAACA GTTAC-3' (105 nt)	[35-37]
	Padlock probe	S5	5'-TAGCA CGGAC ATATA TGATG GACCG CAGTA TGAGT ATCTC CTATC ACTAC TAAGT GGAAG AAATG TAACT GTTTC CTTC-3' (79 nt)	[16]

	sF probe	S6	5’-Cy3-TTTTA GTATG AGTAT CTC-3’ (18 nt)	This work

Note: The colored portions in S1 are respectively complementary with those labeled in S2. The italic portion in S2 has sequences complementary to those of *E. coli* O157:H7 aptamer. The underlined portions in S2 and S3 are the same sequences. The italic sequence in S4 is *E. coli* O157:H7 aptamer and the colored portion are the primers whose sequences are respectively complementary with those red and green sequences in S5. The underlined portion in S5 has the same sequence as that in S6. S5 is used to form circular template for sRCA which produces strands containing tandem repeated complementary sequences for Cy3 fluorescent probe (sF probe, S6) binding and thus enhancing the fluorescence detection.

5.2.3 Microfluidic device fabrication and surface modification

Microfluidic device fabrication and surface modification procedures were described elsewhere [34, 38]. In brief, PDMS stamps prepared by a standard lithography method were cut and sealed with glass slides after oxygen plasma treatment. Subsequently, PAMAM dendrimers were conjugated to the inner surface of the PDMS microchannel via a silane coupling process. Amino group capped oligonucleotides were immobilized to the dendrimer PDMS with surface functional carboxyl groups via NHS/EDC chemistry.

5.2.4 Rolling circle amplification reactions

Rolling circle amplification reactions for both cRCA and sRCA were conducted in similar fashions. Both RCA reactions start with a ligation process. To prepare ligation solution, DNA sequences solutions (primer and padlock probe) were firstly hybridized at 37 °C for

30 min. Subsequently, 10 × T4 reaction buffer (400 mM Tris-HCl, 100 mM $MgCl_2$, 100 mM DTT, 5 mM ATP, pH 7.8) and 10 U of T4 DNA ligase were added to form the circular templates for further RCA reactions at room temperature for 30 min. More specifically, in a typical RCA reaction (based on a total volume of 100 µl), 50 µl ligation solution (cRCA: 2 µM ligation products of primer S1 and padlock probe S2; sRCA: 200 nM ligation products of aptamer-primer S4 and padlock probe S5), 10 µl of 10 × phi29 reaction buffer (330 mM Tris-acetate, 100 mM Mg-acetate, 660 mM K-acetate, 1% (v/v) Tween 20 and 10 mM DTT, pH 7.9), 4 µl dNTPs and 10 U of phi29 DNA polymerase were mixed thoroughly and allowed to react at 37 °C. To terminate the RCA, the reaction mixture was heated at 65 °C for 10 min to inactivate both phi29 DNA polymerase and T4 DNA ligase when reactions ended. All the DNAs were denatured by heating at 95 °C for 5 min and quickly cooled on ice for 1 min prior to use [39, 40].

The optimized cRCA reactions were conducted in microchannels to coat the dendrimer-PDMS surface with aptamers produced by cRCA. With catalysis of NHS and EDC, ligation products containing primer (5' end capped with -NH_2) and padlock probe complexes were conjugated and react with –COOH groups on dendrimer-PDMS surface which has been immobilized on PDMS channel surface. RCA reagents as stated above were injected to initiate the rolling circle process to produce tandem repeated aptamers (cRCA-aptamers) at a flow rate of 0.01 mL/h at 37°C for 10 h. Solutions spiked with *E. coli* O157:H7 bacterial cells at different concentrations were then injected and captured by the modified cRCA-dendrimer-PDMS microchannel. sRCA was optimized in our previous work and conducted in the developed microchannel after the *E. coli* O157:H7 cells were captured

[16]. Fluorescently labeled probes (*i.e.* sF probes) were introduced to hybridize with sRCA products and gave off fluorescent signals. PBS buffer (pH 7.4) was used to wash the channels between different injections and all the injection flow rates were 0.05 mL/h at room temperature unless otherwise specified.

5.2.5 Characterization of RCA products

Agarose gel (2%) was used to analyze RCA products. Gel electrophoresis was conducted in TBE buffer (44.5 mM Tris, 44.5 mM H_3BO_3, and 1 mM EDTA, pH 8.5) at room temperature for 50-90 min under 75 V. An AlphaImager (HP Imaging System, San Jose, CA) was used for capturing gel images. RCA products were also analysed by AFM. RCA product solution was drop-casted on a freshly cleaved mica surface (V-1 Grade, SPI Supplies Division of Structure Probe Inc., West Chester PA) pre-treated with 5 mM $NiCl_2$ where Ni^{2+} was used to increase affinities between RCA products and the mica surface, both of which are negatively charged. The air-dried mica surfaces were imaged by a Multimode AFM with NanoScope V controller (Bruker Nano Surfaces Division, Santa Barbara, CA) in either Bruker's ScanAsyst or PeakForce QNM modes. Gwyddion (http://gwyddion.net/) was used to process and analyse the obtained images.

5.2.6 Fluorescence signals collection and analysis

To investigate whether the fluorescently-labeled oligonucleotides (Cy3 labeled primer S1 and cF probes S3) successfully hybridized with the modified PDMS surfaces, the fluorescence intensities were analyzed before and after the hybridization process. Fluorescent images (n=20) were captured after washing the redundant fluorescent

nucleotides and ImageJ was used to analyze the fluorescence intensities [41]. To collect the fluorescent detection signals, sF probes (S6) were injected into the microchannel at 37 °C for 30 min after sRCA. PBS buffer was used to wash out unbound sF probes. Subsequently, fluorescence images of the microchannels were obtained using an inverted Olympus fluorescence microscope (IX81, Richmond Hill, ON) equipped with a high-resolution camera (QImaging, Surrey, BC). Specifically, twenty fluorescent images for each sample from random areas were captured and analyzed by ImageJ software [41]. Dendrimer-PDMS channel without cRCA coating were used as controls.

5.3 Results and discussion

5.3.1 Surface modification of the PDMS microchannel

The fabrication of the PDMS microfluidic device was based on soft lithography and detailed procedures were described in our previous study [38]. Subsequently, PAMAM dendrimer G7 was successfully immobilized onto PDMS inner channel surface by a silane coupling method (surface (i) to surface (iii), Figure 5-2A) in our previous report [34]. To further conjugate cRCA ligation products of primers and padlock probes onto the PAMAM dendrimer (surface (iii) to surface (iv), Figure 5-2A), the primers capped with -NH_2 were hybridized and ligated with padlock probes to form circular templates prior to introducing onto the dendrimer-COOH coated PDMS surface. To verify that the ligation products successfully reacted with the dendrimer-PDMS surface, fluorescent dye Cy3 was used to label the ligation products at the 5'-end of primer portion and fluorescence changes were observed and analyzed after excess ligation products were washed by PBS buffer. In Figure

5-2C, the fluorescence intensities of surface (iv) are significantly increased ($p < 0.05$) in comparison with those of surface (iii) when the applied ligation product concentrations are 100 nM, 1 µM and 10 µM. Moreover, higher concentrations of Cy3 labeled ligation products resulted in higher fluorescence intensities. However, the fluorescence of the surface modified with 10 µM ligation products showed only slightly higher intensity than that of one modified with 1 µM, suggesting that the modified surface might reach saturation. Therefore, 1 µM-concentration was selected as optimal to use in the rest of the study unless indicated otherwise. Non-specific binding was checked by applying different concentrations of fluorescent ligation products onto the same surfaces without catalysis of NHS and EDC. Results (blue bars in Figure 5-2C) showed slight non-specific binding compared with the specific binding groups (red bars in Figure 5-2C), which is consistent with our previous result [16]. Thus, it is confirmed that the ligation products of primers and padlock probes were successfully immobilized onto the dendrimer-PDMS surfaces.

In the next step, the surface was further modified with cRCA products by initiating the RCA reactions based on the ligation products immobilized-surface (iv). cRCA products consisting of tandem repeating *E. coli* O157:H7 aptamers (surface (v) in Figure 5-2A) were propagated from the dendrimer-PDMS surfaces in order to increase target cell recognition and likelihood of capture improved in comparison with the mono-layer aptamer modified dendrimer-PDMS surface (Figure 5-2B).

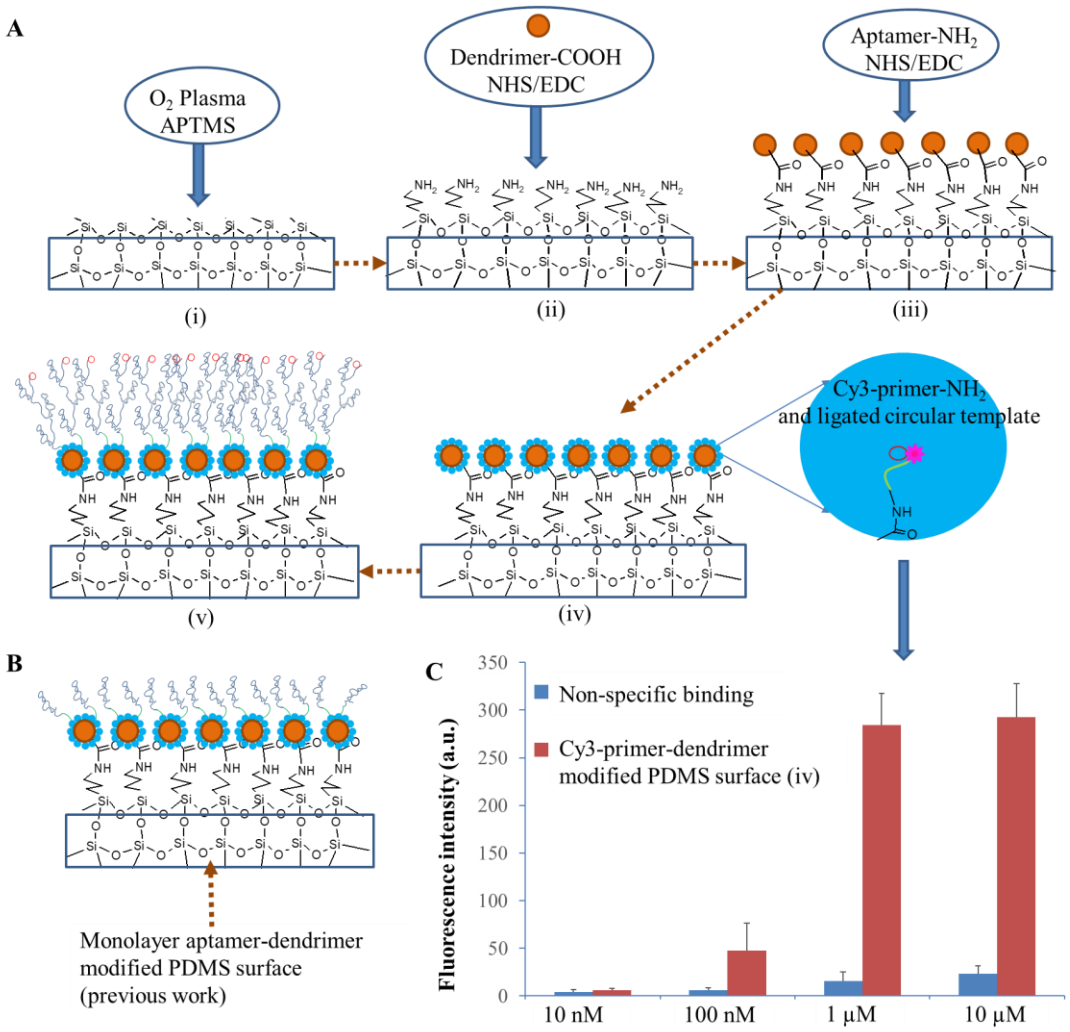

Figure 5-2 Surface modifications of PDMS surfaces. A. schematic drawing of cRCA-aptamer modification on dendrimer coated PDMS surface: (i) original PDMS surface; (ii) aminated PDMS surface after treatment with oxygen plasma and APTMS; (iii) PAMAM dendrimer conjugated PDMS surface; (iv) fluorescently labeled ligation products immobilized on the dendrimer surface; (v) *in situ* cRCA reaction on top of dendrimer modified surface; B. monolayered aptamers modified on PAMAM dendrimer-conjugated PDMS surface from our previous work; C. fluorescence signal intensities of dendrimer conjugated PDMS surfaces before and after the immobilization of ligation products for

further cRCA. The values of fluorescence intensities of ligation product-modified surfaces (including non-specific binding groups) were subtracted by values from the dendrimer-PDMS surfaces.

5.3.2 cRCA optimization and characterizations

In this study, *in situ* cRCA was used to produce tandem repeating *E. coli* O157:H7 aptamers (cRCA-aptamers). The process was followed by agarose gel electrophoresis and AFM. In Figure 5-3A, the primers and padlock probes showed small molecular weight, which are around 30 nt and 80 nt respectively. These results have slight discrepancy with their actual lengths as shown in Table 5-1 (S1 is 36 nt and S2 is 98 nt) due to that the DNA markers used in this agarose gel electrophoresis are double stranded DNA and the DNA sequences for cRCA are single stranded [42]. After the hybridization and ligation between primers and padlock probes, the resulting ligated complexes showed an evident increase in molecular weight which was around 100 nt (bright band in Lane 3, Figure 5-3A). This molecular weight roughly combined the molecular weight of the primer and that of the padlock probe sequences, confirming the success of the ligation reaction. cRCA was initiated by adding phi29 DNA polymerase and dNTPs, and products from different reaction times ranging from 0.5 h to 20 h were collected and loaded onto the agarose gel. As shown in Figure 5-3B, within the first two hours of cRCA reaction, there were no significant amount of high molecular weight cRCA products detected by agarose gel. However, the amount of cRCA products (larger than 10 kbp) gradually increased with increasing cRCA reaction time from 2 h to 20 h. In contrast, it is noted that the sRCA reaction proceeded at a much faster rate, since the side-by-side comparison between

Figures 5-3B and 3C suggests that there were more sRCA products detected - indicating a faster reaction rate for sRCA than cRCA - for a given reaction time under otherwise identical reaction conditions. This observation is interesting as it seems to suggest that RCA reactions do not necessarily "roll" at an approximately constant rate of 50 nt/sec, as has been reported elsewhere [43]. While it is unclear why there was such a significant rate difference between the two RCA reactions in this study, but the length of circular template might play an important role [44]. It should be mentioned that although the agarose gel electrophoresis experiments demonstrated the success of the cRCA reaction, it also indicated that a reaction time of 10 to 20 hours would be required to sufficiently develop the required long tandem chains to enable more effective target capturing. However, this time requirement might not be a significant concern since it would be possible to prepare microfluidic devices pre-modified with the cRCA products.

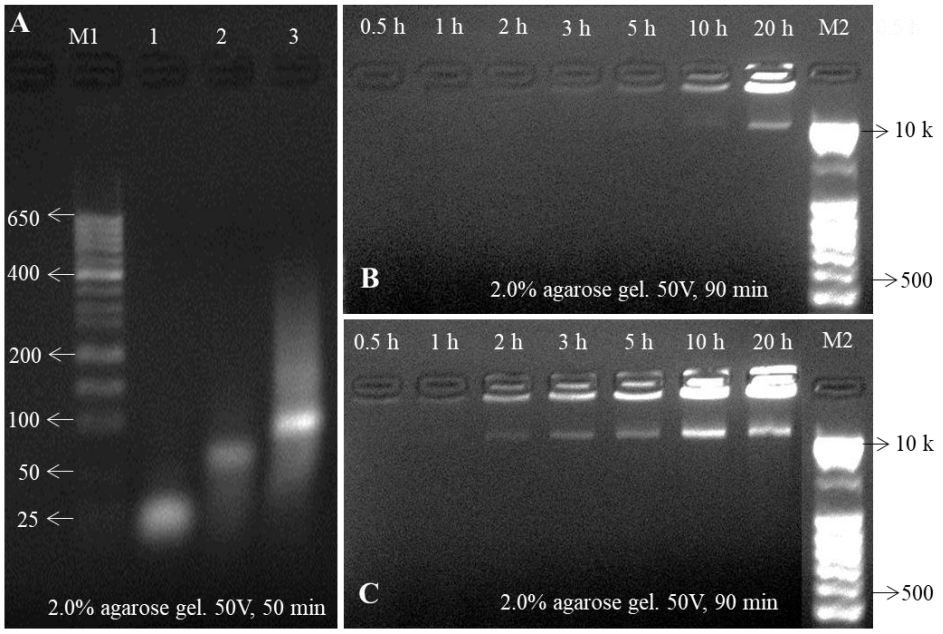

Figure 5-3 RCA reactions as characterized by agarose gel electrophoresis. A. original primers (Lane 1) and padlock probes (Lane 2) and their ligation products (Lane 3); B. cRCA products from varied reaction times as indicated on the top of lanes. Lanes M1 and M2 are DNA markers with the top band at 650 bp and 10 kbp, respectively; C. sRCA products collected from different reaction times as comparisons.

cRCA products collected from varied reaction times were also characterized by AFM as shown in Figure 5-4. For 2 h reaction time, a large percentage of products were observed as short strands (dotted structures on AFM image). This result suggested that the rolling circle process was initiated, and cRCA products were formed; however, the RCA reaction is still at the preliminary stage. At 3 h of reaction, chains of cRCA products grow obviously longer. Whereas, the small round shaped dots still account for more than 50% of all the products. At 5 h, the quantity of longer strands increased and those round shaped dots were decreased. At 10 h of reaction, a high density of extremely long chains of cRCA products

were observed. When the reaction time further increased to 20 h, a good network of cRCA products was formed. Moreover, the density of products was further increased and aggregations of cRCA products were easily found. Overall, to produce a relatively large amount of long strands, reaction time as long as 10 h was required.

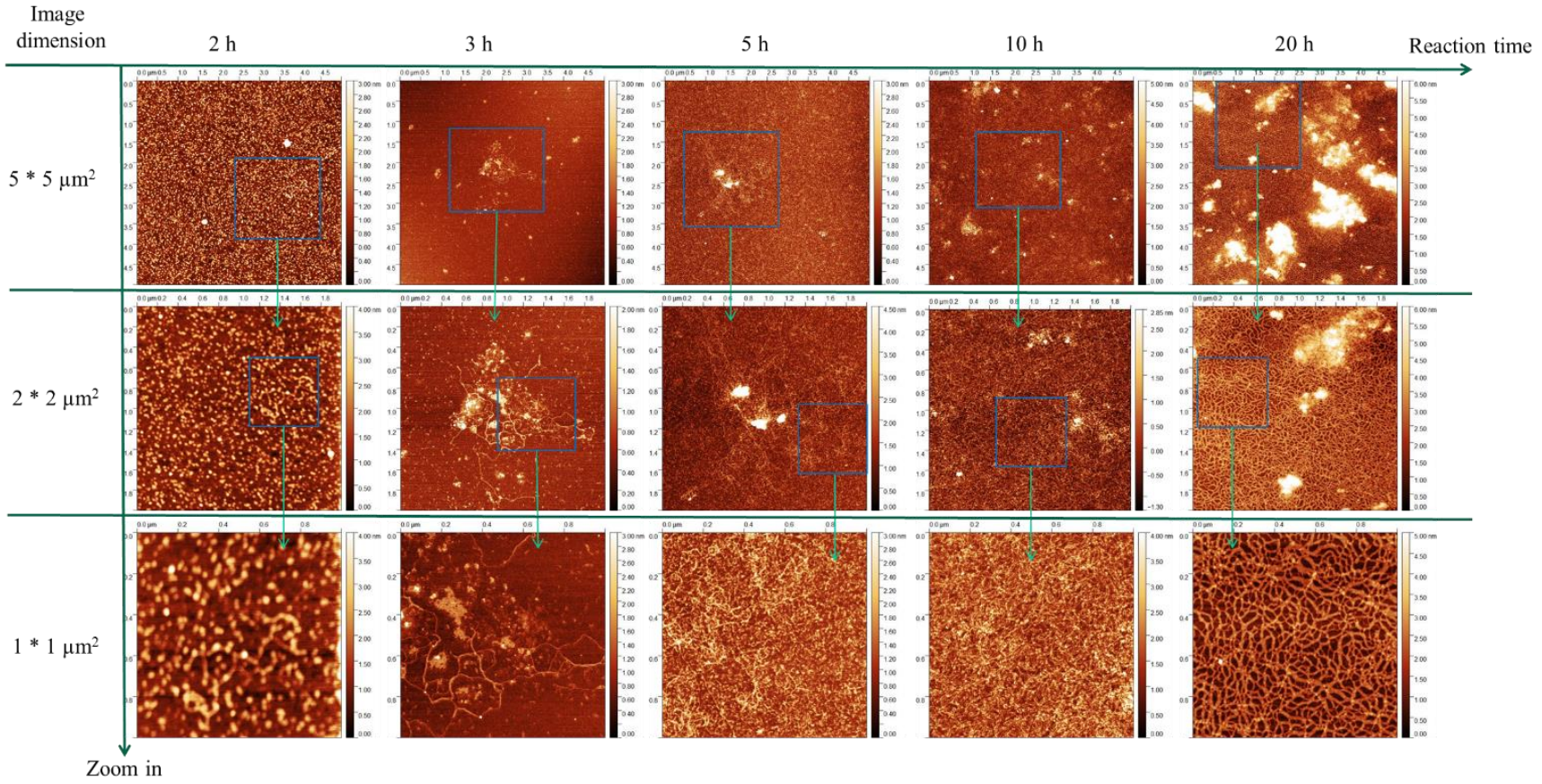

Figure 5-4 Morphologies changes of cRCA products along reaction time from 2 h to 20 h. The downward arrow shows the corresponding zoom-ins.

5.3.3 cRCA on dendrimer

The feasibility of cRCA has been confirmed and the reaction time was optimized above. To further confirm that cRCA products can be synthesized *in situ* on dendrimer and dendrimer-PDMS surfaces, cRCA ligation products were separately conjugated with PAMAM dendrimer and dendrimer-PDMS surfaces using NHS/EDC chemistry. To characterise the cRCA products by AFM, cRCA reactions were carried out *in situ* on PAMAM dendrimers and deposited on a mica substrate, and the results are shown in Figure 5-5. In particular, an AFM image of PAMAM dendrimers deposited directly on mica is shown in Figure 5-5A. The heights of the particulates, most likely PAMAM dendrimer molecules under the AFM, were measured to be 1.5-4 nm (see Figure 5-5B). This measured value is less than a theoretical PAMAM dendrimer (G7) diameter value of 8.1 nm [45], which can be attributed to the fact that dendrimer molecules generally deform from spherical into dome-shaped after deposited and dried on mica surfaces [46]. As expected, when cRCA reactions were conducted on dendrimer molecules, long strands of cRCA products were evident as shown in Figure 5-5C. Unfortunately, further attempts to image cRCA products on dendrimers that were originally immobilized on PDMS surfaces were unsuccessful by AFM due to excessively high noises as a result of the unevenness of the PDMS surfaces.

To confirm that the *in situ* cRCA products are available to provide repeating aptamers, cF probes were used to hybrid with the *in situ* cRCA reaction products on PAMAM dendrimer modified PDMS surfaces, and the intensity of the fluorescence emitted from the surfaces of interest were measured. As shown in Fig 5D, it is clear that the intensities of fluorescence

emitted from the surfaces of interest increased with increasing concentrations of cF probes and levelled off at 10 µM after which further increase in cF probe did not result in significant increase in signal intensities. These results confirmed that the cRCA were successfully carried out *in situ* on PAMAM dendrimer modified PDMS.

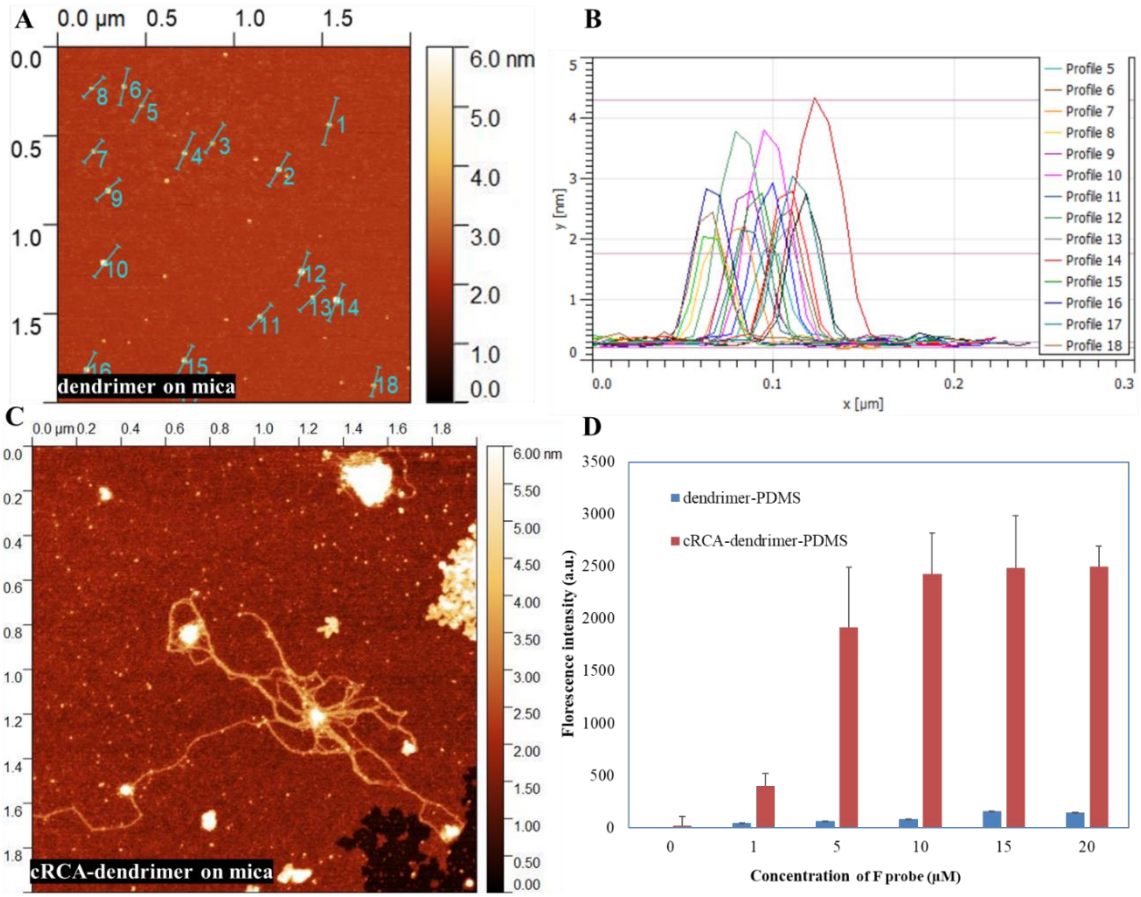

Figure 5-5 AFM characterization of *in situ* cRCA products on PAMAM dendrimer. A. AFM image of PAMAM dendrimer on mica; B. height profiles of dendrimer molecules marked in (A); C. AFM image of cRCA products *in situ* synthesized on dendrimer deposited on mica; D. fluorescence intensities of *in situ* synthesized cRCA-dendrimer-PDMS substrate after hybridization with cF probes (S3, Table 5-1) and the controls.

5.3.4 Target Capturing Performance

Capture performance of the cRCA modified PDMS microchannels for target *E. coli* O157:H7 cells was investigated and compared with that of sRCA modified PDMS microchannels. As evident in Figure 5-6, both aptamer-modified microchannels captured increasing total number of target cells as the concentrations of target cells increased. More importantly, it should be noted that for all the target cell concentrations investigated, the cRCA modified microchannel captured approximately 3 times more cells than the previous monolayer aptamer modified microchannel, exhibiting more effective target cell capturing performance. This significant performance difference is most likely explained by the presence of repeating aptamer of the cRCA products that would likely result in more surface area and increased binding probability for target capturing. In addition, it has been reported that the long strands of tandem repeating aptamers produced by RCA exhibit stronger adhesion to target cells [32], which would be significantly beneficial for target capture efficiency in flow systems where shear forces are know to influence target capturing [47-49]. When the injection flow rate was reduced from 0.05 mL/h to 0.01, as shown in Figure 5-6B, the cRCA-channel performed better capture ability than monolayer aptamer modified channel when the *E. coli* O157:H7 cell concentration was 10^5 cells/mL.

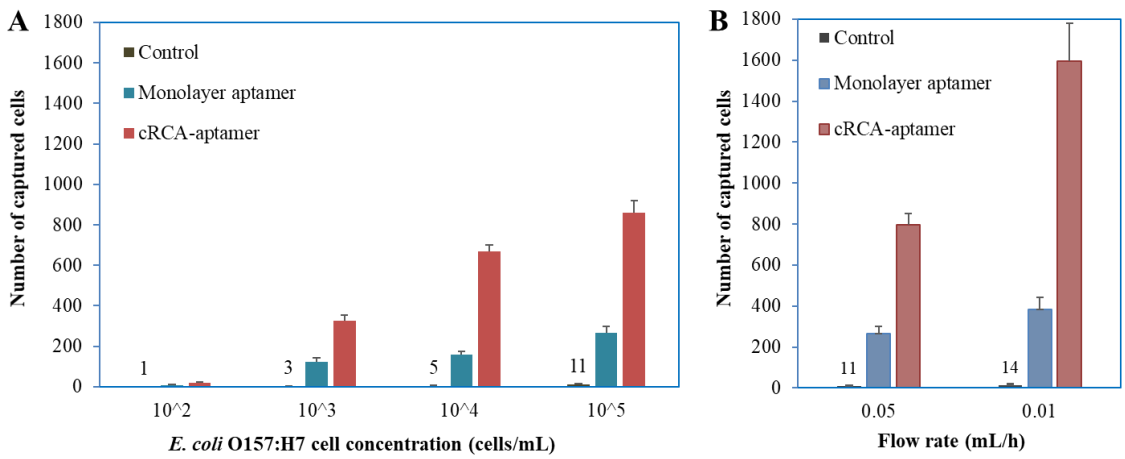

Figure 5-6 Capture performance of both monolayer aptamer and cRCA-aptamer modified microchannels. A. investigations with different concentrations of *E. coli* O157:H7; B. investigations under different injection flow rates. Numbers of captured cells were counted manually under microscope. Experiments were conducted in triplicate.

5.3.5 Detections of *E. coli* O157:H7 using dual-RCA microchannel system

To demonstrate the performances of the dual-RCA microchannel detection system, the dual-RCA modified system was used to detect different concentrations of target *E. coli* O157:H7 cells in PBS solutions; the cRCA reaction was used to produce *in situ* capture aptamers while the sRCA was employed to transduce and enhance detection signals [16, 35]. As a comparison, a monolayer aptamer detection approach was also used, in which immobilized monolayer aptamers were used to capture the target cells and sRCA was employed to transduce and enhance detection signals. Fluorescence signals were collected from both sets of experiments. As shown in Figure 5-7, here are linear relationships between fluorescence signals and *E. coli* O157:H7 concentrations from 10^2 to 10^4 cells/mL.

Relative fluorescence signals increased with the bacterial concentrations. It is clear, cRCA-aptamers microchannels displayed higher fluorescence signals in comparison with those of monolayer aptamer microchannels. This is because cRCA-aptamer modified microchannel captured more target bacterial cells as shown in Figure 5-6. The slope of the cRCA-aptamer microchannel increases dramatically compared with the monolayer aptamer group, indicating the cRCA enhanced detection sensitivity [50, 51].

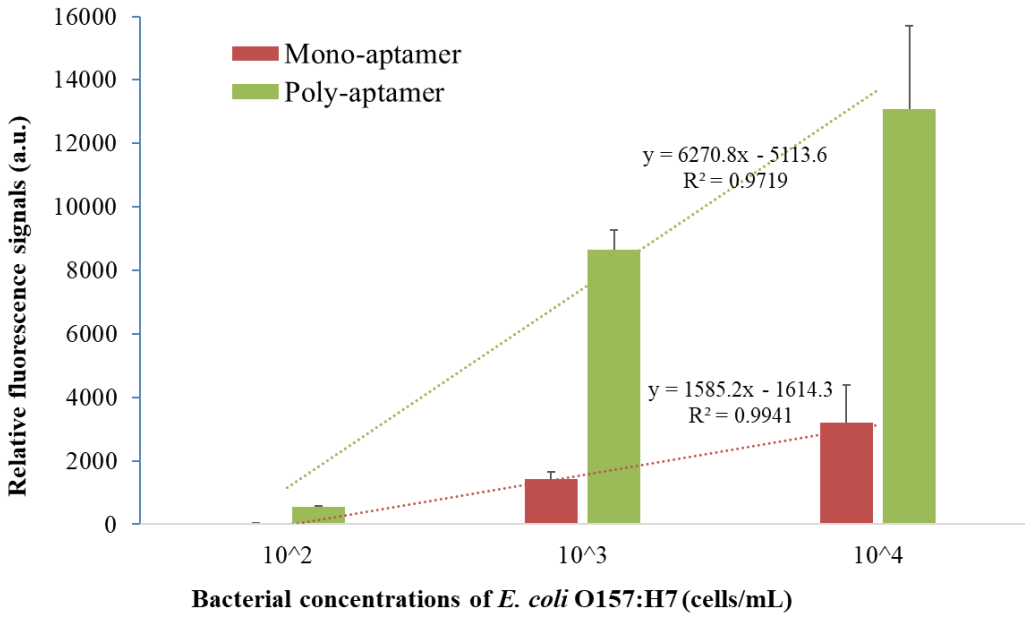

Figure 5-7 Detections of *E. coli* O157:H7 at different concentrations using two different detection systems. Mono-aptamer represents PAMAM dendrimer-coated microchannels further modified with single-layered *E. coli* O157:H7 aptamers; cRCA-aptamer represents cRCA-produced repeated *E. coli* O157:H7 aptamers that were immobilized on the PAMAM dendrimer coated microchannels.

5.3.6 Specificity test

The detection specificity of this dual-RCA aptamer-based microchannel for *E. coli* O157:H7 detection was tested by comparing signals from several non-target bacteria with signals from target bacteria. Fluorescence signals of non-target bacteria including *E. coli* K12, *E. coli* ER2420 and *Listeria innocua* were collected after sRCA, which were compared with that of target *E. coli* O157:H7. As shown in Figure 5-8, the fluorescence signals from target bacteria are significantly higher than those from non-targets when the concentrations for all used bacteria are 10^4 cells/mL, which suggests the proposed dual-RCA detection method exhibits good specificity for *E. coli* O157:H7 cells.

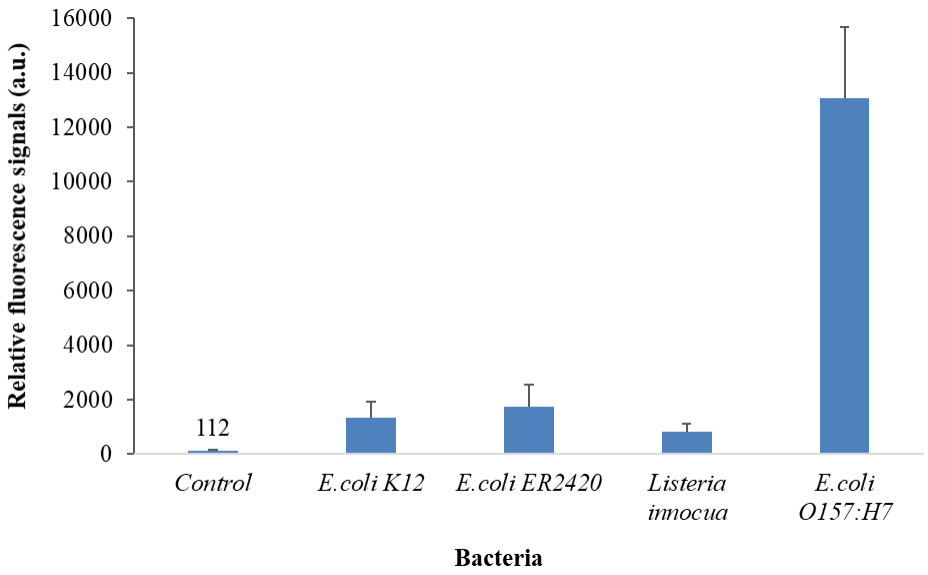

Figure 5-8 Specificity tests of the developed dual-RCA aptamer-based detection microchannel for target *E. coli* O157:H7 by comparison to non-target bacteria at a concentration of 10^4 cells/mL. Error bars represent standard deviations (n=3).

5.4 Discussion and conclusion

In summary, two RCA reactions with different capture sequences were used in this biosensing work. cRCA produces tandemly repeated aptamers for *E. coli* O157:H7, while sRCA produces tandem repeated binding sites for complementary fluorescent probes. cRCA was newly designed and characterized for maximum reaction time. AFM and agarose gel electrophoresis were employed to visualize the long strands of cRCA products formed, which were further immobilized on the inner surface of microchannels for the enhancement of *E. coli* O157:H7 cell capture. Compared with a monolayer aptamer modified channel, the cRCA immobilized channel was able to capture about 3 times more cells when the bacterial concentrations ranged from 10^2 to 10^4 cells/mL. An established sRCA was then introduced for signal transduction and the collected fluorescence signals were enhanced mostly likely due to better *E. coli* O157:H7 cell capture. Our results show that cRCA-aptamers increased detection signal by 3-5 folds while maintaining high specificity for target *E. coli* O157:H7, in comparison with a monolayer aptamer microchannel after sRCA signal transduction.

sRCA transduces detection reactions into signals and enhances detection signals by producing long chains of repeated binding sites for fluorescent probes. Essentially, the transduced signal is based on the number of captured cells. Therefore, strategies to increase capture efficiency of the current detection system are desired. cRCA for production of longer capturing agents (repeated aptamers) is one strategy to increase the amounts of captured cells. Due to the linear structure of this microchannel, the flow rate used and dimensions of the current microchannel, the flow pattern of this system is laminar flow. In a laminar flow channel, most of target bacteria do not have the opportunity to touch the

inner channel surface and be captured. Strategies to stir laminar flow into helically-shaped fluidic streamlines are based on adding grooves on the inner surface of microchannels, which will should enhance the interactions of bacterial cells and aptamer-modified channel surface. Therefore, strategies to increase capture efficiency of the current device are an important direction for future research.

5.5 References

1. Castillo-León, J., *Microfluidics and lab-on-a-chip devices: history and challenges*, in *Lab-on-a-Chip Devices and Micro-Total Analysis Systems*. 2015, Springer. p. 1-15.
2. Vilkner, T., D. Janasek, and A. Manz, *Micro total analysis systems. Recent developments.* Analytical Chemistry, 2004. **76**(12): p. 3373-3386.
3. Dittrich, P.S., K. Tachikawa, and A. Manz, *Micro total analysis systems. Latest advancements and trends.* Analytical Chemistry, 2006. **78**(12): p. 3887-3908.
4. Haeberle, S. and R. Zengerle, *Microfluidic platforms for lab-on-a-chip applications.* Lab on a Chip, 2007. **7**(9): p. 1094-1110.
5. Gupta, K., et al., *Lab-on-a-chip devices as an emerging platform for stem cell biology*. Lab on a Chip, 2010. **10**(16): p. 2019-2031.
6. Boehm, D.A., P.A. Gottlieb, and S.Z. Hua, *On-chip microfluidic biosensor for bacterial detection and identification.* Sensors and Actuators B: Chemical, 2007. **126**(2): p. 508-514.
7. Varshney, M. and Y. Li, *Interdigitated array microelectrode based impedance biosensor coupled with magnetic nanoparticle–antibody conjugates for detection of Escherichia coli O157: H7 in food samples.* Biosensors and Bioelectronics, 2007. **22**(11): p. 2408-2414.
8. Mujika, M., et al., *Magnetoresistive immunosensor for the detection of Escherichia coli O157: H7 including a microfluidic network.* Biosensors and Bioelectronics, 2009. **24**(5): p. 1253-1258.
9. Sefah, K., et al., *Development of DNA aptamers using Cell-SELEX*. Nature Protocols, 2010. **5**(6): p. 1169-1185.
10. Tuerk, C. and L. Gold, *Systematic evolution of ligands by exponential enrichment: RNA ligands to bacteriophage T4 DNA polymerase.* Science, 1990. **249**(4968): p. 505-510.

11. Ellington, A.D. and J.W. Szostak, *In vitro selection of RNA molecules that bind specific ligands.* Nature, 1990. **346**(6287): p. 818-822.
12. Citartan, M., et al., *Aptamers as the 'capturing'agents in aptamer-based capture assays.* Microchemical Journal, 2016. **128**: p. 187-197.
13. Nery, A.A., C. Wrenger, and H. Ulrich, *Recognition of biomarkers and cell-specific molecular signatures: Aptamers as capture agents.* Journal of Separation Science, 2009. **32**(10): p. 1523-1530.
14. Baumstummler, A., et al., *Specific capture and detection of Staphylococcus aureus with high-affinity modified aptamers to cell surface components.* Letters in Applied Microbiology, 2014. **59**(4): p. 422-431.
15. Suh, S.H. and L.-A. Jaykus, *Nucleic acid aptamers for capture and detection of Listeria spp.* Journal of Biotechnology, 2013. **167**(4): p. 454-461.
16. Jiang, Y., S. Zou, and X. Cao, *A simple dendrimer-aptamer based microfluidic platform for E. coli O157: H7 detection and signal intensification by rolling circle amplification.* Sensors and Actuators B: Chemical, 2017. **251**: p. 976-984.
17. Bi, S., et al., *A chemiluminescence imaging array for the detection of cancer cells by dual-aptamer recognition and bio-bar-code nanoprobe-based rolling circle amplification.* Chemical Communications, 2013. **49**(33): p. 3452-3454.
18. Beyer, S., P. Nickels, and F.C. Simmel, *Periodic DNA nanotemplates synthesized by rolling circle amplification.* Nano Letters, 2005. **5**(4): p. 719-722.
19. Pang, D., A.R. Thierry, and A. Dritschilo, *DNA studies using atomic force microscopy: capabilities for measurement of short DNA fragments.* Frontiers in Molecular Biosciences, 2015. **2**: p. 1.
20. Lee, J., et al., *Diffractometric detection of proteins using microbead-based rolling circle amplification.* Analytical Chemistry, 2009. **82**(1): p. 197-202.
21. Fischer, N.O., T.M. Tarasow, and J.B.-H. Tok, *Protein detection via direct enzymatic amplification of short DNA aptamers.* Analytical Biochemistry, 2008. **373**(1): p. 121-128.
22. Nilsson, M., *Lock and roll: single-molecule genotyping in situ using padlock probes and rolling-circle amplification.* Histochemistry and Cell Biology, 2006. **126**(2): p. 159-164.
23. Zhou, L., et al., *Aptamer-based rolling circle amplification: a platform for electrochemical detection of protein.* Analytical Chemistry, 2007. **79**(19): p. 7492-7500.
24. Banér, J., et al., *Signal amplification of padlock probes by rolling circle replication.* Nucleic Acids Research, 1998. **26**(22): p. 5073-5078.

25. Nallur, G., et al., *Signal amplification by rolling circle amplification on DNA microarrays.* Nucleic Acids Research, 2001. **29**(23): p. e118-e118.
26. Ge, J., et al., *A highly sensitive target-primed rolling circle amplification (TPRCA) method for fluorescent in situ hybridization detection of microRNA in tumor cells.* Analytical Chemistry, 2014. **86**(3): p. 1808-1815.
27. Strömberg, M., et al., *Multiplex detection of DNA sequences using the volume-amplified magnetic nanobead detection assay.* Analytical Chemistry, 2009. **81**(9): p. 3398-3406.
28. Cheng, W., et al., *Cascade signal amplification strategy for subattomolar protein detection by rolling circle amplification and quantum dots tagging.* Analytical Chemistry, 2010. **82**(8): p. 3337-3342.
29. Hu, B., et al., *A sensitive colorimetric assay system for nucleic acid detection based on isothermal signal amplification technology.* Analytical and Bioanalytical Chemistry, 2017. **409**(20): p. 4819-4825.
30. Zhang, Z., et al., *A polyvalent aptamer system for targeted drug delivery.* Biomaterials, 2013. **34**(37): p. 9728-9735.
31. Cheglakov, Z., et al., *Increasing the complexity of periodic protein nanostructures by the rolling-circle-amplified synthesis of aptamers.* Angewandte Chemie International Edition, 2008. **47**(1): p. 126-130.
32. Zhao, W., et al., *Bioinspired multivalent DNA network for capture and release of cells.* Proceedings of the National Academy of Sciences, 2012. **109**(48): p. 19626-19631.
33. Chang, E.K., et al., *Facile supermolecular aptamer inhibitors of L-selectin.* PloS One, 2015. **10**(3): p. e0123034.
34. Qin, Y., et al., *Developing an ultra non-fouling SU-8 and PDMS hybrid microfluidic device by poly (amidoamine) engraftment.* Colloids and Surfaces B: Biointerfaces, 2015. **127**: p. 247-255.
35. Zhou, L., et al., *Aptamer-based rolling circle amplification: a platform for electrochemical detection of protein.* Analytical Chemistry, 2007. **79**(19): p. 7492-7500.
36. Bruno, J. and J. Chanpong, *Methods of producing competitive aptamer fret reagents and assays*. 2009, US Application. Patent No. US20090186342A1.
37. Wu, W., et al., *An aptamer-based biosensor for colorimetric detection of Escherichia coli O157: H7.* PloS One, 2012. **7**(11), p. e48999.
38. Yeh, P.Y., et al., *Nonfouling hydrophilic poly (ethylene glycol) engraftment strategy for PDMS/SU-8 heterogeneous microfluidic devices.* Langmuir, 2012. **28**(46): p. 16227-16236.

39. Tong, P., et al., *Double-probe signal enhancing strategy for toxin aptasensing based on rolling circle amplification.* Biosensors and Bioelectronics, 2012. **33**(1): p. 146-151.
40. Yi, X., et al., *A universal electrochemical sensing system for small biomolecules using target-mediated sticky ends-based ligation-rolling circle amplification.* Biosensors and Bioelectronics, 2014. **57**: p. 103-109.
41. Collins, T.J., *ImageJ for microscopy.* Biotechniques, 2007. **43**(1 Suppl): p. 25-30.
42. Stellwagen, N.C. and E. Stellwagen, *Effect of the matrix on DNA electrophoretic mobility.* Journal of Chromatography A, 2009. **1216**(10): p. 1917-1929.
43. Dean, F.B., et al., *Rapid amplification of plasmid and phage DNA using phi29 DNA polymerase and multiply-primed rolling circle amplification.* Genome Research, 2001. **11**(6): p. 1095-1099.
44. Joffroy, B., et al., *Rolling circle amplification shows a sinusoidal template length-dependent amplification bias.* Nucleic Acids Research, 2017. **46**(2), p. 538-545.
45. Esfand, R. and D.A. Tomalia, *Poly (amidoamine)(PAMAM) dendrimers: from biomimicry to drug delivery and biomedical applications.* Drug Discovery Today, 2001. **6**(8): p. 427-436.
46. Li, J., et al., *Visualization and characterization of poly (amidoamine) dendrimers by atomic force microscopy.* Langmuir, 2000. **16**(13): p. 5613-5616.
47. Didar, T.F. and M. Tabrizian, *Adhesion based detection, sorting and enrichment of cells in microfluidic Lab-on-Chip devices.* Lab on a Chip, 2010. **10**(22): p. 3043-3053.
48. Wan, Y., et al., *Velocity effect on aptamer-based circulating tumor cell isolation in microfluidic devices.* The Journal of Physical Chemistry B, 2011. **115**(47): p. 13891-13896.
49. Tsao, S.C.-H., et al., *Capture and on-chip analysis of melanoma cells using tunable surface shear forces.* Scientific Reports, 2016. **6**: p. 19709.
50. Ingle Jr, J., *Sensitivity and limit of detection in quantitative spectrometric methods.* Journal of Chemical Education, 1974. **51**(2): p. 100.
51. Norrod, K.L., et al., *Quantitative comparison of five SERS substrates: sensitivity and limit of detection.* Applied Spectroscopy, 1997. **51**(7): p. 994-1001.

Chapter 6 General discussion and conclusions

Chapter 6

General discussion and conclusions

6.1 Conclusions

In this thesis, dendrimer-aptamer based microfluidic platforms for *E. coli* O157:H7 detection with signal intensification by RCA were developed. Using a layer-by-layer method, dendrimers and aptamers were modified on the inner surfaces of PDMS microchannels. Aptamer-primer induced sRCA was designed and visualized using atomic force microscopy and agarose gel electrophoresis. To enhance capture performance of the dendrimer-aptamer modified microchannels, cRCA was designed to produce tandem repeating cRCA-aptamers to replace the original monolayer aptamers. Results based on the objectives of this work are summarized as follows:

- **A simple dendrimer-aptamer based microfluidic platform for *E. coli* O157:H7 detection with signal intensification by rolling circle amplification.** The recognition between capturing aptamers and target *E. coli* cells were characterized. The performance of dendrimer-aptamer modified PDMS channels for capture were tested by injecting *E. coli* O157:H7 cells of different concentrations from 10^2 to 10^5 cells/mL. sRCA was characterized by AFM and agarose gel electrophoresis before applied in the dendrimer-aptamer modified PDMS microchannels. sRCA enhanced detection signals

by up to 50 times compared with no signal amplification and the limit of detection of the system was reduced to 10^2 cells/mL with high detection specificity.

- **A study on rolling circle amplification and its signal enhancing capability in a dendrimer-PDMS microfluidic system.** sRCA products were characterized during the whole reaction process, including the ligation of aptamer-primer and padlock probe. The formation of ligation products was demonstrated visually and the rolled RCA products were imaged. A non-inhomogeneous RCA initiation phase in early to mid stage of the RCA reaction was observed. Results showed a linear relationship between detection signals and *E. coli* O157:H7 cell concentrations after RCA signal intensification. Our results also indicate that the sRCA is able to enhance detection signals by up to 100-fold and that the observed signal enhancement and detection sensitivity increase with increasing RCA reaction time.
- **Developing a dual-RCA aptamer-based microfluidic platform for sensitive whole-cell detection of *E. coli* O157:H7.** A cRCA was developed to produce repeating aptamer units (cRCA-aptamers) for enhanced target capturing surface area, theoretically increasing the likelihood of capture. *In situ* synthesized cRCA on microchannels showed more than 3 times higher capture efficiency and 3-5 times more intensive fluorescence detection signals after sRCA than those with monolayer aptamers. Linear relationships between fluorescence signals and *E. coli* O157:H7 concentrations in the range of 10^2 to 10^4 cells/mL were obtained with good specificity.

6.2 General discussion and recommendations

Conventional methodologies for food safety analysis such as chromatography, immunoassays and PCR are reliable. However, those methods are time consuming and can be expensive and require trained personnel. In addition, food samples contain complicated matrices and the new detection methods are expected to monitor food safety from farm to table. Therefore, a detection method that can integrate food sample preparation and detection will be attractive. Microfluidic detection based on microchannels are high throughput, and convenient to integrate with a sample preparation module of microchannel design. Thus, microfluidic biosensing devices are potential alternatives to conventional analytical methods, due to their features of rapid, specific and sensitive detection.

In this thesis, research efforts focused on the detection module of aptamer-based dendrimer coated PDMS microchannels. Aptamers specific to bacterial cells can be selected by the cell-SELEX process, which provides high affinity aptamers binding to whole cells. The sequences of aptamers are convenient to synthesize and reproduce. Aptamers were chosen as the recognition elements due to their stability and ease of incorporation with RCA. RCA is versatile to produce functional sequences for complementary fluorescent probes and even aptamers themselves. Therefore, cRCA-aptamers produced by cRCA reactions have significantly more aptamer sequences for bacterial capture than monolayer aptamers. In this way, the total number of captured cells are increased when compared with that of the monolayer aptamer method, theoretically improving the detection sensitivity of the proposed detection microfluidic device. sRCA products provide multiple binding sites for fluorescent probes, enhancing fluorescence signals and increasing detection sensitivity.

Several aspects should be considered to improve the current detection systems and are worthy to be discussed.

6.2.1 RCA efficiency

Both cRCA and sRCA products are important to the detection system developed in this work. However, RCAs with different sequences showed different reaction efficiencies. The current sRCA reaction needs 2 h to produce sufficiently long product chains; this takes 10 h for cRCA. This time needs to be reduced. Therefore, RCA reaction parameters, such as reaction time, temperature, dNTP, and polymerase need to be further investigated and optimized. Besides, the sequences of padlock probes for different RCAs may influence the reaction efficiency. It is not convenient to change the padlock probe sequence of cRCA because it is designed to produce specific products (*E. coli* O157:H7 aptamer sequence) and therefore once the desired aptamer sequence is determined, the padlock probe sequence is pre-determined. However, the cRCA step provides surface modification of microchannels, like the PAMAM dendrimer, which is done prior to detection, while manufacturing the device. This extended time appears less important. The sRCA, on the other hand, is part of the detection signal transduction and its reaction time is included in the whole detection time. Therefore, it is necessary to optimize or find strategies to enhance sRCA reaction speeds. Increasing reaction temperature should be the first choice. The reported RCA reaction temperatures range from room temperature to 42 °C, while the temperature used in this work is 37 °C. Another critical reaction temperature is the annealing temperature for the primer hybridizing with the padlock probe, which was not optimized in this study. Moreover, the GC content of the primer influences the annealing

and thus affects RCA efficiency [1, 2]. Another suggestion is to change the length of the padlock probe of sRCA or otherwise find a better design which would achieve rapid RCA production, such as different polymerase. In addition, reducing ligation time by optimizing ligation reaction conditions could be another strategy. For example, optimizing the ligation concentrations, the annealing temperature, the molar ratio between primers and padlock probes, the amount of T4 DNA ligase, or the reaction temperatures could all be investigated.

6.2.2 Characterization of RCA reaction efficiency

It is of great importance to quantify the RCA products in this study. AFM was used to characterize the morphology of the RCA chains. However, it is difficult to measure the length of the long chains, as the scanning size is several micrometers and the RCA chains exhibit in a random cross-over pattern. On the other hand, gel electrophoresis was supposed to provide the molecular size of DNA molecules, but the low mobility of RCA products makes them trapped in the loading wells of the agarose gel. To make the RCA products move from the loading wells for better evaluations on molecular sizes and reaction efficiencies, I tried to digest the RCA products by a restriction enzyme (BfaI) after the complementary probes hybridized with RCA products for providing the specific cutting sites. Unfortunately, this method did not work well nor showed any positive results. The RCA products were also denatured by heating at 95 ℃ for 5-10 min or purified by a purification kit (Wizard® SV Gel and PCR Clean-Up System, Promega Corporation, Canada) before loading the RCA products onto the agarose gel, but these approaches did not solve the problem neither. My suggestion to characterize the reaction efficiency of RCA is to measure the contour lengths of RCA chains by AFM images at the beginning

stage when the strands are not too long and confined within a single scanning spot. The length of the DNA strands is related to the molecular size (0.2 – 0.3 nm/nt). Therefore, the reaction efficiency could be calculated by assuming the reaction rate is constant.

6.2.3 Capture efficiency improvement

The limits of detection of the aptamer-sRCA system and the cRCA-aptamer-sRCA (dual-RCA) system are both 100 cells/mL. It is desirable to further decrease the LOD of the detection systems. The limit of detection is closely related to the capture efficiency, which is fundamental for the final detection signals. Therefore, it is crucial to improve the capture efficiency of the current detection system. The capture efficiency of the current dual-RCA system is below 10% when the concentration of *E. coli* O157:H7 is 10^5 cells/mL. Herein, capture efficiency is defined as the percentage of captured target bacterial cells divided by the total target bacterial cells being injected. The Reynold number of microfluidic systems is very low and the flow pattern of this system is laminar flow [3]. The layered flow behavior of laminar flow in detection channels has the advantage of easier control of fluids and manipulation of particles. However, this layered flow creates complications for the detection of bacteria in food samples because sample solutions flowing in the center streamline of the microchannel have little chance to interact with channel surfaces. To increase the likelihood of capture, the interaction and contact between sample solution and aptamer-modified channel surface should be increased, especially for food samples with ultra-low concentrations of bacteria. Therefore, the capture efficiency must be enhanced to ultimately achieve reduced detection limits. In order to do these, perturbing the layered laminar flow patterns into chaotic ones could increase the possibility of interaction between

bacteria in the sample solution and the aptamer-modified channel surface. Patterning ridges (grooved floor) on the surface of microchannels has been found to be a promising strategy to induce chaotic flow in straight channels [4]. Another strategy to improve capture efficiency is to enhance the affinity between recognition elements and target bacterial cells. While cRCA-aptamers produced by the cRCA reaction improved the capture efficiency of the recognition elements, reaction conditions such as flow rate of injected reagents, reaction buffer, concentrations of cRCA-aptamers can be further optimized. Once the capture efficiency is increased, the detection limit should be reduced and thus improve the detection sensitivity. Effects of flow rates of samples to be tested on capturing efficiencies require further explorations. Besides, the capture efficiencies at static incubation conditions between fluidic samples and the modified microchannel should be compared with those under varied dynamic flow rates.

6.2.4 Specificity tests

The aptamer used in this work was selected from an US patent and was tested by another group for specificities (four non-target *E. coli*, four *Salmonella*, two *Shigella* strains and five other foodborne bacterial types) with a colorimetric aptamer-based biosensor and showed an excellent specificities [5, 6]. The specificities of the aptamer-RCA system and the dual-RCA system were tested by comparing detection signals with several strains of non-target bacteria. It is expected to further explore the detection specificity by evaluating a larger variety of bacteria including *E. coli* cells of different serotypes and broader foodborne bacterial species that are commonly found in food samples. Besides, as non-pathogenic bacteria are generally spread in food samples, it is also necessary to confirm

the specificity by testing bacterial types that are non-hazardous. Moreover, these specificity studies could be expanded by using a mixture of various bacterial types, including target or/and not, with the aptamer-RCA and the dual-RCA detection systems. To further explore the specificity of this *E. coli* O157:H7 aptamer, the binding affinity should be tested and compared with other reported *E. coli* O157:H7 aptamers (Table S1) and *E. coli* O157:H7 antibodies.

6.2.5 Effects of food matrices and sample preparations

The complex and diverse food matrices bring challenges and difficulties for rapid and sensitive detection methods. Therefore, it is virtually impossible to achieve a universal method for all kinds of food samples. Besides, although the best efforts are applied to prepare the food samples before detections, it is still unavoidable to remove all the residual food-associated compounds [7]. Those compounds usually interfere with the recognition elements or signal transduction process, thus affect the detection sensitivity and quantification of the rapid detection methods. The cultural enrichment is an effective method to transform the food matrix into purified prepared food sample for the detection steps. This enrichment method has been well employed as a standard procedure for decades. Whereas, the multistep enrichment procedures, consist of pre-enrichment, selective enrichment and separation of bacterial colonies, are time consuming and impede rapid detection methods far from giving off real-time results [7, 8]. In addition to the food debris, there usually exist non-target or non-pathogenic microorganisms in food which also can interfere with the detection assays [8].

Food sample preparation and concentration methods have been developed to reduce the interference by food debris and non-target bacteria, in this way the cultural enrichment steps can be eliminated and thus reduce the whole detection time. Separation of samples is to remove a selected population of particles from a complex mixture, while concentration is to reduce sample volume while simultaneously retain the original bacterial population of interest. The common goal is to mostly remove the complex food matrixes and keep the bacterial cells. The most commonly used methods for food sample separation and concentration are filtration, centrifugation, adsorption, dilution, and extraction [9-11]. There have been a few food sample separation and concentration methods, such as micro-fabricated filters, were integrated with biosensing detection systems [12, 13]. This makes it one step forward to achieve on-chip analysis for raw food samples, as most of pre-treatment procedures are operated off-chip. Given that our system is based on microfluidics, microchannel-based method is preferred to be used to separate the food sample prior to be led to the detection channel. Spiral microchannel is chosen to separate ground food sample due to its high efficiency. This will be beneficial to the integration of our microfluidic detection device. Among the separation microchannels, spiral microchannel is a simple inertial one which has been reported to possess the capability of efficient size-dependent separation of multiple particles. Bhagat *et al*. used a 5-loop spiral microchannel to separate 7.32 μm from 1.9 μm particles [14]. Johnston *et al*. cleaned 93 % of 3.2 μm and 87 % of 2.1 μm microparticles from 1 μm particles [15]. As stated, a mortar grinder can prepare food samples into final fineness < 10 μm while the bacterial size is among the range of 1-3 μm [15]. Thus, it is possible to separate bacteria and bacterial sized particles from larger food matrix particles, and finally obtain enriched food samples with bacterial cells by spiral

microchannels. Spiral microchannels can achieve size-dependent separation by the advantages of laminar flow and inertial flow effects. There are several types of spiral channels categorized by the shape of the sectional faces. Rectangular spiral microchannel is the most popular type due to ease of fabrication and manipulation. In a rectangular spiral microchannel, curvature-induced secondary flows develop two major counter-rotating Dean vortices producing the Dean drag forces, which coupled with the dominant inertial forces causing the particles immigrate and focus in a single stream and equilibrate near the inner channel wall. Consequently, particles equilibrate at the center of the inner wall and form a single stream of particles due to the laminar flow and can be extracted if suitable outlets are designed [16]. As a result, particles can be separated by their size and be collected at different outlets. This kind of inertial size-dependent separations by special designed microchannels show convenient operation and high efficiency. In addition, the pre-treatment methods are expected to be based on microchannels, by which they can be coupled with the detection microchannel to obtain an integrated multi-functional device.

6.2.6 Device capability

The dendrimer coated on the PDMS microchannel provides multiple binding sites for aptamer immobilization and reduces non-specific binding of particles. However, the stability of the dendrimer under different flowing conditions have not been studied. The dendrimer-PDMS surfaces should be evaluated after washing at varied flow rates for different time and be compared with the original modified dendrimer-PDMS surface. Similarly, the conjugated aptamers or cRCA products on dendrimer-PDMS surfaces should also be studied for stability evaluations after washing with varied flow rates of PBS buffer

or fluidic samples. The surfaces can be evaluated by the roughness, water contact angles, XPS analysis, etc. Besides, the capture efficiencies should be compared between the original modified functional microchannels and those treated with repeated fluidic washes. The shelf life of the modified aptamer-RCA system and the dual-RCA system, under different storage conditions, is worthy to be studied. As single stranded nucleic acids, aptamers are chemically stable and have long shelf lives. However, the aptamers can be degraded if nucleases contained in the tested food samples. This degradation issue may be solved by chemical modifications of nucleic acid aptamers, such as modifications on the sugar ring or 3' end capping strategies [17]. Aptamers are advantageous to antibodies in terms of "catch and release" property, which makes it possible to reuse the microfluidic devices. The nucleic acid modifications within the microchannel can be cleaved by nucleases [18, 19], thus the captured cells can be released, while the devices can be cleaned for recycled uses. Temperature mediated and trypsin-induced releases of captured cells were also reported [20-22].

6.2.7 Perspective of this detection system

According to the site of use, a detection method can be evaluated in perspectives of sensitivity, specificity, limit of detection, speed, simplicity, potability, and cost. The current detection methods described in this thesis are still at their infant stage, and there are many aspects to be improved as discussed. It is potential to be regularly used in a laboratory if raw food samples are well prepared. It is also possible to be used personally at home or remote sites if the signal transduction module is integrated with a smartphone. The current detection system can also be developed as a preliminary screening method for

foodborne pathogens, as a large throughput of a liquid sample can be introduced to the microchannel.

6.4 References

1. Kumar, A. and J. Kaur, *Primer based approach for PCR amplification of high GC content gene: Mycobacterium gene as a model.* Molecular Biology International, 2014. **2014**: p. 1-7.
2. Wei, C., et al., *An improved DNA marker technique for genetic characterization using RAMP-PCR with high-GC primers.* Genetics and Molecular Research Journal, 2016. **15**: p. 1-12.
3. Stone, H.A. and S. Kim, *Microfluidics: basic issues, applications, and challenges.* AIChE Journal, 2001. **47**(6): p. 1250-1254.
4. Fodor, P.S. and M. Kaufman, *Time Evolution of Mixing in the Staggered Herringbone Microchannel.* Modern Physics Letters B, 2011. **25**(12n13): p. 1111-1125.
5. Bruno, J. and J. Chanpong, *Methods of producing competitive aptamer fret reagents and assays*. 2009, US Application. Patent No. US20090186342A1.
6. Wu, W., et al., *An aptamer-based biosensor for colorimetric detection of Escherichia coli O157: H7.* PloS One, 2012. **7**(11), p. e48999.
7. Brehm-Stecher, B., et al., *Sample preparation: the forgotten beginning.* Journal of Food Protection, 2009. **72**(8): p. 1774-1789.
8. Benoit, P.W. and D.W. Donahue, *Methods for rapid separation and concentration of bacteria in food that bypass time-consuming cultural enrichment.* Journal of Food Protection, 2003. **66**(10): p. 1935-1948.
9. Fukushima, H., et al., *Rapid separation and concentration of food-borne pathogens in food samples prior to quantification by viable-cell counting and real-time PCR.* Applied and Environmental Microbiology, 2007. **73**(1): p. 92-100.
10. de Mello, A.J. and N. Beard, *Dealing with real samples: sample pre-treatment in microfluidic systems.* Lab on a Chip, 2003. **3**(1): p. 11N-19N.
11. Stevens, K.A. and L.-A. Jaykus, *Bacterial separation and concentration from complex sample matrices: a review.* Critical Reviews in Microbiology, 2004. **30**(1): p. 7-24.

12. Andersson, H., et al., *Micromachined flow-through filter-chamber for chemical reactions on beads.* Sensors and Actuators B: Chemical, 2000. **67**(1-2): p. 203-208.
13. Chu, W.-H., et al., *Silicon membrane nanofilters from sacrificial oxide removal.* Journal of Microelectromechanical Systems, 1999. **8**(1): p. 34-42.
14. Bhagat, A.A.S., S.S. Kuntaegowdanahalli, and I. Papautsky, *Continuous particle separation in spiral microchannels using dean flows and differential migration.* Lab on a Chip, 2008. **8**(11): p. 1906-1914.
15. Johnston, I., et al., *Dean flow focusing and separation of small microspheres within a narrow size range.* Microfluidics and Nanofluidics, 2014. **17**(3): p. 509-518.
16. Chatterjee, A., S.S. Kuntaegowdanahalli, and I. Papautsky. *Inertial microfluidics for continuous separation of cells and particles*. in *Microfluidics, BioMEMS, and Medical Microsystems IX*. 2011. International Society for Optics and Photonics.
17. Ni, S., et al., *Chemical Modifications of Nucleic Acid Aptamers for Therapeutic Purposes.* International Journal of Molecular Sciences, 2017. **18**(8): p. 1683.
18. Zhao, W., et al., *Bioinspired multivalent DNA network for capture and release of cells.* Proceedings of the National Academy of Sciences, 2012. **109**(48): p. 19626-19631.
19. Li, S., et al., *Endonuclease-responsive aptamer-functionalized hydrogel coating for sequential catch and release of cancer cells.* Biomaterials, 2013. **34**(2): p. 460-469.
20. Enomoto, J., et al., *Catch-and-Release of Target Cells Using Aptamer-Conjugated Electroactive Zwitterionic Oligopeptide SAM.* Scientific Reports, 2017. **7**: p. 43375.
21. Zhu, J., et al. *Reusable microfluidic chip for cell capture and releaseusing surface-immoblized aptamers*. in *Int. Conf. on Miniaturized Chemical and Biochemical Analysis Systems (MicroTAS'10)*. 2010.
22. Zhu, J., et al., *Spatially selective release of aptamer-captured cells by temperature mediation.* IET Nanobiotechnology, 2014. **8**(1): p. 2-9.

Appendix A

Table S1 Summary on aptamer candidates of *E. coli* O157:H7

Sequence (5'-3')	Size (mer)	Type	Reference
ATCCG TCACA CCTGC TCTGG TGGAA TGGAC TAAGC TAGCT AGCGT TTTAA AAGGT GGTGT TGGCT CCCGT AT	72	DNA	[1]
ATCCG TCACA CCTGC TCTGC CGGAC CATCC AATAT CAGCT GTGGT GTTGG CTCCC GTAT	59	DNA	[1]
ATCCG TCACA CCTGC TCTGT AAGGG GGGGG AATCG CTTTC GTCTT AAGAT GACAT GGTGT TGGCT CCCGT AT	72	DNA	[1]
ATCCG TCACA CCTGC TCTAT CCGTC ACGCC TGCTC TATCC GTCAC ACCTG CTCTG GTGTT GGCTC CCGTA T	71	DNA	[1]
ATCCG TCACA CCTGC TCTAT CAAAT GTGCA GATAT CAAGA CGATT TGTAC AAGAT GGTGT TGGCT CCCGT AT	72	DNA	[1]
ATCCG TCACA CCTGC TCTGT AGATG GCAAG GCATA AGCGT CCGGA ACGAT AGAAT GGTGT TGGCT CCCGT AT	72	DNA	[1]
ATCCG TCACA CCTGC TCTGT AGATG GCAAG GCATA AGCGT CCGGA ACGAT AGAAT GGTGT TGGCT CCCGT AT	72	DNA	[1]
ATACG GGAGC CAACA CCACC TTTTA AAACG CTAGC TAGCT TAGTC CATTC CACCA GAGCA GGTGT GACGG AT	72	DNA	[1]
ATACG GGAGC CAACA CCATG TCATC TTAAG ACGAA AGCGA TTCCC CCCCC TTACA GAGCA GGTGT GACGG AT	72	DNA	[1]
ATACG GGAGC CAACA CCACA GCTGA TATTG GATGG TCCGG CAGAG CAGGT GTGAC GGAT	59	DNA	[1]
ATACG GGAGC CAACA CCAGA GCAGG TGTGA CGGAT AGAGC AGGCG TGACG GATAG AGCAG GTGTG ACGGA T (71)	71	DNA	[1]
ATACG GGAGC CAACA CCATC TTGTA CAAAT CGTCT TGATA TCTGC ACATT TGATA GAGCA GGTGT GACGG AT	72	DNA	[1]
ATACG GGAGC CAACA CCATT CTATC GTTCC GGACG CTTAT GCCTT GCCAT CTACA GAGCA GGTGT GACGG AT	72	DNA	[1]
ATACG GGAGC CAACA CCATT CTATC GTTCC GGACG CTTAT GCCTT GCCAT CTACA GAGCA GGTGT GACGG AT	72	DNA	[1]

ATCAA ATGTG CAGAT ATCAA GACGA TTTGT ACAAG AT	37	DNA	[2]
CGTGA TGATG TTGAG TTGGG GTGAT GGGTG CATGT GATGA AAGGG GTTCG TGCTA TGCTG TTTTG TCTAA TAATA CTAGT CCTTG CCAAG GTTTA TTCCA GTAAT GCCAA CCAAT CT	117	DNA	[3]
GGGAU ACCAG CUUAU UCAAU UUGAU UCCAU CUUCC UGGAC UGUCG AAAAU UCAGU AUCGG GAGGU UACGU AUUUG GUUUA UAGAU AGUAA GUGCA AUCU	99	RNA	[4]
GGGUC UUCCU GGACU GUCGA AAAUU CAGUA UCGGG AGGUU ACGUA UUUGG UUUAU AGAUA GUAA	64	RNA	[5]
TGAGC CCAAG CCCTG GTATG CGGAT AACGA GGTAT TCACG ACTGG TCGTC AGGTA TGGTT GGCAG GTCTA CTTTG GGATC	80	DNA	[6]
TGGTC GTGGT GAGGT GCGTG TATGG GTGGT GGATG AGTGT GTGGC	45-mer	DNA	[7]

References

1. Bruno, J. and J. Chanpong, *Methods of producing competitive aptamer fret reagents and assays*. 2009, US Application. Patent No. US20090186342A1.
2. Wu, W., et al., *An aptamer-based biosensor for colorimetric detection of Escherichia coli O157: H7.* PloS One, 2012. **7**(11), e48999.
3. Amraee, M., et al., *DNA aptamer identification and characterization for E. coli O157 detection using cell based SELEX method.* Analytical Biochemistry, 2017. **536**: p. 36-44.
4. Lee, Y.J., et al., *In vitro selection of Escherichia coli O157: H7-specific RNA aptamer.* Biochemical and Biophysical Research Communications, 2012. **417**(1): p. 414-420.
5. Apta-Index™ (Aptamer Database). https://www.aptagen.com/aptamer-index
6. Zou, Y., et al., *Selection , Identification and Binding mechanism Studies of an ssDNA Aptamer Targeted to different stages of E.coli O157:H7.* Journal of Agricultural and Food Chemistry, 2018. Published online first.
7. Yu, X., et al., *Whole-bacterium SELEX of DNA aptamers for rapid detection of E. coli O157: H7 using a QCM sensor.* Journal of Biotechnology, 2018. **266**: p. 39-49.